

# POLITECNICO DI TORINO

Collegio di Ingegneria Energetica

**Corso di Laurea Magistrale  
in Ingegneria Energetica e Nucleare**

Tesi di Laurea Magistrale

## **Analysis of the Calcium Looping process for chemical storage of solar energy aimed at decarbonizing power cycles and carbon intensive industries**



### **Relatori**

*firma del relatore (dei relatori)*

prof. Andrea Lanzini

.....

Dott. Stefano Stendardo

.....

### **Candidato**

*firma del candidato*

Salvatore Francesco Cannone

Marzo 2019



## Abstract

This Thesis proposes a novel solution for CO<sub>2</sub> capture and energy storage by means of combination and hybridization of a calcium-based process (Calcium Looping, CaL) and concentrated solar power (CSP) technologies.

These processes either make use of relatively abundant cheap materials (e.g. dolomite, limestone) with several outlet markets for spent materials (iron, steel, cement industries) or focus on the design of active material with long lifetimes and hence small environmental footprints. These technologies are aimed at reducing the size of the carbon footprint associated with the fossil fuel and capturing the CO<sub>2</sub> at high temperature.

This work is focused on the implementation of CaL for the decarbonisation of power and steel making process and to store the excess of renewable energy.

The iron and steel industry are the largest energy consuming manufacturing sector and the second-largest industrial consumer of energy, after the chemical sector. It produces around 7% of total world greenhouse gas emissions in 2016.

The first part of thesis is focused on the decarbonisation of an electric arc furnace (EAF) based process. A bi-reforming process is used to convert methane into a mixture of CO and H<sub>2</sub> via steam methane reforming (SMR) and dry methane reforming (DMR) at 950°C. The **CaL** technology is **used to enhance the production of the hydrogen via the intensification of the water gas shift (WGS) reaction** with the capture of CO<sub>2</sub> (Sorption Enhanced Water Gas Shift, SE-WGS) at 650°C. Hydrogen is used as reductant in the production of DRI (Direct Reduction Iron) into a shaft furnace in order to reduce the emission of CO<sub>2</sub>. The heat demand requested during the production of DRI is furnished by the combustion of conventional fuels. Flue gas will be decarbonised into carbonator reactor.

In the second part the integration of concentrating solar power (CSP) system is investigated in order to exploit the solar energy and regenerate the CaCO<sub>3</sub> into CaO. Calcium carbonate produced is sent to the calciner reactor run at 900°C to regenerate the spent solid back to calcium oxide. Solar energy is harvested into central tower receiver and transferred into calciner reactor by heat transfer fluid or, alternatively, calcination reaction can happen directly into solar receiver.

The third part of the thesis is focused on the **integration of the calcium looping process for thermochemical energy storage (TCES) of solar power**. The solar energy is used to decompose CaCO<sub>3</sub> into CaO and CO<sub>2</sub> at high temperature and stored at ambient temperature. Solar energy is harvested into central tower receiver and transferred into calcination reactor by heat transfer fluid or, alternatively, calcination reaction can happen directly into solar receiver. The produced CO<sub>2</sub> is cooled, compressed at high pressure and sent to a storage tank whereas the CaO stream is cooled and transported to a CaO reservoir (e.g. silos). The solar energy is then stored in chemical form which can be used in a different place and in different times without heat loss overcoming the fluctuation of power generation from solar energy. During energy release, CO<sub>2</sub> is expanded into a turbine and sent into a carbonator where it reacts with CaO coming from a silos, and releasing reaction heat at high temperature, used for power production. This work analyses two power cycle configurations with the main goal of optimizing the performance of the overall system integration. In particular an **integration with Rankine cycle** and **supercritical CO<sub>2</sub> Bryton cycle** are proposed and a pinch analysis is performed to optimize these energy systems. A parametric analysis was carried out to forecast the reduction of plant's efficiency when the CaL process coefficients (e.g. carbonation extent, temperature and pressure of carbonation reactor) changes.

The positive results obtained are encouraging: The CO<sub>2</sub> emission **from the steel industry** dropped by 70% with CSP to respect Midrex NG/EAF steel plant and the analysis **allows an important energy storage efficiency around 80%** and a good performance of power plant higher than 35%.

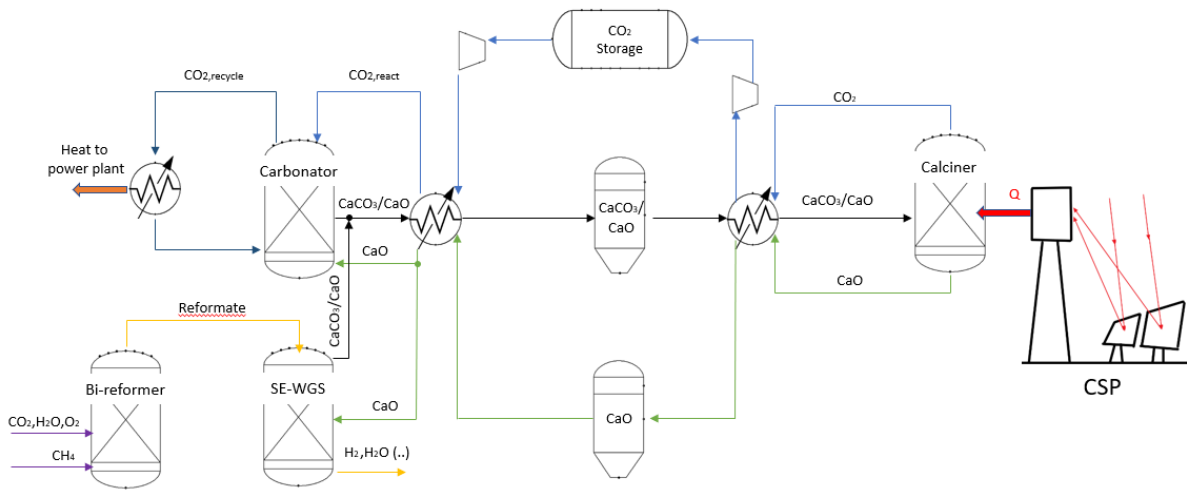


Figure 0: Conceptual CSP-CaL integration for sorption enhanced water gas shift (WGS) and thermochemical energy storage via CaL process

## Table of contents

Nomenclature .....	1
<b>1. Introduction .....</b>	<b>1</b>
1.1. Iron and steel Industry .....	2
1.2. Emission in the Iron and Steel Industry .....	3
1.3. Carbon capture and storage system (CCS).....	4
1.4. Methane reforming and sorption enhanced water gas shift.....	5
1.5. Electricity overview and CO <sub>2</sub> emission.....	7
1.6. Solar tower technology.....	8
1.7. Storage system.....	9
1.8. Research object.....	11
1.9. Thesis outlet .....	11
References.....	13
<b>2. Calcium Looping technology.....</b>	<b>15</b>
2.1. Fundamentals.....	15
2.2. Materials.....	16
2.3. Integration of CaL with Concentrated Solar Plants.....	18
2.4. Calcium looping utilization .....	20
2.4.1. Bi-Reforming and Sorption Enhanced Water Gas Shift.....	21
2.4.2. Carbon capture from flue gas .....	22
2.4.3. Calcium Looping for power production .....	23
2.5. Bubbling fluidized bed reactor .....	24
References.....	26
<b>3. Implementation of decarbonisation systems to iron and steel industry .....</b>	<b>28</b>
3.1. Plants layout .....	29
3.1.1. Reference iron plant.....	29
3.1.2. Integrated solar calcium looping iron plant .....	32
3.2. Modelling .....	33
3.2.1. Benchmark configuration .....	34
3.2.2. Integrated solar calcium looping iron plant .....	34
3.2.3. Material and energy balance of CaL solution.....	37
3.3. Energy assessment.....	39
Reference iron and steel plant.....	40
Integrated solar calcium looping iron and steel plant .....	40
3.4. Avoided emissions and environmental performance .....	42
3.5. SPECCA AND SPECCA* .....	43
References.....	45

4.	Implementation of a storage system and Rankine power production in IS-CaL .....	46
4.1.	Integrated Solar Calcium Looping .....	46
4.1.1.	Balance equation.....	48
4.2.	Rankine power cycle .....	50
4.2.1.	Rankine Power cycle integrated CaL technology.....	53
4.2.2.	Pinch analysis: design with minimal energy requirements.....	53
4.2.2.1.	Pinch analysis of calciner side .....	54
	Identification and characterization of flows.....	54
	Definition of constraints and boundary conditions .....	54
	Calculation of energy requirements .....	55
	Fluid coupling and representation of the exchanger network .....	55
4.2.2.2.	Pinch analysis of carbonator side.....	57
4.2.3.	Modelling.....	60
4.2.4.	Optimum configuration and parametric analysis.....	63
	References.....	69
5.	Supercritical Carbon Dioxide Power Cycle .....	70
5.1.	System configuration.....	71
	Recompression cycle.....	71
	Partial cooling with recompression cycle .....	72
	Recompression with Main-Compression intercooling.....	73
5.2.	Modelling approach.....	73
5.3.	S-CO <sub>2</sub> Brayton power cycle integrated with Solar CaL technology .....	78
5.4.	Modelling .....	81
5.4.1.	Optimum configuration and parametric analysis.....	84
	References.....	91
6.	Conclusion .....	92

## Nomenclature

<b>UNFCCC</b>	<b>United Nations Framework Convention on Climate Change</b>	
<b>BF</b>	Blast Furnace	
<b>DRI</b>	Direct Reduction Iron	
<b>HBI</b>	Hot Briquetted Iron	
<b>BOF</b>	Blast Oxygen Furnace	
<b>EAF</b>	Electric Arc Furnace	
<b>ASU</b>	Air Separator Unit	
<b>PSA</b>	Pressure Swing Adsorption	
<b>VSA</b>	Vacuum Swing Adsorption	
<b>VPSA</b>	Vacuum Pressure Swing Adsorption	
<b>SMR</b>	Steam Methane Reforming	
<b>DMR</b>	Dry Methane Reforming	
<b>WGS</b>	Water Gas Shift	
<b>SE-WGS</b>	Sorption Enhanced Water Gas Shift	
<b>HTF</b>	Heat transfer fluid	
<b>TES</b>	Thermal Energy Storage	
<b>PCM</b>	Phase Change Material	
<b>TCES</b>	Thermochemical Energy Storage	
<b>CaL</b>	Calcium Looping	
<b>SE-SMR</b>	Sorption Enhanced steam methane reforming	
<b>BMR</b>	Bi-Methane Reformer	
<b>IS Cal</b>	Integrated Solar Calcium Looping	
<b>t ls</b>	Tonnes of steel liquid	
<b>DC</b>	Direct Current	
<b>AC</b>	Alternating Current	
<b>CC7</b>	ChemCad <sup>TM7</sup>	
<b>LHV</b>	Low Heating Value	MJ/kg
<b><math>\dot{n}</math></b>	Mole flow rate	kmol/s
<b><math>\epsilon</math></b>	Extent of reaction	
<b><math>\Delta H_{react}</math></b>	Heat of reaction	kJ/kmol
<b>h</b>	Enthalpy	kJ/kmol
<b><math>\emptyset</math></b>	Power heat	kW
<b>W</b>	Mechanical or electrical power	kW
<b><math>c_p</math></b>	Specific heat capacity	kJ/(kmol K)
<b>SPECCA</b>	Specific Primary Energy Consumption for CO <sub>2</sub> avoided	GJ/t CO <sub>2</sub>
<b>HR</b>	Heat Requirement	GJ/t ls

# 1. Introduction

The CO<sub>2</sub> emissions from global energy rose progressively from 1971 excepted for a few years and reached an important value of 32.5 Gt [1] in 2016.

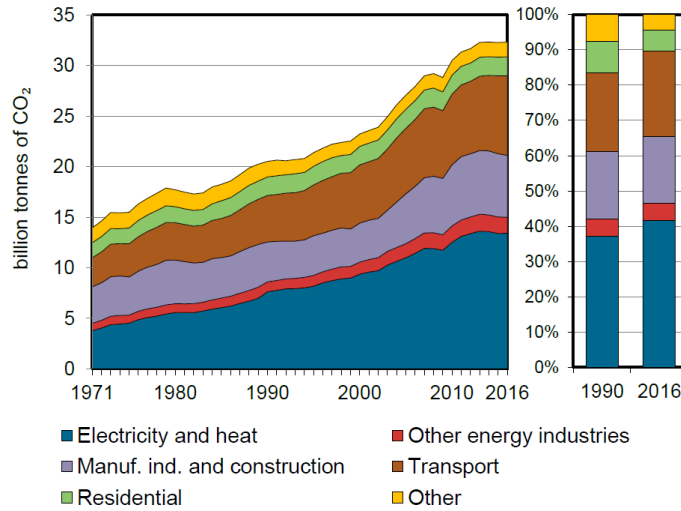


Figure 1.1: CO<sub>2</sub> emissions by sector in the world

Industry become the largest emitter if the emission from electricity and heat are reallocated to the effective consuming sectors as illustrated in the follow figure for the only 2016 [1].

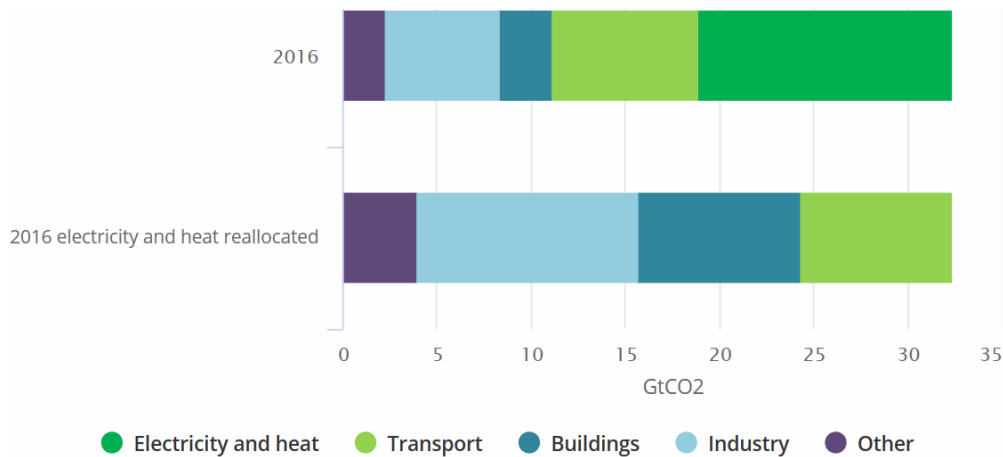


Figure 1.2 CO<sub>2</sub> world emissions by sector in 2016 [1]

A climate change represents a critical issue for all people in the world and now it is time to intensify our efforts to counter it. For this purpose, on 12 December 2015, the nations that are part of UNFCCC reached an agreement with the aim to limit the global warming below 2.0°C above pre-industrial level in this century and try to reduce it until 1.5°C [2].

To reach the 2°C target, starting from 2018 to 2100 only 720 Gt of CO<sub>2</sub> can be emitted into the atmosphere while the current rate is 32.5 Gt/year [2].

## 1.1. Iron and steel Industry

The following processes have to be analysed during the production of steel:

- Raw material preparation;
- Iron making process;
- Steel making process;
- Manufacturing steel product that is outside the scope of the thesis.

Coke is a fundamental material in this industry: it is the reducing agent in the Blast Furnace (BF) where reduce the iron ore with its combustion and gasification, providing the reducing gas and the heat to melt the iron ore and driving the endothermic process.

Obviously, the second main raw material is iron ore that in natural states occurs as lump ore. The energy needs of the BF depend on the quality of the ore. The higher the metal quantitative, the lower the energy consumption and CO<sub>2</sub> emissions [3]. A certain amount of scrap, DRI, and hot briquetted iron (HBI) inserting into BF with iron ore, increase the metal content and energy efficiency.

Iron making is the process in which iron ore is reduced removing oxygen and producing Fe. This process needs a certain amount of energy and produce the largest quantity of CO<sub>2</sub> among the main steel making processes.

A carbon-based and/or hydrogen-based reducing gas remove the oxygen from iron ore producing inevitably CO<sub>2</sub>.

The reduction of iron occurs either above or below melting temperature and the following reactions can take place:



The BF is the common method to produce iron reaching the 90% of iron production in the world. Iron coke and limestone are fed into the top of furnace while enriched oxygen air blast and reductant auxiliary are blown from below. The hot air convert coke in reducing gas to reduce the descending iron ore in counter-current. The time of reaction is around 6-8 hours [3]. The hot metal produced is sent to Blast Oxygen Furnace (BOF).

An alternative making iron of BF is the DRI and is based on natural gas. In this process the reducing agents are generated by reforming of methane or carbon gasification both in separately reactor. The solid DRI produced contains around 85-94% of metallic iron, carbon and gangue [3]. Energy consumption for coal-based processes is ~11.7–16 GJ/t DRI while natural gas-based processes consume ~10.5–14.5 GJ/t DRI assuming 100% lump ore operation [3].

The only process studied in this thesis is the production of DRI using shaft furnace with natural gas based Midrex process. In the shaft furnace process lump iron or iron ore are charged into the top of the vertical reactor and reducing by counter-current reduction gas. In Midrex the desulphurised natural gas is sent in an external reformer operated at ~950°C producing reductant gas. The DRI produced usually contains 90-94% of iron and it can be cooled and stock, discharged hot and fed briquette machine or fed directly EAF [4].

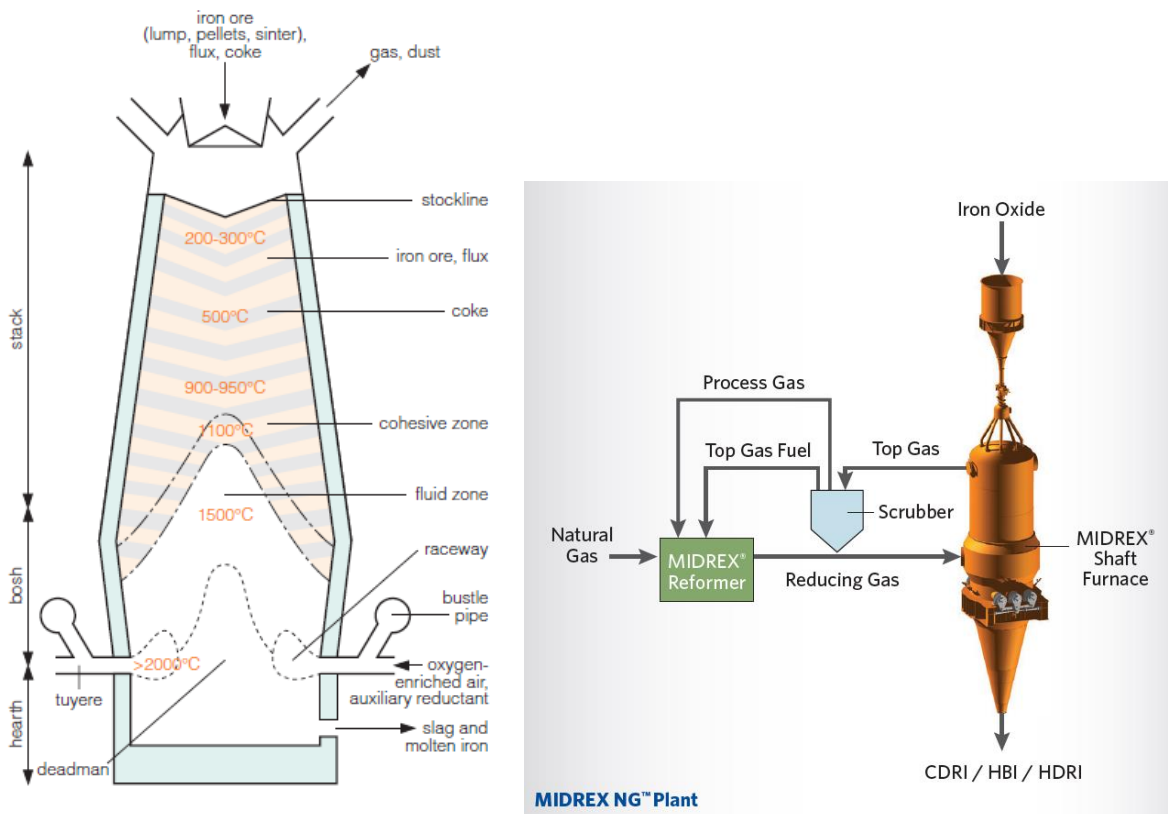


Figure 1.3: Blast Furnace cross section (left) and Midrex shaft furnace (right)

The hot metal produced in both reactors contain impurities which are removed in basic oxygen furnace BOF or in electric arc furnace EAF.

The hot metal is charged into the BOF in which silicon, carbon, and other impurities are removed. To remove this material, oxygen flow into reactor and oxidize all impurities releasing heat and forming a molten slag. The hot metal ratio into the charge influence the energy consumption.

The main charge material into EAF reactor is scrap but also DRI and HBI are inserted. The impurities of the charge are removed in a batch process. When hot metal, scrap and others are charged at the top of the furnaces, an electric arc carbon-based raises the temperature until 1600°C above melting temperature. Part of energy can be supplied with oxyfuel burns.

## 1.2. Emission in the Iron and Steel Industry

Manufacturing steel estimated for 22% of industry energy use and they are responsible for 31% of industrial direct CO<sub>2</sub> in 2012 and therefore one of the major contributors to global anthropogenic CO<sub>2</sub> emissions [5]. The CO<sub>2</sub> emitted in the air vary widely between country and it is function on the quality and type of raw materials (iron ore, scrap based, DRI based), technology used (BOF, EAF), efficiency process, fuel mix and carbon intensity of the fuel mix and electricity respectively. For every tonne of steel cast is emitted an average 1.8 t of CO<sub>2</sub> [5].

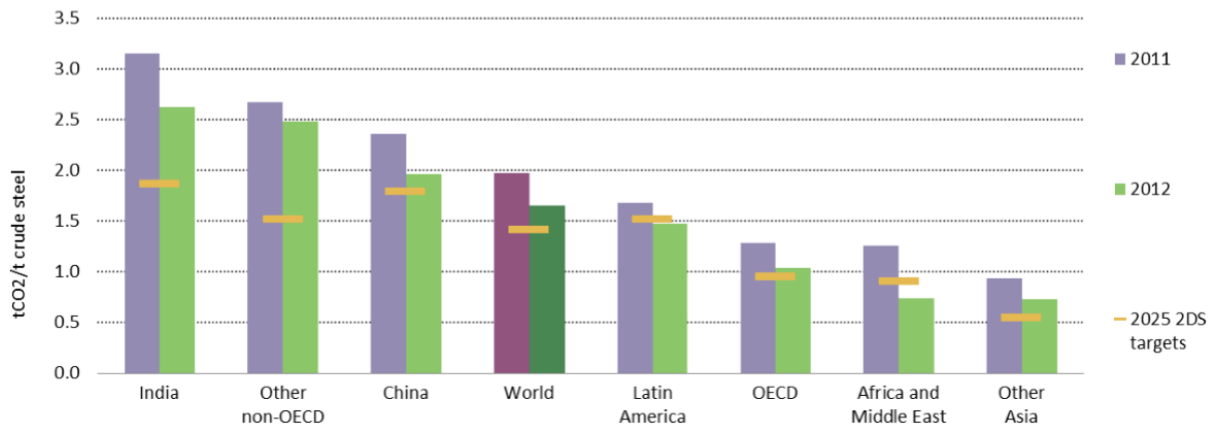


Figure 1.4: Direct CO2 emissions intensity of crude steel production [5]

An increase of process efficiency, minimizing the energy consumption, using carbon capture storage and the reuse of industrial wastes should be improved to drop the impact of climate change.

CO<sub>2</sub> is emitted during different processes:

- Combustion of fossil fuel (natural gas, carbon) that are include in direct emission;
- Emission from internal-process as the oxidise of gas reduction also include in direct emission;
- Electricity consumed into the plant (auxiliary or EAF) include in indirect emission;

CO<sub>2</sub> emitted from power consumed varies from country to country based on the different ratios of thermal, nuclear and renewable power generation accounted.

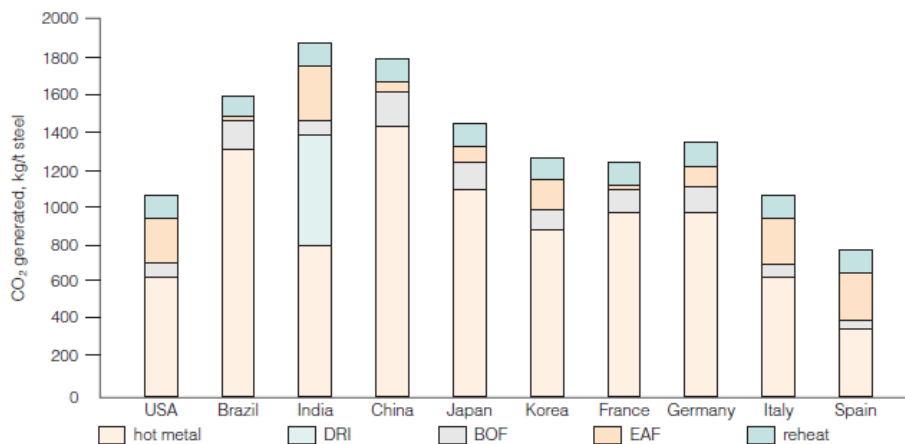


Figure 1.5: Estimated CO2 emissions/t for different country in 2009 [5]

The difference of the CO<sub>2</sub> emitted for the same process is due to plant size, energy recovery, quality of raw material and so. Waste energy is often recovery for power generation while increasing scrap recycle help to increase efficiency of the whole process.

### 1.3. Carbon capture and storage system (CCS)

Generally, the CO<sub>2</sub> can be separate into power plant and industry in three way:

- pre-combustion process used largely in integrated gasification combined cycle [6];
- oxyfuel combustion carbon capture producing only CO<sub>2</sub> and water easily separated [7];
- post-combustion capture unit [8-11].

Oxy-combustion process uses pure oxygen as oxidant replacing air oxygen produced by an Air Separation Unit (ASU). Usually oxygen is mixed with CO<sub>2</sub> or steam to reduce the exhaust operating temperature safeguarding the combustion chamber. Existing several commercial technologies to

separate oxygen as cryogenic process, Pressure swing adsorption (PSA), Vacuum swing adsorption (VSA) and Vacuum pressure swing adsorption (VPSA). Benchmark technology is cryogenic air separator with a power demand of 200 kWh/t O<sub>2</sub> in 2005 [12].

Pre-combustion capture process removes CO<sub>2</sub> from fossil fuel before combustion. Fossil fuel is converted into synthetic fuel gas (syngas) usually at high temperature and with low quantity or without oxygen, Syngas is a mixture of hydrogen, carbon monoxide and carbon dioxide at the outlet of the gasification process. This syngas can be sent to a further step where Water Gas Shift reaction happens concentrating the gaseous stream in H<sub>2</sub> and CO<sub>2</sub> that can be easily separated.

Post-combustion carbon capture removes diluted carbon dioxide from flue gas after a conventional combustion of carbonaceous fuel (e.g. coal, biomass, methane).

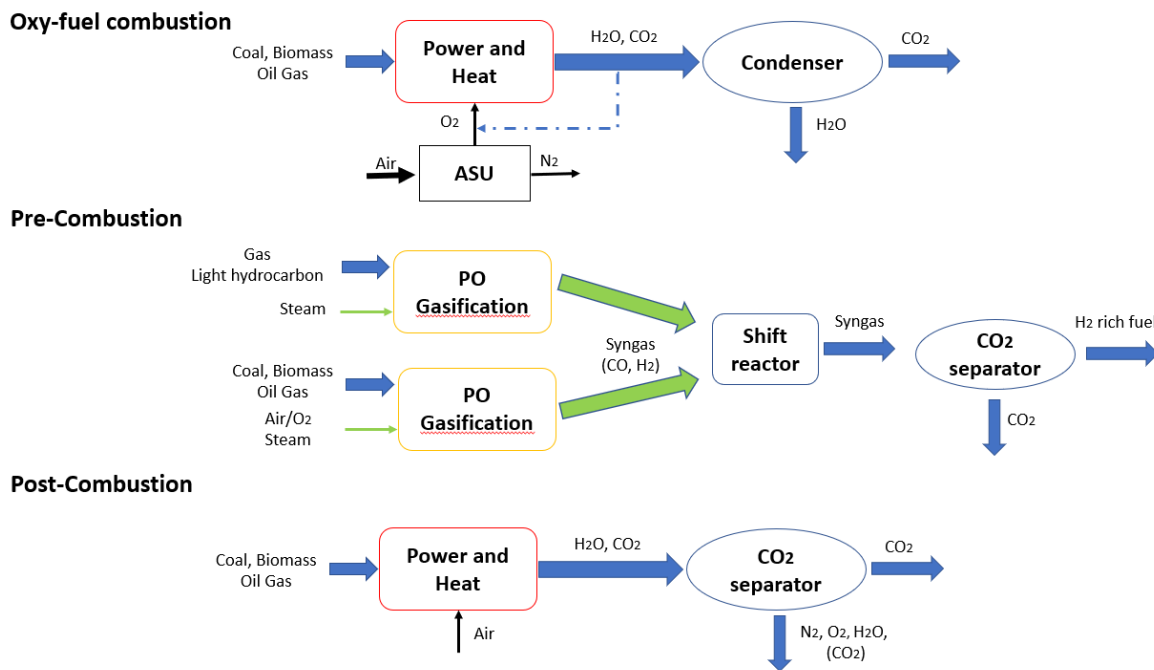


Figure 1.6: CO<sub>2</sub> Capture Processes

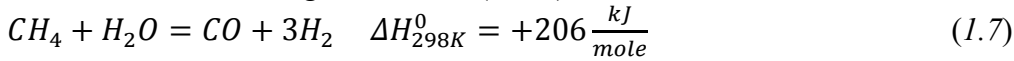
Post and pre-combustion processes could be based on the same technologies: polymers membrane, liquid or solid solvents, cryogenic liquefaction is used to capture the CO<sub>2</sub>.

Currently, the absorption process can be divided into physical absorption where the CO<sub>2</sub> forms electrostatic bond with the CO<sub>2</sub> acceptor and chemical absorption where the CO<sub>2</sub> and the solvent form chemical bonds. Chemical scrubbing with amines is one of the most used (H<sub>2</sub>O-MEA-CO<sub>2</sub> system). An emerging technology for the separation of CO<sub>2</sub> from gaseous stream happens during an exothermic reaction (carbonation). The spent material is the regenerated at high temperature (calcination) to decompose CaCO<sub>3</sub> into the respective oxide (CaO) producing a high CO<sub>2</sub> concentrated stream. Generally, the CO<sub>2</sub> capture is carried out in the fluidised bed reactor (carbonator) at approximately 600-700 °C whereas the regeneration occurs in a fluidised environment at temperature not below than 850 °C and atmospheric pressure.

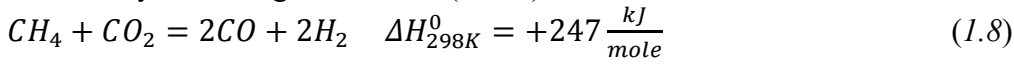
#### 1.4. Methane reforming and sorption enhanced water gas shift

The reductant gas can be produced via reforming of methane with steam (SMR, steam methane reforming) and carbon dioxide (DMR, dry ethane reforming). Usually, reforming of methane is followed by water gas shift, when the main goal is hydrogen production. Into a bi-reformer of methane the following reaction are coupled and carried out in a single reactor:

- Steam reforming of methane (SMR)



- Dry reforming of methane (DMR)



The endothermic reactions can occur only with high temperature and in presence of catalyst usually metal-based (e.g. nickel, cobalt). High temperature and low pressure enhance the conversion of methane. Tubular reformers are a typical design contain many tubes and burner arrangements (see Fig 1.7). The heat necessary for the reaction is given from a furnace gas where the heat released by the fuel combustion heat is used for the reforming reaction and for preheating the inlet gas [13].

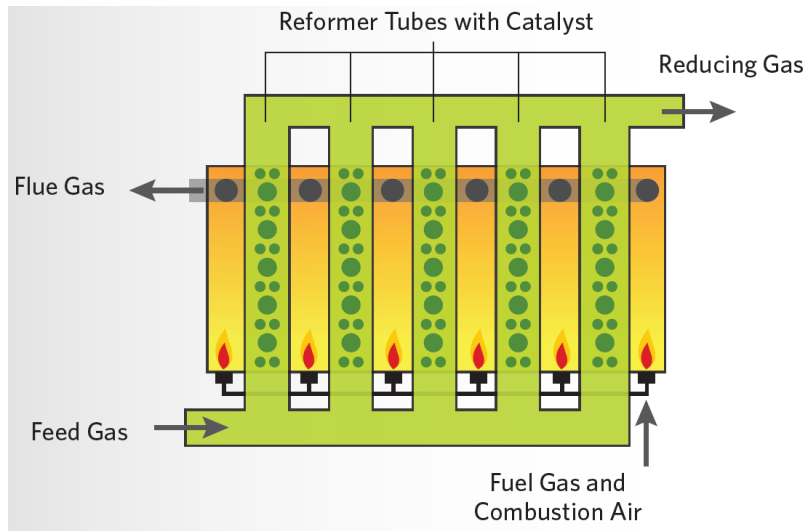
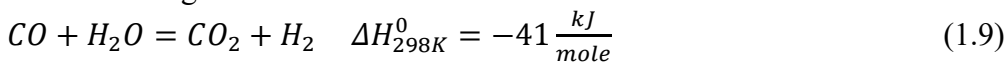


Figure 1.7: Tubular reformer used in Midrex process

The water gas shift (WGS) reaction (eq. 1.9) is used to change the H<sub>2</sub>/CO ratio of the syngas: this is an exothermic reaction and low temperature increase reaction advancement instead change of pressure does not affect the WGS reaction.

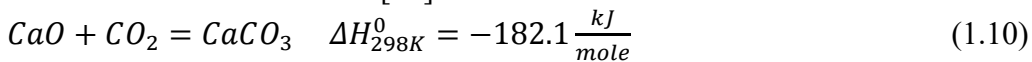
- Water gas shift reaction



The high temperature WGS is typically carried out in adiabatic reactor at 500°C [12] using robust catalyst as Fe-Cu-Cr.

The Sorption Enhanced water gas shift (SE-WGS) is a novel process for hydrogen production. This process integrates capture of CO<sub>2</sub> by CaO based technology (Calcium looping) and typical WGS in a single reactor. The production of hydrogen take advantage of the Le Chatelier principle due to simultaneous in-situ CO<sub>2</sub> sorption that shift the thermodynamic equilibrium toward the products.

- Carbonation reaction [14]



Solid sorbent can be regenerated decomposing at high temperature (>850°) calcium carbonate into CaO which is sent again into SE-WGS reactor making continuous the CO<sub>2</sub> capture cycle.

## 1.5. Electricity overview and CO<sub>2</sub> emission

The production of gross electricity has been increasing since 1974, except during economic crisis that caused a drop in global production. Recently, the largest part of electricity is produced with combustion fuel (67.3% of total electricity production [15] in 2016) provided by fossil fuel, biofuel and wastes.

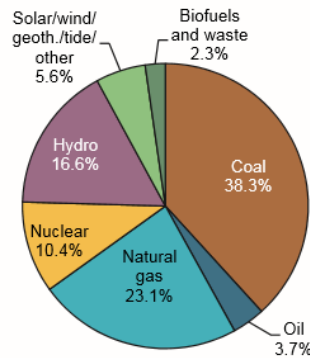


Figure 1.8: Global electricity production, by source, in 2016 [15]

Gross electricity production in countries belonging in Organisation for Economic Co-operation and Development (OECD) from fossil fuel decrease a growth from renewable source has been recorded.

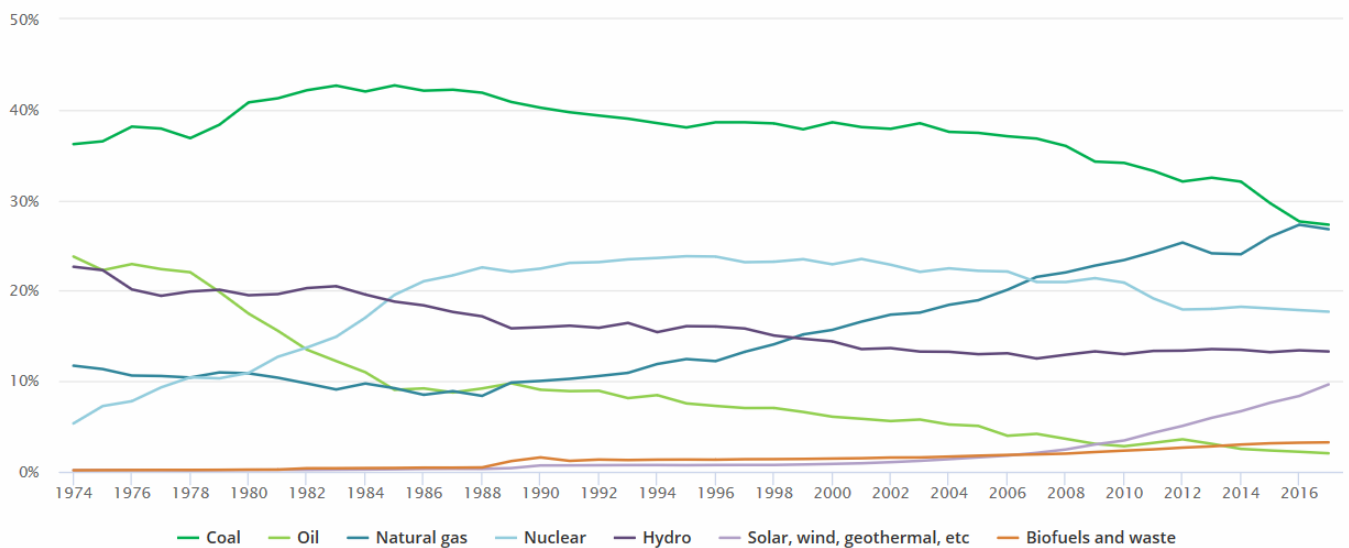


Figure 1.9: OECD gross electricity production by source [15]

The phase-out of coal-fired power and the increase of the use of natural gas and renewable for power generation lead to a gradual decline of CO<sub>2</sub> emission. Recently, higher efficiency of natural gas-fired and the slump in prices, made natural gas an attractive choice for baseload demand previously met by coal-fired generation.

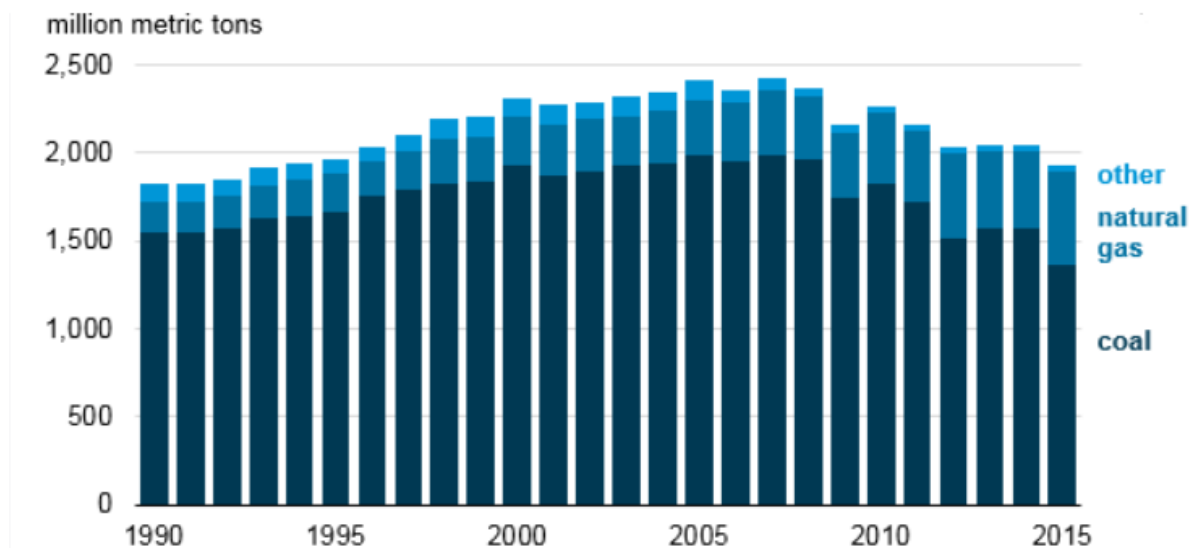


Figure 1.10: Carbon dioxide emission from electricity generation [16]

In the next five years the almost 30 percent of power demand will be provided by renewables reaching also 70 percent of electricity [17]. Concentrated solar power will have the highest growth to respect the last five years with new plant focused in China, Morocco and South Africa but technology risk, long construction times and inability to perform efficient energy storage continue to curb the development of this technology. Generally increasing the variable renewable energy plants there will be same period during the day in which the energy produced exceeds power demand [18]. Concentrated solar power depends on the availability of direct sunlight and to increase the energy production capacity and to correct the mismatch between the discontinuous renewable energy supply and demand, storage system and more widely flexibility needs to be improved [19]. Thus, cheaply and efficient energy storage [20] can help to give up fossil fuel and mitigate global warming.

### 1.6. Solar tower technology

The limitation of the fossil fuel and the critical issue of the climate change motivated many countries to support development of the renewable energy. Concentrated Solar Power (CSP) generate electricity by the concentration of the direct solar beam and the use of a conventional power plant. Therefore, it can be used in regions with excellent solar resource. CSP is a renewable system capable to provide base load electricity and consequently, it has been considered the major substitute of the fossil power plant.

CSP technology can be classified in two system: Parabolic trough and linear Fresnel are line concentrating systems while the Sterling system and solar tower technology are point concentrating system. In line concentrating system, solar beams are concentrated along the length of the receiver, this means that not high concentration ratio is reached, and the temperature are not very high.

Solar tower power plant consists of a large number of sun-tracking mirror (heliostats) which concentrate the solar irradiation onto an absorber, called receiver, usually located atop of a tower. The concentrated irradiation is transformed into heat that is transferred by the heat transfer fluid and used to produce electricity. Exist many different receiver technologies which work with different heat transfer fluid.

The heliostats field of the solar tower plant are equipped by two-axes tracking system to track the sun's path during the day and they reflect the solar beam onto a comparatively small area of the receiver. The heliostats field is usually very expansive and cover until 50% of the investment cost (150 €/m<sup>2</sup>) [22].

The efficiency of the solar tower plant is influenced by optical efficiency and thermodynamic efficiency. The optical loss due mainly to the heliostats field are:

- Cosine loss: The effective mirror area is less than actual mirror area caused by the angle between incident irradiance and normal at surface;
- Blocking loss: One heliostat cannot reflect part of irradiance onto the receiver because a front heliostat blocks them;
- Shadowing loss: A front heliostats blocks the direct irradiance from solar to the other heliostat;
- Spillage loss: Not all light reflected hit the receiver due to mirror quality, tracking system accuracy;
- Atmospheric attenuation;
- Part of reflected irradiance are absorbed or scattered by the air;

Typical value of the heliostats field efficiency is included between 0.55-0.80 [22]

On the contrary, the main goal of the receiver is absorbing the reflected solar irradiation and transfer the energy heat into a heat transfer fluid. Usually thermal loss occurs into receiver and HTF pipes. Increasing the operational temperature, and therefore the temperature difference between the receiver and the surrounding air, thermal losses increase, and they are generated by the thermal radiation, convection and heat conduction.

The CSP efficiency is strongly depend on the receiver technology, heat transfer fluid used and operating temperature.

### 1.7. Storage system

In this last years, different technologies are used to store energy from CSP plants based in three main concepts:

- Thermal energy storage (TES) store heat through temperature difference. The material with high heat capacity used are molten salts [23] (nitrates, carbonates, chlorides) and solids [10] (ceramic materials or graphite);
- Phase-change materials use latent heat to store energy (sodium nitrate [24], slurries [25]);
- Finally, thermochemical energy storage (TCES) converting solar energy into separately chemical materials through endothermic reaction [26].

Both sensible and latent heat storage are low efficiency due to loss energy in short-medium term instead TCES storage avoid the loss of heat producing chemical materials. During cloudy day or, generally, when energy is needed, the produced chemical materials are brought together in a favourable condition in which an exothermic reaction can occur. Then, the heat released during the reaction is used to produce electricity.

Thermochemical storage systems have several advantages. The energy density is more than five times higher than PCM and TES systems. The storage period is indefinite because there is no thermal loss during storage.

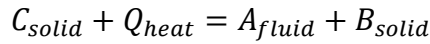
Nevertheless, sensible and latent heat storage systems are mature technology.

The first step to develop a TCES system is the choice of the medium material which has to respect the following criteria [13]:

- During energy storage, the temperature of endothermic reaction should be lower than 1000 °C;
- During release of energy stored, the temperature of exothermic reaction should be higher than 500°C;

- To maximize the storage capacity is necessary a high enthalpy of reaction and small molar volume of product;
- Completely reversible reactions and cycling behaviour;
- Both reactions should be fast;
- Chemical compounds should be easy to handle, stable with the storage environment and cheap;

The basic reaction process in equilibrium is the follow:



During charge of storage, the solid C, adding solar heat, decompose in compound A and B, in endothermic reaction, at temperature higher then turnover temperature. The products A and B are stored separately at ambient temperature in order to avoid side reactions. For the release of energy, the two compounds are mixed together at temperature lower than turnover temperature of reaction to produce heat.

Table 1.1: Promising materials for thermochemical energy storage [27]

Thermochemical Material (C)	Solid Reactant (A)	Working fluid (B)	Energy storage density (GJ/m <sup>3</sup> )	Charging reaction temperature (°C)
<b>MgSO<sub>4</sub> * 7H<sub>2</sub>O</b>	MgSO <sub>4</sub>	7H <sub>2</sub> O	2.8	122
<b>FeCO<sub>3</sub></b>	FeO	CO <sub>2</sub>	2.6	180
<b>Ca(OH)<sub>2</sub></b>	CaO	H <sub>2</sub> O	1.9	479
<b>Fe(OH)<sub>2</sub></b>	FeO	H <sub>2</sub> O	2.2	150
<b>CaCO<sub>3</sub></b>	CaO	CO <sub>2</sub>	3.3	837

One of the best and promising technologies is the Calcium Looping (Calcium-based) process in which calcination and carbonation reaction occur [14].

- Charging process: During the off-peak period or sunny day, Calcium carbonate is sent into calciner reactor and will be decompose through high solar energy input. The high temperature of the reactor produces the two compounds CaO and CO<sub>2</sub>. These two compounds are at higher temperature and therefore their sensible heat have to be recovered to store them at ambient temperature. Calcination reaction is an endothermic process.
- Storing process: Calcium oxide and carbon dioxide are separately stored at ambient temperature. The storage of the energy could be used after month or in another part of the world with the simply transport of the products.
- Discharging process: Calcium oxide and carbon dioxide are combined in an exothermic reaction (carbonation) during which heat is released at high temperature (800°C, 1-3 bar).

## 1.8. Research object

This work has been structured to analyse the Calcium looping technology for abroad implementation. An integration with Concentrated Solar tower is studied to regenerate the material at high temperature.

In this Thesis the CaL is investigated mainly as process for the decarbonisation of power and steel making process.

The CaL technology is used to enhance the production of hydrogen with the capture of CO<sub>2</sub> into water gas shift reactor. Is also used for the decarbonisation of flue gas which provide heat required by bi-reformer.

Specifically, a conventional around one million tpa (tons per annum) of steel making plant with and without carbon capture was assessed. The integration of the CaL with CSP, has the main goal to evaluate a thermodynamic optimum (e.g. energy penalty and CO<sub>2</sub> captured).

The novelty introduced in this first study, focus on applying CCS technologies in the iron industry, was combining the different research concepts previously introduced: CaL integrated with CSP for steel making's decarbonisation and SE-WGS for hydrogen production.

The second part of this work is focused on the integration of the Calcium looping process for thermochemical energy storage collected by CSP. Carbonator reactor is coupling with two power cycle at high temperature: 320 MW steam power plant and 305MW supercritical CO<sub>2</sub> Brayton cycle. To find the best design a pinch analysis was performed. A parametric analysis was carried out to evaluate the reduction of plant's efficiency when carbonation extent, temperature and pressure of carbonation reactor change.

In this last part, the use of the process as TCES at high temperature ~800°C and 1-3 bar represent the novelty of the thesis.

The major objectives of the Thesis are the:

- Development of thermodynamic characterization of carbonator reactor: evaluation of the minimum pressure as function of the operating temperature of the carbonator and carbonation reaction extent and the evaluation of heat released at different condition;
- Development of a simplified short-cut model to simulate the Carbonator as well as the Sorption-Enhanced Water Gas Shift (SE-WGS) reactors for the decarbonisation of steel making process;
- Development integration between CSP and CaL as thermochemical energy storage and different power cycle using pinch analysis to maximize thermodynamic efficiency;
- Evaluate the storage volumes off compounds and storage efficiency when the degree of CaO conversion varies;

## 1.9. Thesis outlet

In chapter 2, a background of calcium looping process is given. The fundamentals and the several materials used as sorption are described. The integration of the calciner reactor within the solar tower plant are discussed. The sorption-enhanced Water-gas-Shift (SE-WGS), carbon capture, storage/release of energy applications are introduced, and a general description of the fluidized bed reactors is presented.

In Chapter 3, the implementation of CCS technologies in iron and steel plant is discussed. For comparison reason, a conventional iron making with an output of 1 Mt/y is firstly introduced. Then, the alternative concepts to capture CO<sub>2</sub> from iron mills is presented: a novel calcium looping process integrated with CSP is showed: The CaL technology is used to enhance the WGS and to capture CO<sub>2</sub> from flue gas. Finally, a simulation model for the iron and steel with and without the CO<sub>2</sub> capture system considered is proposed and developed in Chemcad™ 7, putting in evidence the main assumptions and compute some significant parameter (e.g. SPECCA).

In Chapter 4, the proposed CaL technology is used to store the energy excess of renewable energy. The energy is released into the carbonator reactor integrated with a conventional Rankine power cycle of 320 MW. A pinch analysis is carried out to optimize the heat exchanger network with the main goal to reduce the heat required. Successively, a parametric analysis is performed changed several key parameters (e.g. CaO conversion, carbonator pressure and temperature).

In Chapter 5, the same CaL optimize is integrated with supercritical CO<sub>2</sub> Brayton cycle. At first, the more efficient cycle is chosen between three. The optimum configuration is found and consequently the best performance configuration is considered. A parametric analysis at different CaO conversion was performed.

Lastly, in Chapter 7 the most significant results are resumed, and conclusions are drawn together with future works.

## References

- [1] International Energy Agency, «CO<sub>2</sub> emissions from fuel combustion,» OECD/IEA, 2018.
- [2] U. Nation, «Adoption of the Paris Agreement,» in *Framework Convention on Climate Change*, Paris, 2015.
- [3] A. Carpenter, «CO<sub>2</sub> abatement in the iron and steel industry,» IEA: International Energy Agency, 2012
- [4] Midrex Technology Inc , «The Midrex Process,» technical paper, 2019
- [5] K. West, «ETP 2015: Iron & steel findings,» IEA International Energy Agency, 2015.
- [6] US Department of Energy (DOE), «Kemper County Integrated Gasification Combined-Cycle (IGCC) Project, Draft Environmental Impact,» 2009.
- [7] B.J.P. Buhre, et al, «Oxy-fuel combustion technology for coal-fired power generation,» *ELSEVIER*, vol. Progress in Energy and Combustion Science 31 (2005) , 205.
- [8] Antonio Perejón, et al, «The Calcium-Looping technology for CO<sub>2</sub> capture: On the important roles,» *ELSEVIER*, 2015.
- [9] M. C. Romano, et al, «Modeling the carbonator of a Ca-looping process for CO<sub>2</sub> capture from power,» *ELSEVIER*, 2011.
- [10] Yuan Wang, et al «A Review of Post-combustion CO<sub>2</sub> Capture Technologies from,» *ELSEVIER*, 2016.
- [11] C. Ortiz, et al, «A new model of the carbonator reactor in the calcium looping technology,» *ELSEVIER*, 2015.
- [12] Sandeep Alavandi, et al, «Emerging and Existing Oxygen Production Technology Scan and Evaluation », 2018
- [13] J.R. Nielsen, et al, « Concepts in syngas manufacture », Imperial College Press, 2011
- [14] B.R. Stanmore and P. Gilot, « Review—calcination and carbonation of limestone during thermal cycling for CO<sub>2</sub> sequestration », *ELSEVIER*, 2005
- [15] International Energy Agency, « Electricity information: Overview » OECD/IEA, 2018.
- [16] International Energy Agency, « Monthly Energy Review » OECD/IEA, 2019.
- [17] International Energy Agency, « Market Report Series: Renewables 2018. Analysis and Forecasts to 2023 »; 2018.
- [18] Tim Schmidla, et al, « Prospective Integration of Renewable Energies with High Capacities Using Combined Heat and Power Plants (CHP) with Thermal Storages »; *ELSEVIER*, 2016
- [19] International Energy Agency, « Status of power system transformation »; 2018.
- [20] Otto Koskinen, et al, « Energy Storage in Global and Transcontinental Energy Scenarios: A Critical Review »; *ELSEVIER*; 2016
- [21] J. Sattler, et al « Solar Tower Technology »; ENERMENA
- [22] Solar-Institut Jülich, Heinrich-Mußmann-Str. 5, D-52428 Jülich, [www.sij.fh-aachen.de](http://www.sij.fh-aachen.de)
- [23] N. Braidenbach, et al; « Thermal Energy Storage In Molten Salts: Overview Of Novel Concepts And The DLR Test Facility TESIS »; *ELSEVIER*; 2016
- [24] U. Nepustil, et al; « High Temperature Latent Heat Storage with Direct Electrical Charging – Second Generation Design »; *ELSEVIER*; 2016
- [25] S. Niedermaier, et al; « Characterisation and Enhancement of Phase Change Slurries »; *ELSEVIER*; 2016

- [26] P. Pardo, et al; « A review on high temperature thermochemical heat energy storage »;  
ELSEVIER; 2014
- [27] Ali H. Abedin, et al; « A critical review of TCES »; The Open Renewable Energy Journal;  
2011

## 2. Calcium Looping technology

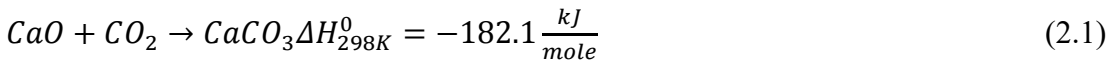
The largest energy consuming manufacturing sector as cement plants, steel mills, paper mills, together with power plants emit a large quantity (20 Gt CO<sub>2</sub> in 2016 [1]) of greenhouse in atmosphere. Capturing CO<sub>2</sub> from flue and fuel gases has become one of the main research activities in recent years. Several processes are suggested (e.g. ammine, membrane) but in this work a novel solution for CO<sub>2</sub> capture and energy storage by means of combination and hybridization of a calcium-based process (Calcium Looping, CaL) and concentrated solar power (CSP) technologies is proposed.

Calcium looping process makes use of two fluidised bed reactors to capture CO<sub>2</sub> from flue gas or synthetic fuel gas (syngas) producing CaCO<sub>3</sub>. The solids product is sent into a further reactor (regenerator), where calcium carbonate is decomposed to CaO and CO<sub>2</sub> at high temperature. In case of energy production, the carbonator is fluidised by means of pure CO<sub>2</sub> stream releasing a certain quantity of energy (approximately 182 kJ/kmol) during the reaction with the CaO.

### 2.1. Fundamentals

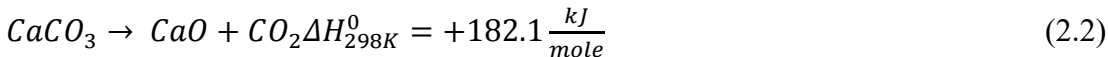
Calcium oxide is content in relatively abundant cheap materials (e.g. dolomite, limestone) with several outlet markets for spent materials (iron, steel, cement industries).

Shimitzu et al [2] proposed for the first time the reaction of CaO with CO<sub>2</sub>, calcium looping process CaL, with the main goal of decarbonizing flue gas. Carbonator reactor operates in a temperature range between 600 – 850°C with the operating pressure ranging from 1 bar to 3 bar and the CO<sub>2</sub> is adsorbed from CaO as shown in the follow equation:



Since carbonation reaction is an exothermic reaction, heat is released and steam can be produced to generate electricity by membranate walls or/and immersing heat exchange in the carbonator reactor.

The produced CaCO<sub>3</sub> can be stored and successively transported to the calciner reactor. Into the calciner reactor, the equilibrium temperature of CO<sub>2</sub> is 895°C at atmospheric pressure. Therefore, the regeneration of the calcium oxide has to take place at temperature above 900°C.



Since calcination reaction is an endothermic reaction, the heat of reaction is supplied usually by oxy-fuel combustion into the reactor. This work proposes a novel integration of CaL process with a concentrated solar power at high temperature for the regeneration of spent material. The CO<sub>2</sub>-rich stream leaving the regenerator is cooled and compressed in supercritical condition for its temporary (seasonal) storage. The produced CaO is cooled and stored in a common silos ready to be sent back into carbonator reactor releasing the heat during the carbonation reaction.

The carbonation/calcination reactions depend strictly on the decomposition pressure of CaCO<sub>3</sub>. This latter pressure is determined by equilibrium thermodynamic considerations. The equilibrium decomposition pressure cited by Stanmore and Gilot [3] is:

$$P_{eq} = 4.137 \cdot 10^7 \exp\left(-\frac{20474}{T}\right) atm \quad (2.3)$$

Fig. 2.1 plots the decomposition pressure of  $\text{CaCO}_3$  with the temperature:

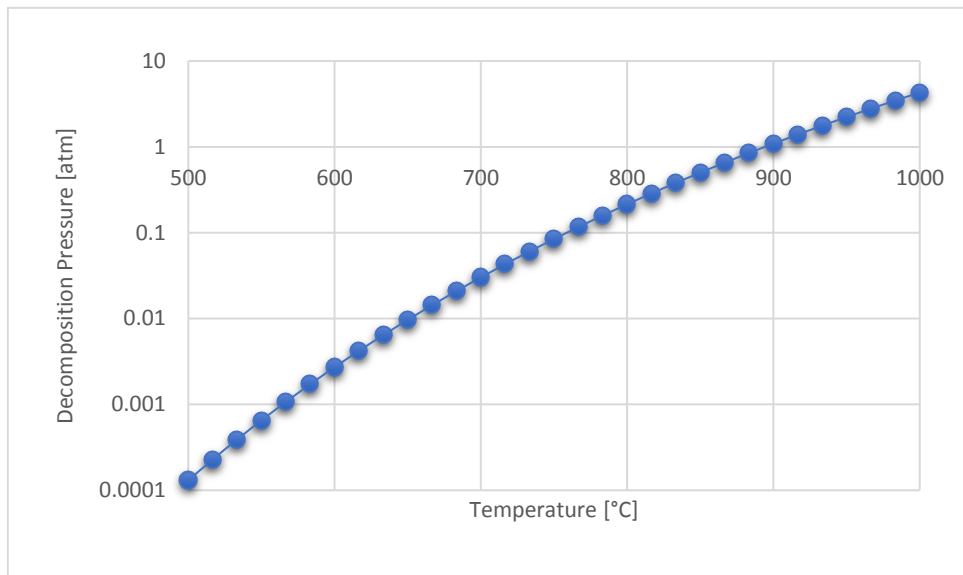


Figure 2.1: Decomposition pressure of  $\text{CaCO}_3$  plotted with the expression of Stanmore and Gilot

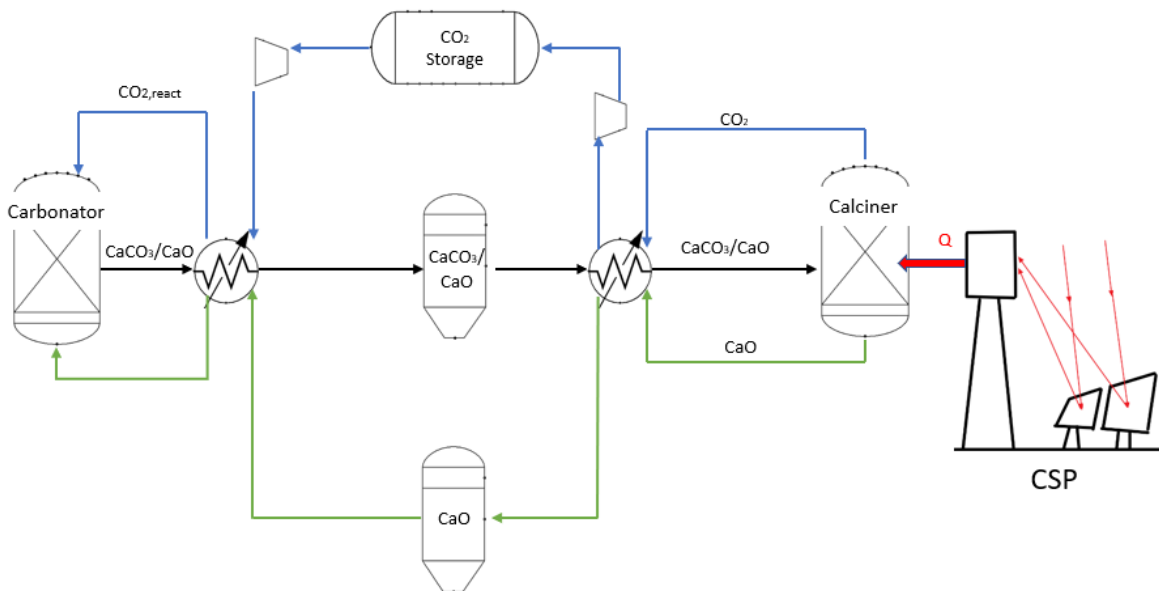


Figure 2.2: General scheme of CaL with CSP integration

## 2.2. Materials

The main advantages of the CaL process is the low price (10 \$/ton [4]) of the  $\text{CO}_2$  acceptor material:  $\text{CaO}$  from naturally occurring material as limestone or dolomite, its wide availability and harmlessness towards the environment. Commercial limestone rock generally contains more than 90% of calcium carbonate. As Fig 2.1 illustrates, carbonation and calcination reaction occur at high temperature (at 1 bar the equilibrium temperature is around 900 °C). Thus, it is possible to use the sensible heat of gas leaving carbonator at high temperature to produce steam to be expanded in a conventional turbine and generate electricity. Direct expansion of  $\text{CO}_2$  at the exit of the two reactors is not recommended because it may contain solid particles that would damage the blades of the turbines placed downstream.

It is demonstrated from several experimental works that calcite and dolomite can be used as sorbent for high temperature CO<sub>2</sub> capture [5]. However, it is also known that CaO-based solid sorbent are never fully utilized displaying the existence of maximum degree of carbonation conversion. A further drawback of this material is the dramatically drop in carbonation conversion with a short number of carbonation/calcination cycle.

Stendardo and Foscolo [5] considered two type (A and B) of naturally occurring dolomite whose chemical composition and physical characteristics are showed in Table 2.1. They proposed a grain model to interpret the CaO conversion to CaCO<sub>3</sub> during time (see Fig 2.3). It is presented only one step for sample A at 700°C and a multi-cycle carbonation for sample B.

As can be seen sample A reach quickly the 85% of conversion and the behaviour at the first cycle of sample B is like the previous. The figure shows also the progressively decline of CaO conversion which drops to 65% after only 4 cycles.

Table 2.1: Value of parameter used in simulation [5]

Parameter	Sample A	Sample B
fCaO (-)	0,274	0,215
fMgO (-)	0,155	0,164
ε <sub>0</sub> (-)	0,571	0,260
d <sub>p</sub> (m)	1,65E-04	1,95E-04
δCaO (m)	1,50E-06	1,50E-07
Sh <sub>e</sub> (-)	5,770	15,140
β (-)	0,017	1,40E-03
Φ (-)	0,048	0,237
Γ (-)	1292,200	1014,400
V <sub>CaO</sub> (m <sup>3</sup> /kmol)	1,69E-02	
V <sub>CaCO<sub>3</sub></sub> (m <sup>3</sup> /kmol)	3,69E-02	
V <sub>MgO</sub> (m <sup>3</sup> /kmol)	1,11E-02	
V <sub>MgCO<sub>3</sub></sub> (m <sup>3</sup> /kmol)	2,75E-02	
Z (-)	2,180	

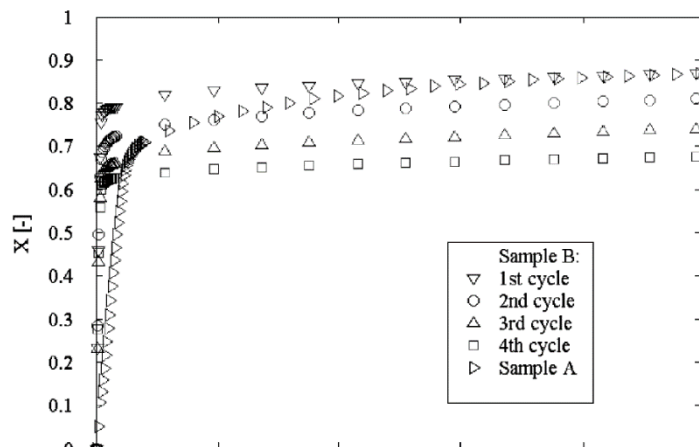


Figure 2.3: Experimental data for CaO conversion at 700°C obtained during a single step carbonation with sample A and multi-cycle carbonation with sample B [5]

A good strategy could be replaced a natural dolomite with synthetic CaCO<sub>3</sub> or doped limestone that maintain high degree of sorbent capture capacity. There are many reports in the literature focused on the research of synthesis CaCO<sub>3</sub>-based sorbents that enhance CaO conversion in a multi cycle carbonation including [6-7].

An important works with optimum results has been published by Chen et al [8] in which are considered three sorbent pellets described in table 2.2 while the experimental conditions are reported in table 2.3

Table 2.2: Composition with CaO pellet with aluminate cement

Sample	CaO	MgO	SiO <sub>2</sub>	Al <sub>2</sub> O <sub>3</sub>	Others	LOI
L-A	51,96	1,73	1,89	7,76	1,47	35,19
CP-A	59,74	2,21	1,48	6,95	1,93	27,69
CaO-0,5% CLS-A	43,67	2,21	2,25	14,35	1,9	35,54
Original limestone	54,98	2,07	0,21	0,08	0,34	42,32
LOI= Loss on ignition						

Table 2.3: Operation condition of carbonator and calciner reactor

	Pressure [bar]	Temperature [°C]	%CO <sub>2</sub> /air
<b>Carbonator</b>	5	700	15
<b>Calcine</b>	1	950	100

Fig 2.4 shows the calcium oxide conversion during multiple cycle. The CO<sub>2</sub> capture capacity of the new materials decline gradually and much slower than original limestone during multi-cycle. The addition of alumina has slowed down the drop in CaO conversion allowing up to 70% percent of CO<sub>2</sub> capture capacity after 50 cycle.

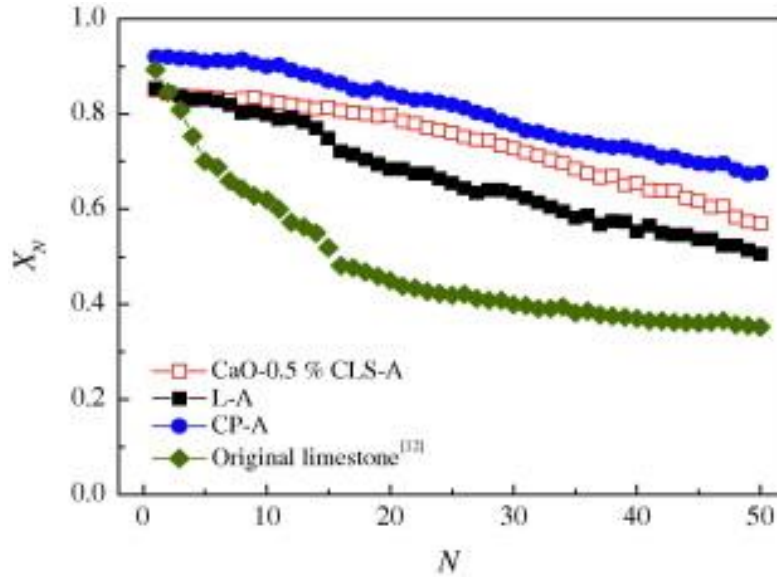


Figure 2.4: CaO conversion versus Number of cycles for different samples respect original limestone [8]

A good conversion degree after high number of cycles allows to save material and increase the efficiency of the system. It is also true we must go on sintering CaO-based, considering the costs of the new material and the CO<sub>2</sub> emitted to make it.

### 2.3. Integration of CaL with Concentrated Solar Plants

This section is devoted to the analysis of integration of the CaL process used as Thermo-Chemical Energy Storage (TCES) process to the concentrated solar power unit. In [9] the authors have proposed an efficient integration between CaL process and CSP power plant in which the heat released by carbonation reaction is carried out by the excess of CO<sub>2</sub> and employed for power generation by means of a closed CO<sub>2</sub> cycle. It is investigated the application of the CaL technology in pre-combustion capture systems and energy integration, and the coupling of the CaL technology with other industrial plants (e.g. cement plant) [10]. Tregambi et al [11] have studied the CaL process for post-combustion CO<sub>2</sub> capture and storage technique. Ortiz et al have analysed several power cycle configurations as closed carbon dioxide Brayton power cycle, Rankine cycle or a supercritical carbon dioxide Brayton cycle [4]. The key drawback to couple CaL with direct closed Brayton power cycle is the fines entrained by the CO<sub>2</sub> stream leaving carbonator that can cause problems at turbine during the expansion.

According to thermodynamic condition and kinetic reaction high temperature is necessary to drive the calcination reaction when operating under high CO<sub>2</sub> concentration [12, 13]. Nevertheless, the use of superheated steam or easily separable gas in calcination environment could allow to decrease the calcination temperature down to 700-750 °C to respect 900°C with high CO<sub>2</sub> partial pressure.

The energy storage can take place directly inside a solar receiver or using heat transfer fluid. When solar receiver and calciner are in two different reactors, solar energy is collected into central tower receiver and transferred into calcination reactor by heat transfer fluid (HTF). Several configurations have been proposed to harvest solar radiance. Therefore, several prototypes of solar receiver have been developed as rotary kilns [14-15], cyclone atmospheric reactor [16], falling particle receiver and fluidised bed reactor to efficiently increase the collected solar energy [17].

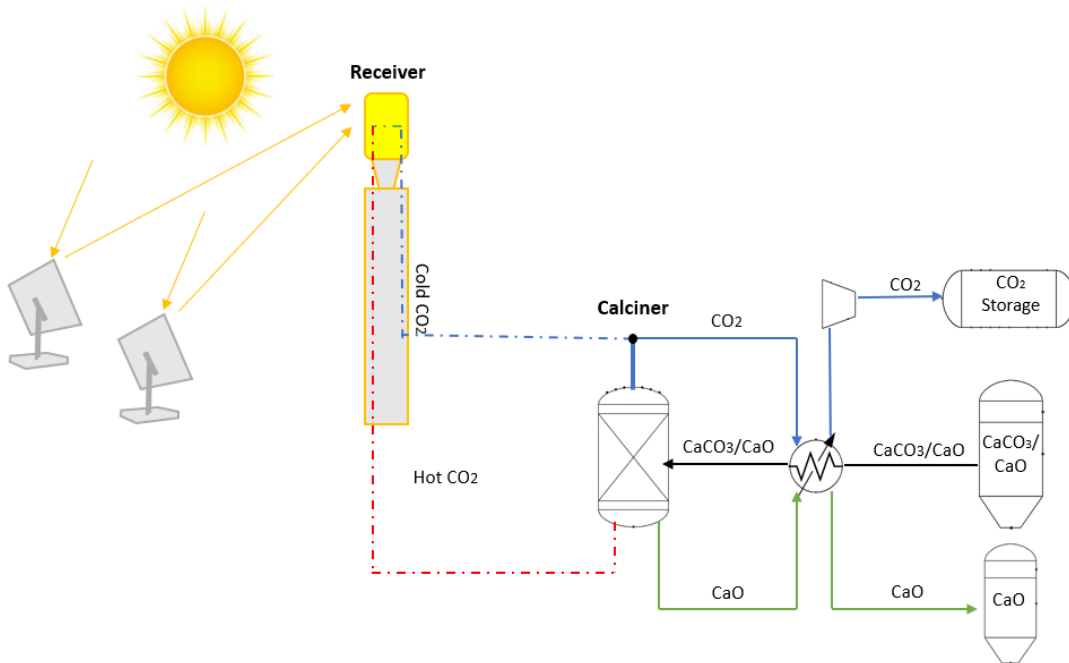


Figure 2.5: Chemical storage of solar energy using heat transfer fluid

In this work, a direct thermo-chemical storage was considered as part of the development of the models. The solar rays coming from the field of the heliostats are concentrated in a single point of

the reactor by means of a Central Reflector. Therefore, it is possible to have a reactor at a lower height than the classic solar towers, reducing the problems of mechanical strength of the structure. The solar irradiance is directly concentrated in the fluidised bed composed of calcium carbonate particles. In this configuration, the solar receiver also has the function of regenerating spent material.

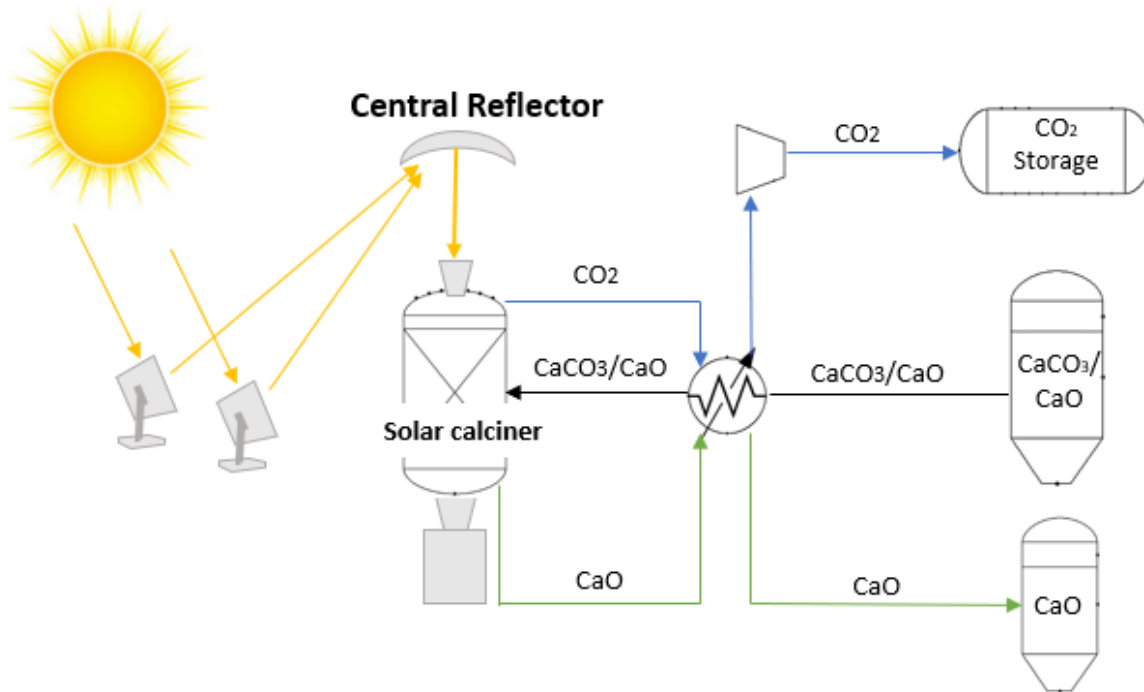


Figure 2.6: Chemical storage of solar energy directly into solar calciner. The reactor has the dual function of harvesting the solar radiance and regenerating the used material.

Solar calciner is a fluidized bed reactor which operates at ambient pressure, temperature above  $900^\circ\text{C}$  and it is fluidized by pure carbon dioxide.

Solids entering in solar calciner, composed by  $\text{CaCO}_3$  and unreacted  $\text{CaO}$ , are pre-heated through a heat-exchanger network by the hot products (i.e.  $\text{CaO}$ ,  $\text{CO}_2$ ) leaving the reactor itself. Then, the cooled  $\text{CO}_2$  is compressed at supercritical conditions and sent to a storage tank whereas the cooled  $\text{CaO}$  stream is transported to a  $\text{CaO}$  reservoir (e.g. silos). In this way we store solar energy in chemical form that can be used in a different place and in different times without heat loss in order to: (i) generate electricity and/or (ii) decarbonize carbon intensive industries (e.g. cement, iron and steel). While the solids reservoirs are at ambient condition, in order to use reasonably sized  $\text{CO}_2$  storage volume, a pressure of 74 bar at ambient temperature was chosen (supercritical conditions of  $\text{CO}_2$ ). The high pressure from 1 to 74 bar requires the installation of intercooling compression to minimize power loss. The sensible heat available at each stage is recovered to feed a district heating network.

#### 2.4. Calcium looping utilization

After storing solar energy as  $\text{CaO}$  and  $\text{CO}_2$ , these reaction products can be used for different purposes:

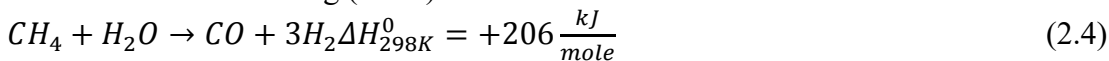
- To produce hydrogen via: (i) a sorption enhanced water gas shift reactor (SE-WGS), (ii) a sorption enhanced steam methane reforming (SE-SMR);
- To capture  $\text{CO}_2$  from: (i) off-gases produced in steel making process, (ii) flue gases leaving a rotary drum for clinker production;
- To generate power at zero  $\text{CO}_2$  emission;

The following sections will outline the three cases studied that will be subsequently explained into the details in the remainder of this work.

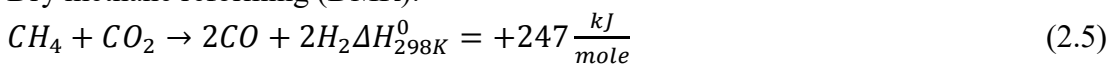
### 2.4.1. Bi-Reforming and Sorption Enhanced Water Gas Shift

Methane reforming process is commonly used for H<sub>2</sub> production releasing CO<sub>2</sub>. Natural gas is the most used fossil fuel for hydrogen production because of its high ratio of H to C (4) compared to other conventional fuels and it is relatively abundant gas. The H<sub>2</sub> content of the reformed gas is approximately (75% in dry reformat [18]) the remainder being composed of CO, CO<sub>2</sub>, H<sub>2</sub>O and traces of unreacted CH<sub>4</sub>. Therefore, water gas shift (WGS) reaction is generally envisaged downstream a reformer for an efficient CO<sub>2</sub> separation. In fact, WGS concentrates the content of CO<sub>2</sub> as CO reacts with H<sub>2</sub>O to produce CO<sub>2</sub> and H<sub>2</sub> and the carbon capture can be simultaneously implemented in an intensification approach to further increase the hydrogen production.

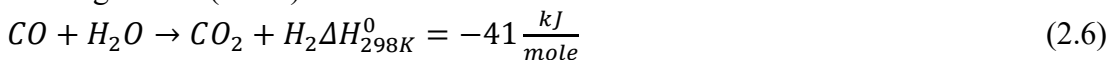
Steam methane reforming (SMR):



Dry methane reforming (DMR):



Water gas shift (WGS):



The figure 2.7 confirm that to attain the highest H<sub>2</sub> content the WGS reactor has to be placed downstream at a lower temperature with respect to the operating temperature of the SMR reactor.

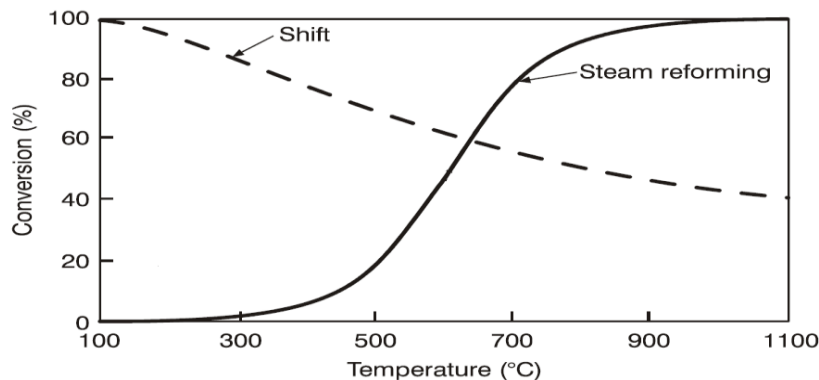


Figure 2.7: Equilibrium for steam reforming and water gas shift [19]

At lower temperature robust catalyst as Fe-Cu-Cr are necessary. Currently, the most used process to obtain H<sub>2</sub>-reach flow, is installing two WGS reactors at different temperature (180 – 400 °C, condensing water vapour and separate hydrogen from syngas into a Pressure Swing Adsorption unit, reaching 99% of purity.

In this Thesis we propose to implement the WGS at relative high temperature (600 °C) with a simultaneous CO<sub>2</sub> capturing in order to further shift the equilibrium controlled WGS towards the H<sub>2</sub> production. CaO produced by solar energy is used to capture the CO<sub>2</sub> thereby increasing the conversion of CO to H<sub>2</sub> by means an intensified process. This process shows several advantages:

- The reaction is performed only in a single reactor reducing capital cost;
- WGS kinetics is favoured at high temperature thus avoiding the use of metal catalyst;
- H<sub>2</sub>-rich gas and spent sorbent leave the reactor.

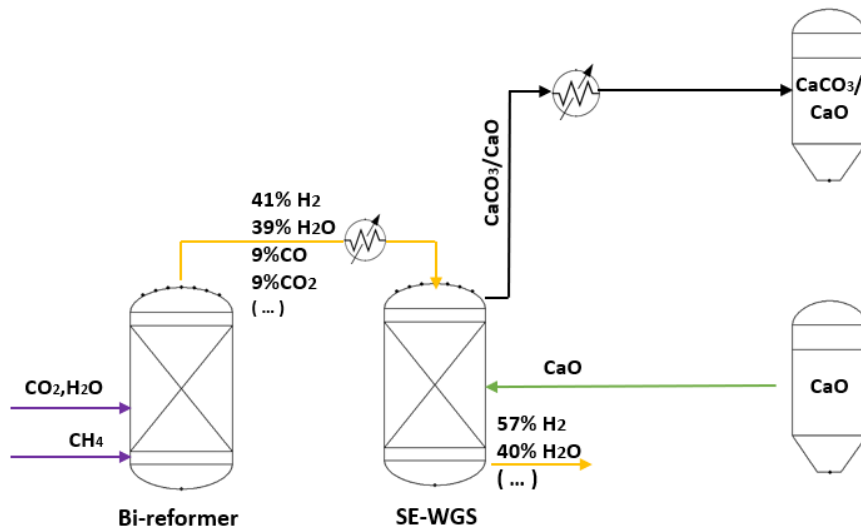


Figure 2.8: Bi reforming and sorption enhanced water gas shift

Methane reforming is enhanced at high temperature and low pressure and therefore Bi-reformer (BMR) is set at 5 bar and 800 °C. The Bi-reformer is a reactor in which the reaction SMR and DMR occur. The heat necessary to drive endothermic reaction between CO<sub>2</sub>, H<sub>2</sub>O and CH<sub>4</sub> is provided by air combustion of methane in a separated combustion chamber. The reformed gas produced in the BMR is cooled and sent into SE-WGS where the CO<sub>2</sub> is captured and the H<sub>2</sub> produced.

The Hydrogen production is enhanced by absorption of CO<sub>2</sub> in situ based on principle of equilibrium mobile of Le Chatelier. Spent materials will be cooled, stored and consecutively regenerated into solar calciner reactor. The SE-WGS operates at 650°C and 5 bar and the heat of reaction can be used to pre-heat the air-combustion.

#### 2.4.2. Carbon capture from flue gas

Another use of the CaL process is the capture of CO<sub>2</sub> from flue gas released from air-blow combustion system. The reaction is as same as 2.1 but the operating condition in which it takes place are different.

The flue gas is produced during the combustion of methane which provide the necessary heat to the BMR above. Part of CO<sub>2</sub> has not been captured and will be released into the atmosphere due to thermodynamic equilibrium.

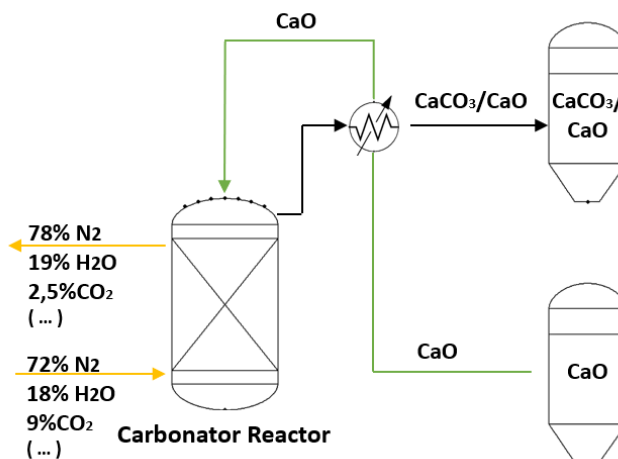


Figure 2.9: Scheme of Calcium Looping process for flue gas decarbonization

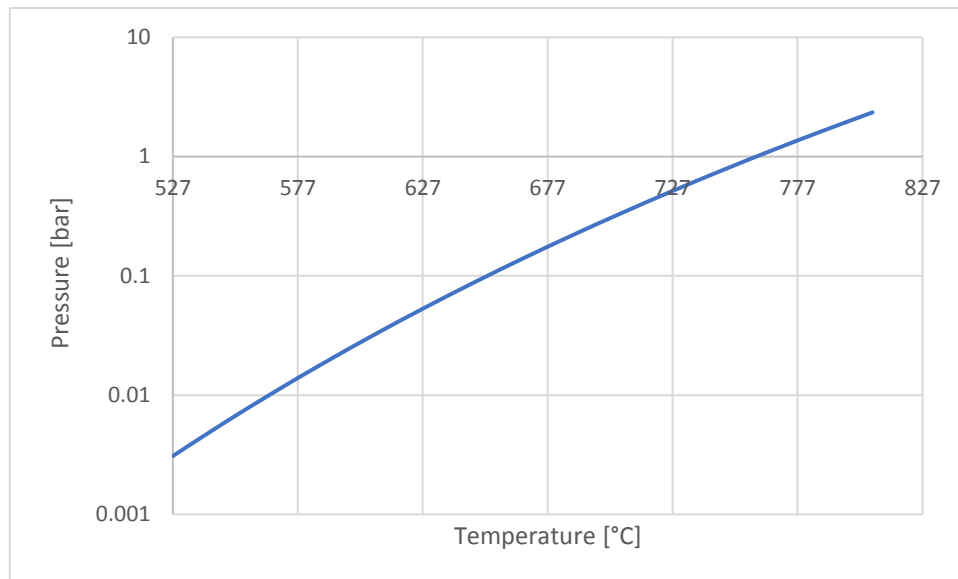


Figure 2.10: Absolute equilibrium pressure of the carbonator reactor with CO<sub>2</sub> molar fraction equal to 0.1

The graph in Fig. 2.10 shows the progress of the equilibrium pressure of the carbonation reactor when the reaction temperature varies. It represents the minimum pressure of the reactor for which the reaction can start at a certain temperature.

Thermodynamically, a further effort to decarbonise could be done by increasing the pressure in the reactor at the expense of the electricity consumption to compress air combustion.

#### 2.4.3. Calcium Looping for power production

The most common energy storage studied in CSP plant are based on molten salts. The mainly components used are nitrates, chlorides, fluorides and carbonates. The fluoride salts have high heat storage capacity but very expansive and toxic [20, 21]; Chloride have an high heat fusion and are very cheaply but highly corrosively [22]; Carbonates have high temperature of phase change but high viscosity and they easy decay [23]; Nitrate salts are low chemical reactivity, low corrosive and have low cost [24] and therefore suitable for thermal storage material in CSP. The issue of these materials is the melting point, in fact also when there is not sun or direct sunlight, the temperature of the storage has to be higher than melting temperature for each salt [25, 26]. The integration between CSP with thermal storage and power cycle is limited by a maximum temperature achievable around 500-600 °C. This limitation is due to degradation of molten salts at high temperature. The coupling of CSP with CaL process avoids this problem reaching temperature higher than 700°C.

During the study of the process coupled to a power cycle, a parametric analysis was performed on the operating parameters of the carbonator. The analysis results in a better efficiency at lower pressure and high temperatures. Therefore, the reactor operates in isothermal conditions at 830 °C and 2 bar. The reactor is fluidized by CO<sub>2</sub> used also as heat transfer fluid.

Starting from CO<sub>2</sub> stored at high pressure, the CO<sub>2</sub> is carried out stoichiometric molar rate. The expansion of stored CO<sub>2</sub> supplies useful electric power via a turbo-expander providing efficient cooling power. Indeed, the expansion from 74 to 2 bar require the use of inter-heating expansion to avoid the condensation of CO<sub>2</sub> and protect the turbine blades.

In the carbonator reactor, under favourable condition, CO<sub>2</sub> and part of CaO react in an exothermic reaction. The heat of reaction is carried out by the heat transfer fluid (Into these reactors the CO<sub>2</sub> is used both fluidised gas and HTF) which will exchange heat with the power cycle fluid used to

generate electricity. The spent solids produced, composed by  $\text{CaCO}_3$  and unreacted  $\text{CaO}$ , are cooled and stored inside silos at ambient condition.

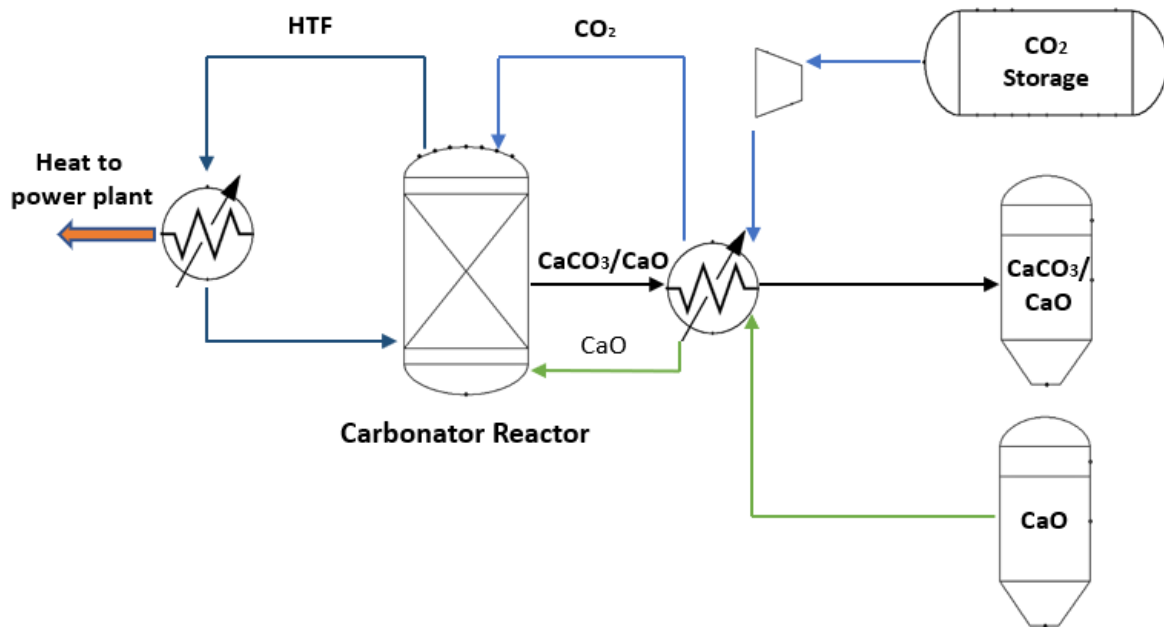


Figure 2.11: Calcium Looping process to power production

## 2.5. Bubbling fluidized bed reactor

The carbonation / calcination processes are usually carried out in a gas-solid fluidized bed reactors. The gas-solid fluidization is an operation in which the solid phase is transformed in a fluid like state through suspension in gas environment. There are several fluidisation regimes with regards to the velocity of the fluid and particles:

- Fixed bed reactor: fluid passes through a bed of fine particles at low flow rate, while particles are stationary;
- Incipiently fluidized bed reactor: at higher velocity of the gas, all particles are suspended. The frictional force between particles and fluid is equal to weight force of the particles.
- Bubbling fluidized bed reactor: at higher flow rate beyond minimum fluidization, the movement of the solid become vigorous forming bubble.
- Turbulent fluidized bed reactor: When fine particles are fluidized at a sufficiently high gas flow rate, instead of bubbles, one observes a turbulent motion of solid clusters and voids of gas of various sizes and shapes.

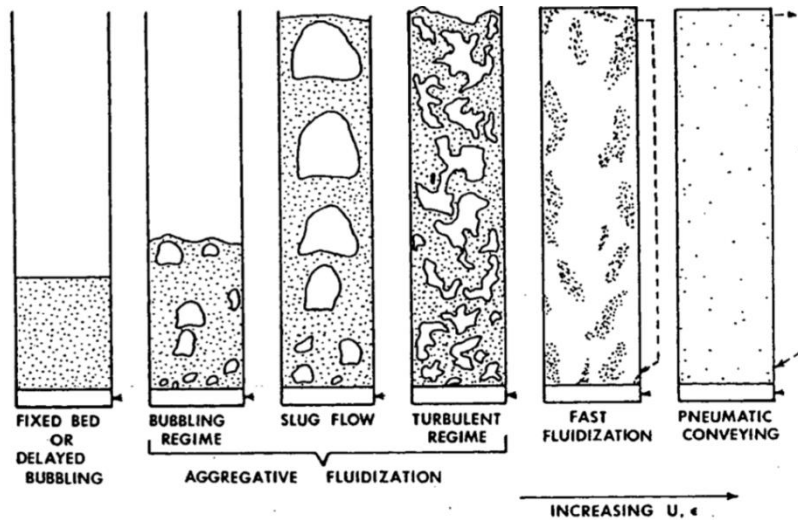


Figure 2.12: Gas-Solid flow regime. Fluidized bed reactor [27]

There are several advantages on the use of fluidized bed for industrial operation:

- The liquid like flow of particles allows a better control operation;
- The rapid mixing of particles allows temperature uniformly in the reactor;
- It is possible remove a large quantity of heat produced in highly exothermic reaction;
- High heat and mass transfer flow rate;

The disadvantages are:

- For bubbling bed, it is difficult to describe the flow of gas;
- Non-uniform residence time of solids into reactor;
- Erosion of pipe and vessel from abrasion by particles;

Each flow regime has unique characteristics that differentiate it from other regimes. Unless special attention is taken, modelling of a reactor within one flow regime should not be extended to another.

## References

- [1] K. West, «ETP 2015: Iron & steel findings,» IEA International Energy Agency, 2015.
- [2] T. Shimizu, et al «A TWIN FLUID-BED REACTOR FOR REMOVAL OF CO<sub>2</sub> FROM COMBUSTION PROCESSES » IChem, 1999.
- [3] B.R. Stanmore and P. Gilot, « Review—calcination and carbonation of limestone during thermal cycling for CO<sub>2</sub> sequestration »,ELSEVIER, 2005
- [4] C. Ortiz, et al;, « Power cycles integration in concentrated solar power plants with energy storage based on calcium looping », ELSEVIER; 2017.
- [5] S. Stendardo, P.U. Foscolo « Carbon dioxide capture with dolomite: A model for gas–solid reaction within the grains of a particulate sorbent » ELSEVIER; 2009
- [6] R. Sun, et al « CO<sub>2</sub> capture performance of calcium-based sorbent doped with manganese salts during calcium looping cycle » ELSEVIER; 2011
- [7] J. M. Valverde« Ca-based synthetic materials with enhanced CO<sub>2</sub> capture efficiency »; Journal of material Chemistry; 2013
- [8] H. Chen, et al; « CO<sub>2</sub> capture and attrition performance of CaO pellets with aluminate cement under pressurized carbonation » ELSEVIER; 2011
- [9] M.Benitez-Guerrero « Multicycle activity of natural CaCO<sub>3</sub> minerals for thermochemical energy storage in Concentrated Solar Power plants» ELSEVIER; 2017
- [10] Antonio Perejón, et al, «The Calcium-Looping technology for CO<sub>2</sub> capture: On the important roles,» *ELSEVIER*, 2015..
- [11] C. Tregambi, et al, « A model of integrated calcium looping for CO<sub>2</sub> capture and concentrated solar power » *ELSEVIER*, 2015.
- [12] J. Strohle, et al, « Carbonate looping experiments in a 1 MWth pilot plant and model Validation » *ELSEVIER*, 2014.
- [13] D.P.Hanak, et al, « A review of developments in pilot-plant testing and modelling of calcium looping process for CO<sub>2</sub> capture from power generation systems» *Energy & Environmental Science*, 2015.
- [14] A. Meier, et al, « Design and experimental investigation of a horizontal rotary reactor for the solar thermal production of lime » *ELSEVIER*, 2004
- [15] A. Meier, et al, « Multitube Rotary Kiln for the Industrial Solar Production of Lime » *Solar Technology Laboratory*
- [16] Arthur Imhof « The cyclone reactor- an atmospheric open solar reactor »; Solar Energy Materiale; 1991
- [17] C. Ho, et al, « Technology advancements for next generation falling particle receivers » *ELSEVIER*, 2013.
- [18] S.K. Dutta « Direct reduction iron; production » ReserchGate, 2009.
- [19] J.R.Nielsen, et al, « Concepts in syngas manufacture », Imperial College Press, 2011
- [20] Christian Le Brun, « Molten salts and nuclear energy production » ELSEVIER, 2007
- [21] M. Fujiwara, et al, « Thermal Analysis and Fundamental Tests on a Heat Pipe Receiver for a Solar Dynamic Space Power System1 » Takasago R&D Center
- [22] M.M. Kenisarin, « High-temperature phase change materials for thermal energy storage» ELSEVIER, 2010

- [23] B.C. Shin « Ternary carbonate eutectic (lithium, sodium and potassium carbonates) for latent heat storage medium » Solar Energy Material; 1990
- [24] M. Kamimoto « INVESTIGATION OF NITRATE SALTS FOR SOLAR LATENT HEAT STORAGE » Solar Energy; 1980
- [25] Q. Peng, et al; « Design of new molten salt thermal energy storage material for solar thermal power plant» ELSEVIER, 2012
- [26] Q. Peng, et al; « The preparation and properties of multi-component molten salts» ELSEVIER, 2009
- [27] Daizo Kunii, et al « Fluidization engineering » Series in Chemical Engineering; 1991

### 3. Implementation of decarbonisation systems to iron and steel industry

One of the important CO<sub>2</sub> emitters is the iron and steel industry responsible for 31% of industry direct anthropogenic emission in 2012 [1]. Therefore, the application of an industrial process to carbon abatement is necessary.

The iron and steel mill investigated in this work is the Midrex process based mill which produces Direct Reduced Iron (DRI) into a shaft furnace. The trend of using alternative technologies compared to the BF/BOF is constantly growing. One of the main processes in the conventional blast furnace (BF) and basic oxygen furnace (BOF) is the production of coke which is a high carbon gas emitting process. The transition from coke to methane is one of the routes for reducing emissions from the steel industry.

Lump iron and/or iron ore and/or scrap are reduced by counter-current reducing gas composed mainly of CO and H<sub>2</sub>. This gas is produced in a reformer reactor in which the methane is reformed to CO and H<sub>2</sub>. The Hot Direct Reduced Iron (HDRI) fed directly an electric arc furnace (EAF) producing liquid iron. Generally, DRI based steel mill produce 1 Mt/year of liquid iron, the largest module can produce up to 1.76Mt/y [2].

In order to meet the environmental directives, the CO<sub>2</sub> emitted by iron industry should be reduced drastically. To achieve this goal:

- Energy efficiency should be improved;
- The consumption of coal and coke should be reduced;
- Biomass, by-product fuel, plastics and renewable energy should be used;

But all these techniques should be complemented by carbon capture and storage (CCS) technologies.

The main sources of CO<sub>2</sub> emissions from the considered process is from the flue gas produced to drive natural gas reformer, the shaft furnace off-gas and EAF off-gas. Part of shaft off-gas are sent into the bi-methane reformer (BMR) where CO and H<sub>2</sub> are produced, re-using the CO<sub>2</sub> produced in the flue gases [2].

The current technology used to capture CO<sub>2</sub> are based on chemical absorption in which the amines are the main solvent used. Another commonly used method is the Pressure Swing Adsorption (PSA) and the Vacuum Pressure Swing Adsorption (VPSA) which works at high pressure to capture CO<sub>2</sub> which is released by reducing the operating pressure.

In this chapter the integration of calcium looping (CaL) technology as pre- and post-combustion CCS is analysed for decarbonisation of iron making process.

The iron mills benchmark was initially analysed and subsequently compared to CaL iron plant at low-carbon emission. In the latter, new processes based on SE-WGS to pre-combustion decarbonisation and CaL to intensify the water gas shift (WGS) reaction with the CO<sub>2</sub> capture via CaL in fluidised bed carbonator reactor. The comparison to the benchmark configuration in terms of CO<sub>2</sub> avoided and energy consumption was performed.

The models are simulated using the software ChemCad 7 capable of easily solving material and energy balances. Chemical components are chosen from the library while the heat capacity of Calcium Carbonate was modified taking into consideration the equation and coefficients from [3]. The equation used by the software to calculate the heat capacity is valid for a limited range of temperature. The Soave-Redlich-Kwong (SRK) model is used for thermodynamic parameters.

### 3.1. Plants layout

Two plants solution were investigated integrating the CaL technology presented in the previous chapter (BMR + SE-WGS in 2.4.1; CO<sub>2</sub> capture in 2.4.2). Hence, the following iron plant design are evaluated in this work:

- Benchmark: conventional iron plant based on Midrex process and EAF;
- Iron IS CaL: iron plant based on Midrex process integrated with SE-WGS reactor and post-combustion capture in a separated reactor and EAF;

It should be noted that the iron plant designed with CO<sub>2</sub> capture system uses the same auxiliary equipment as the conventional reference iron industry.

The main different sections of DRI based process decarbonised with CaL with respect to the benchmark steel mill are:

- SE-WGS reactor is used to capture CO<sub>2</sub> upstream the shaft furnace;
- Carbonator reactor is installed to capture CO<sub>2</sub> from flue gas;
- Seasonal storage of CaO and CO<sub>2</sub>;
- Solar calciner reactor to regenerate spent sorbents;
- Compression unit to efficiently store CO<sub>2</sub> regenerated;

#### 3.1.1. Reference iron plant

DRI production is the second process to iron making and over then 90% is based on natural gas [2]. The DRI technologies operate without the use of coke avoiding the associated CO<sub>2</sub> emission limiting their use only into the EAF. The DRI is produced largely by the Midrex process. The largest module can produce up to 1.76 Mt/y [2] and require high quality of iron ore.

The use of natural gas helps many industries reduce emissions and thus improve the world's air quality. In Midrex the desulphurised natural gas is heated and sent in an external catalytic reformer operated at ~950°C. Natural gas is reformed and consist mainly in hydrogen and carbon monoxide. The Midrex Reformer externally optimizes the Shaft Furnace performance by converting part of recycled gas (from the iron reduction reactions) along with fresh natural gas into H<sub>2</sub> and CO.

The off-gas leaving the shaft furnace is sent back to the BMR where the reaction of SRM (1.7) and DRM (1.8) occur along with the WGS (1.9) reaction.

BMR shows several advantages with respect to conventional reformer [4]:

- Less natural gas is required;
- No steam system is required;
- No CO<sub>2</sub> removal system is required;
- No O<sub>2</sub> required for reforming;

- Hot reducing gas can be directly used into the shaft furnace;

The sensible heat of the flue gas leaving the reformer section is used to preheat the feed gas mixture, the natural gas feed and the burner combustion air. The heat recovery system increases the energy efficiency of Midrex. The remaining part of the off-gas from the shaft furnace provides fuel for the burner in the reformer [5]. Indeed, as described in chapter 1.4, the reactions occurring within the reformer are endothermic. The necessary heat is then supplied by a methane combustor.

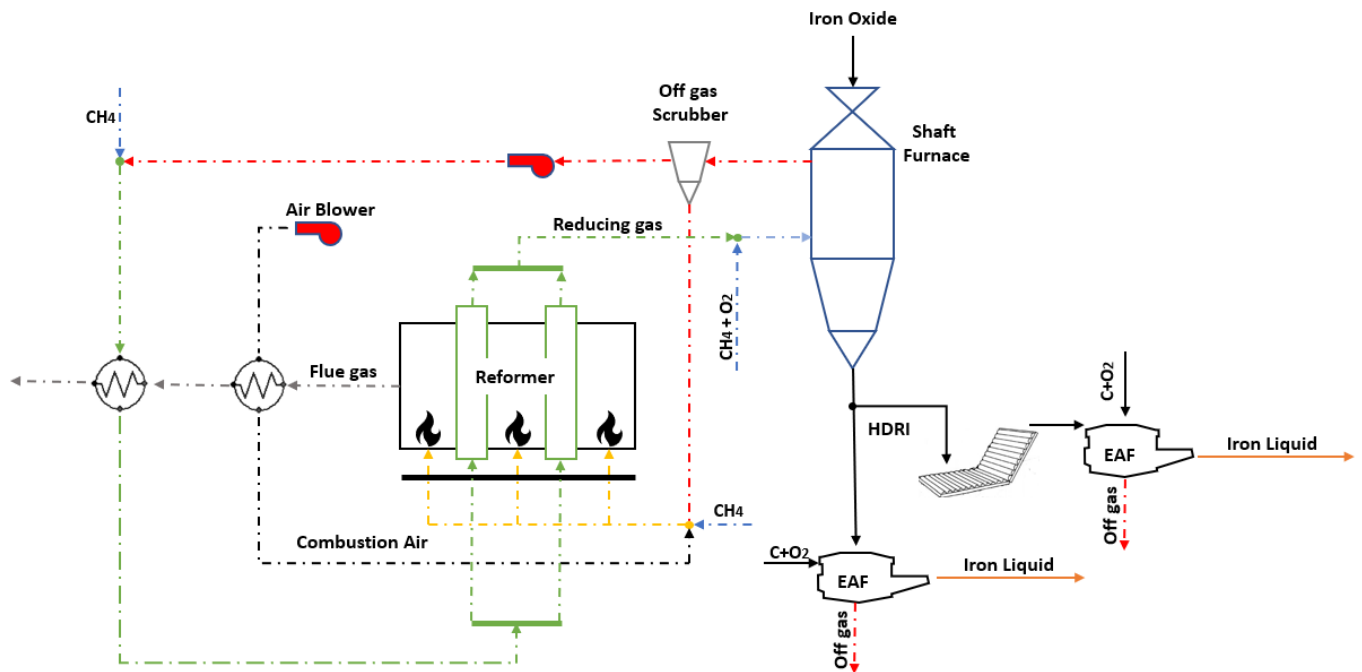


Figure 3.1: Scheme of reference iron and steel plant (Benchmark)

In the shaft furnace process lump iron and/or iron ore are charged into the top of the vertical reactor whereas reducing gas is fed counter-current. Iron oxides react with a hot reducing gas composed of  $H_2$  and  $CO$  largely producing hot metallic iron. This gas reduces iron ore directly in solid state and the gangue remains in solid form. The furnace operates at approximately 0.5 MPa.

The overall reduction reactions are:



The DRI produced contains 91,5% metallic iron, 2,5% carbon and gangue and it is discharged from the furnace at temperature up to 700°C [5]. The HDRI is transported directly into EAF to take advantage of the available sensible heat. Two different process we have considered to feed the HDRI into the furnace [6]:

- Hotlink: Use gravity to feed DRI from the shaft furnace into storage bins located directly above the EAF;
- Hot transport conveyor: Transport HDRI continuously from the shaft furnace to storage bins located directly above the EAF via an inclined bucket conveyor;

The HDRI is charged into the top of the EAF in a discontinuous process. The roof is closed and then carbon electrode are lowered into the furnace. The fusion of materials takes place at 1600°C using an electric arc. Carbon, silicon calcium oxide and other impurities are removed from the iron in a batch process. To reduce electric consumption, usually an additional oxyfuel combustion can happen into the furnace. The molten steel is tapped from the furnace into a ladle and transferred to the ladle furnace where alloys are added to obtain the desired steel properties. The time range of the process from 35 to over 200 minutes according to the quality of the steel produced while the typical capacity is 0.5 to 1 Mt/y. The electricity consumption of EAF is about 365 kWh/t ls using an oxyfuel combustion [2]. The carbon injection is 12 kg/t ls for DRI with 2.2% of carbon content [2]. The loaded coal can be replaced with biomass or other polymers to reduce CO<sub>2</sub> emissions.

The direct CO<sub>2</sub> emitted from EAF is generated during the smelting and refining processes and from the oxyfuel combustion. The off-gas produced is sent to bag-house for removal of particulate and discharged in atmosphere. The indirect CO<sub>2</sub> emission results from the consumption of electricity. The specific emission of CO<sub>2</sub> per MWhe produced in Italy is set at 406 [kg CO<sub>2</sub>/MWhe] [7].

Several techniques can be used to raise the energy efficiency of the system:

- Improve process control;
- Use DC arc furnace instead of AC;
- Oxyfuel burns and oxygen lances;
- Injecting an inert gas as nitrogen or argon to increase heat transfer fluid;
- Inject oxygen above the steel bath in furnace to burn the CO and preheat the next charge;
- Add a sensible heat recovery from the offgas to produce vapour and generate electricity;
- Add a sensible heat recovery from slag but it is not currently practised due to technical and economic reason;

*Table 3.1: Heat recovery for Benchmark plant*

<b>Heat recovery source</b>	<b>Temperature [°C]</b>	<b>Heat recovery strategy</b>
Flue gas from methane reformer	950	Pre-heat combustion air Pre-heat gas to reformer
Offgas from EAF	1600	Steam production for Rankine cycle

### 3.1.2. Integrated solar calcium looping iron plant

To avoid high quantity of carbon dioxide produced into the shaft furnace, H<sub>2</sub>-rich gas is necessary. At the downstream of the BMR, a SE-WGS reactor is added producing a high hydrogen content stream. The heat of reaction released in the BMR is used to pre-heat the air-combustion used by BMR itself.

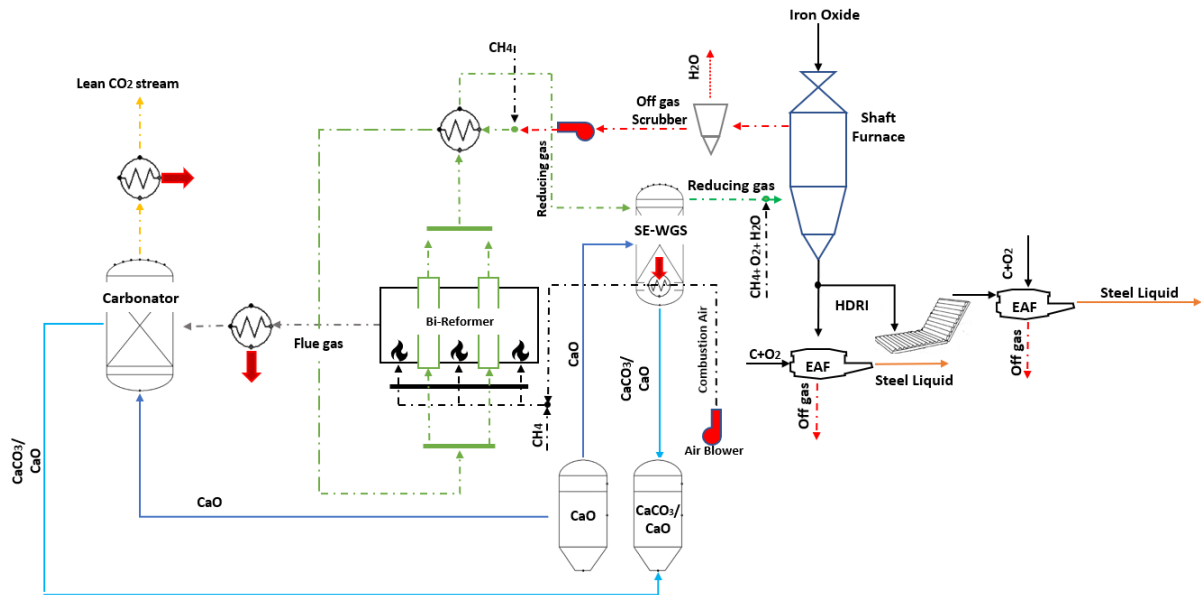


Figure 3.2: Scheme of calcium looping iron plant

The sensible heat of the flue gas released during the combustion can be used to generate electricity (see heat exchanger upstream carbonator in Fig. 3.2). After having released part of their heat, the flue gas is sent to the carbonation reactor where the CO<sub>2</sub> react with calcium oxides producing CaCO<sub>3</sub>. The heat of the carbonation reaction is used to preheat the recycled and dedusted off-gas from shaft furnace. The calcium carbonate and the un-reacted calcium oxide are cooled and conveyed into the silos. The lean CO<sub>2</sub> flue gas are cooled and discharged in atmosphere.

Table 3.2: Heat recovery on CaL Midrex iron plant

Heat source	Temperature [°C]	Heat recovery management
Reformed gas leaving BMR	From 800 to 500	Pre-heat of gas to reformer
Flue gas leaving BMR	From 800 to 300	Steam production for Rankine cycle
Heat produced in Carbonator	650	Pre-heat gas to reformer

Gas and solids from Carbonator	650	Pre-heat stream to Carbonator Steam production for Rankine cycle
Heat produced in SE-WGS	650	Pre-heat air combustion Steam production for Rankine cycle
Off-gas from Shaft furnace	900	Pre-heat reducing gas and mineral iron to Shaft furnace Pre-heat gas to Bi-reformer

### 3.2. Modelling

The commercial software ChemCad™ 7 (CC7) was used for the modelling and simulation of the iron and steel production process with or without calcium looping technology. The CC7 is used to solve mass and energy balances of complex systems and provides with a large database of chemical components and it is specifically designed to simulate chemical reactions. With regards to the iron and steel plant, a steady-state CC7 model was assembled.

Both the iron and steel plant and the CaL unit were simulated by means of several components such as reactors, flow mergers/splitter, heat exchangers. Due to the large amount of sub-processes taking place and to their complexity, some simplifying assumptions had to be made.

Due to the complex reaction into different reactor, it was decided to not model in detail the chemical reactions but to simulate their effects on the gaseous flows inside the reactor

Pre-heating of solid material are supposed to take place in dedicate heat exchangers. A detailed description of these heat exchange is considered outside the scope of this conceptual description of the systems, which involved standard preheating operation of solids typically used in iron and steel plant. Other assumptions are listed below:

- Operation of all components is at steady state;
- The ambient temperature and pressure are constant and equal to 20°C and 1 bar, respectively;
- The pressure losses were neglected in almost all the components with exceptions on Shaft furnace where is considered 1 bar of drop pressure;
- The heat losses in the piping and in the rest of the system were neglected with the exception of the inlet reducing gas into shaft that in benchmark it exits from reformer at 950°C and enters into shaft furnace at 900°C;
- The performance of the main reactors e.g. Bi-reformer, SE-WGS, carbonator, EAF and calciner were represented using the chemical and phase equilibrium through the free energy minimization at the operating temperature;
- A complete calcination of calcium carbonate takes place into solar calciner;

- Minimum temperature difference (pinch temperature) is 20°C for all heat exchangers;
- A natural gas (100% CH<sub>4</sub>) ( $LHV_{\text{methane}} \approx 50 \text{ MJ/kg}$ ) has been selected and it burnt with approximately 20% of air excess.

### 3.2.1. Benchmark configuration

The figure below shows the model of the benchmark steel mill simulated to solve material and energy balances.

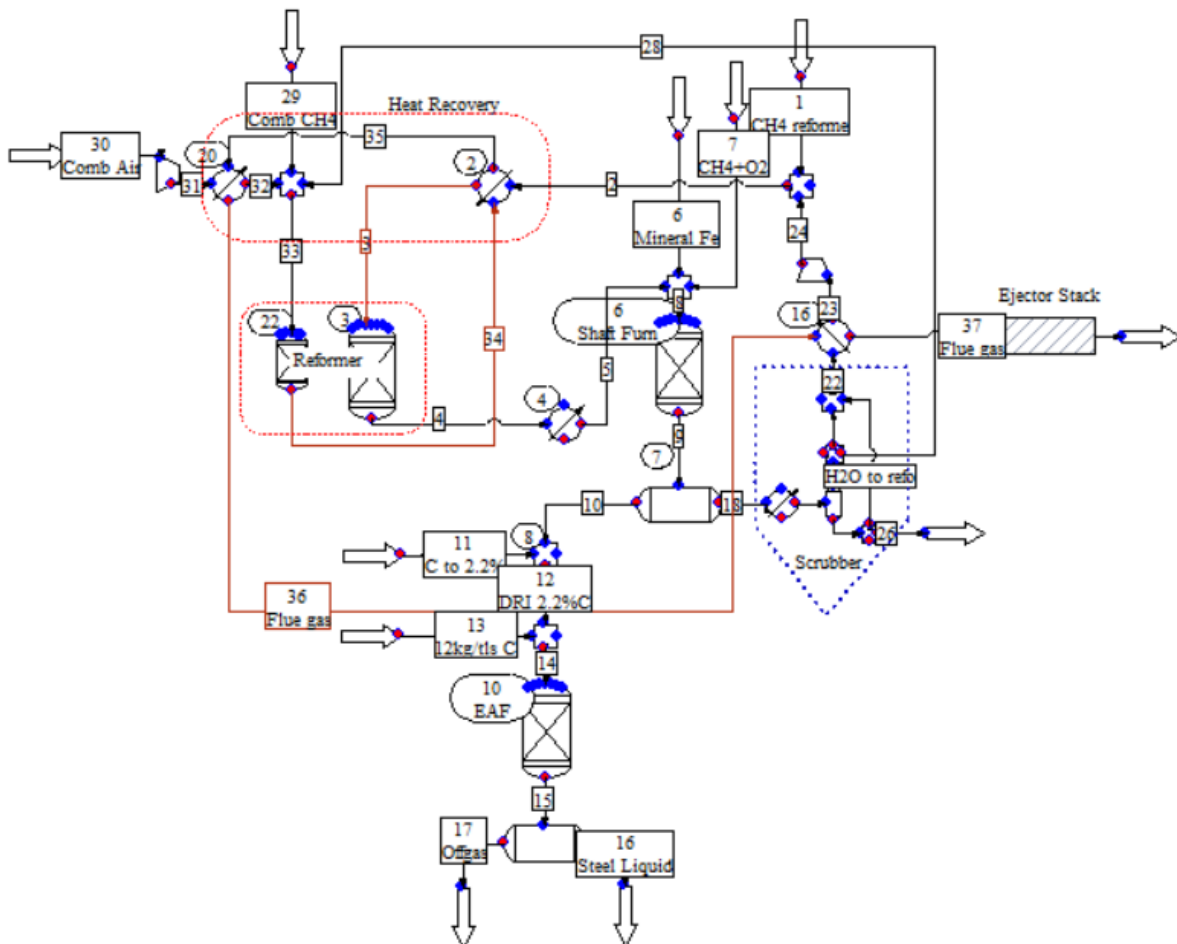


Figure 3.3: CC7 model for iron and steel benchmark plant

### 3.2.2. Integrated solar calcium looping iron plant

Figure 3.4 displays an Integrated Solar Calcium Looping (ISCaL) fitting an iron plant. As for the CaL, it was assumed that the carbonation reaction was formulated in an isothermal GIBBS reactor (a CC7 model based on the free energy minimization).

The thermodynamic equilibrium is supposed to be reached in both SE-WGS and Carbonator reactors: the molar flow of calcium oxide feeding the system was set to capture the CO<sub>2</sub> stream with degree of conversion equal to 0.7. However, the capture efficiency of the carbonator change at every cycle and dynamic analysis should be performed in the next works.

In CC7 the average conversion is considered by introducing a fictitious element with the same chemical property of the CaO but inert in presence of the carbon dioxide and thus does not

produce calcium carbonate. It was introduced in the simulation of the plant in to properly solve the energy balance of the CaL system. It is known that the thermal energy input required by the calciner is mainly due to the decomposition of calcium carbonate. Consequently, the calciner energy consumption is estimated based on the average possible quantities of solids sent into the reactor.

In addition, a complete conversion of  $\text{CaCO}_3$  to  $\text{CaO}$  into the calciner operating at  $900^\circ\text{C}$  has been supposed. The performance of the calciner as well as the carbonator were analysed using the Gibbs free energy minimization model (GIBBS reactor).

The CaL process requires a continuous make-up flow of fresh limestone to counteract the deactivation of lime with the number of carbonation/calcination cycles while a corresponding purge is also extracted from the calciner. The calcined purge is obviously a potential material to be fed to the steel mill plant. Due to the high resistance of the new sorbents at higher number of cycles, a continuous make-up flow is not simulated.

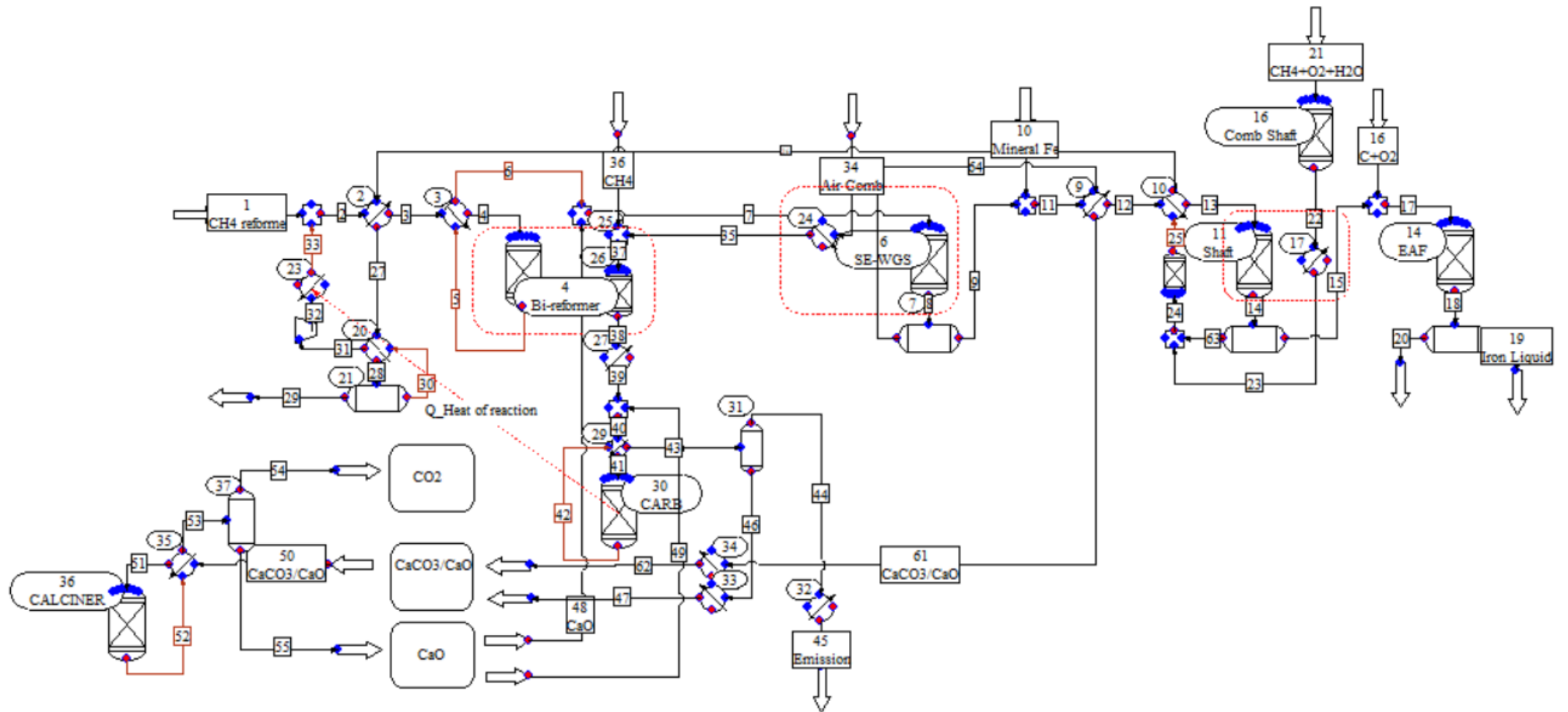


Figure 3.4: ChemCad model of the integrated solar calcium looping in iron and steel industry

It is interesting to observe in detail the balance of mass and energy from the two new components introduced: SE-WGS and carbonator.

### 3.2.3. Material and energy balance of CaL solution

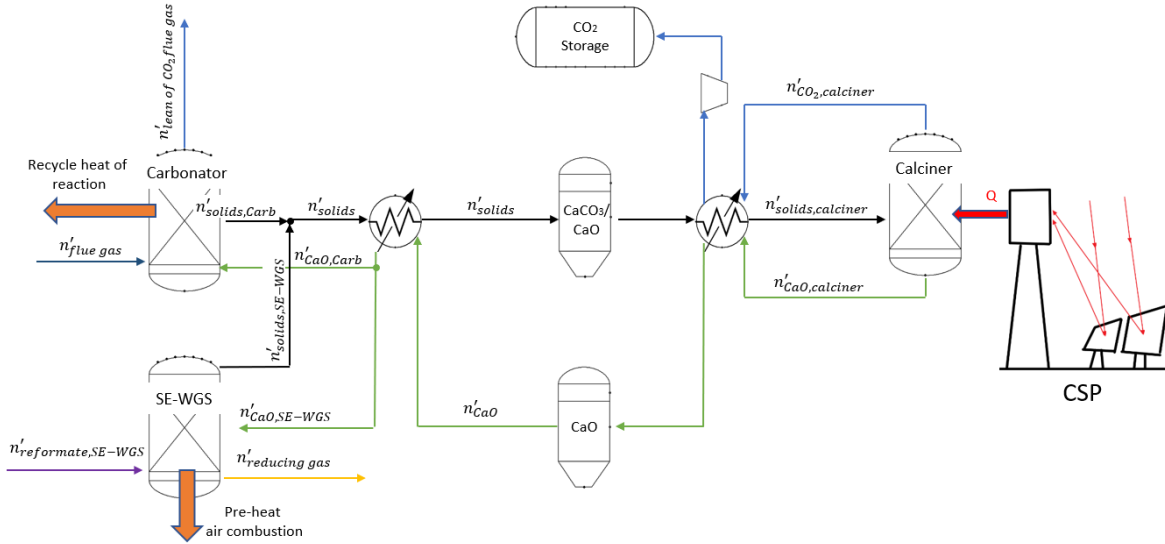


Figure 3.5: Iron and steel industry decarbonisation by CaL process

The CO<sub>2</sub> capture process uses CaO as regenerable sorbent to capture the CO<sub>2</sub> from flue gases and into WGS reactor. In carbonator reactor, CO<sub>2</sub> is captured from combustion flue gas ( $\dot{n}_{flue\ gas}$ ) of a BMR in a bubbling fluidized bed reactor operating at 650°C and 1.2 bar. The solids leaving the carbonator ( $\dot{n}_{solids, Carb}$ ) with a certain conversion of CaO to CaCO<sub>3</sub> are directed to the silos.

$$\dot{n}_{solids} = \dot{n}_{CaO} = \dot{n}_{CaCO_3} + \dot{n}_{CaO, unreact} \quad (3.3)$$

The flue gas ( $\dot{n}_{lean\ of\ CO_2\ flue\ gas}$ ) come out from the reactor lean of CO<sub>2</sub> at the reactor condition. Because of the thermodynamic conditions and the low partial pressure of the CO<sub>2</sub> of the starting flue gas, not all the carbon dioxide can be captured.

At the same time, in order to enhance the water gas shift reaction, calcium oxide ( $\dot{n}_{CaO, SE-WGS}$ ) from the silos enters the SE-WGS reactor. In this reactor chemical reactions 2.7 and 2.8 occur simultaneously and according to the principle of Le Chatelier hydrogen production increases. Only part of CaO reacts with CO<sub>2</sub> from  $\dot{n}_{reformate, SE-WGS}$  and from the WGS reaction, due to both thermodynamic condition and degree of conversion of CaO. The solids ( $\dot{n}_{solids, SE-WGS}$ ) leaving the SE-WGS reactor are cooled and sent to the silos.

During the capture of carbon dioxide into the reactor, the heat of carbonation reaction is released.

It is possible to write  $\dot{n}_{i, in}$  and  $\dot{n}_{i, out}$  the molar rate that came in and come out respectively from one of two Calciner and carbonator reactors, and to define the extent of reaction as:

$$\varepsilon = \frac{\dot{n}_{i, out} - \dot{n}_{i, in}}{\nu_i} \quad (3.4)$$

where  $\nu_i$  is the stoichiometric coefficients the molar rate reacted is written as:

$$\dot{n}_{i,out} - \dot{n}_{i,in} = \varepsilon \nu_i \quad (3.5)$$

Arranging the first law of thermodynamic and considering that the out flow is at the same condition of the reactor, the heat released during several reaction is:

$$\varepsilon \Delta H_{react}(T_{react}) + \sum \dot{n}_{i,in}(h_{i,react} - h_{i,in}) = \sum \Phi_j - W \quad (3.6)$$

Where:

- $\Delta H_{react}$ : Heat of reaction [kJ/kmol];
- $T_{react}$ : Temperature in which reaction occur [°K];
- $h_{i,react}$ : Enthalpy of the compound i, at the out of the reactor [kJ/kmol];
- $h_{i,in}$ : Enthalpy of the compound i, at the inlet of the reactor [kJ/kmol];
- $\Phi_j$ : Heat flux from or to the reactor [kW];
- $W$ : Mechanical or electrical power [kW];
- $c_{p,i}$ : specific heat capacity [kJ/kmol K];

With the heat of reaction defined as:

$$\Delta H_{react}(T_{react}) = \Delta H^{\circ}_{react} + \sum_i \nu_i \cdot \int_{T_{ref}}^{T_{react}} c_{p,i}(T) dT \quad (3.7)$$

The stream at the inlet and outlet of the two reactors, considering the model in Fig 3.4 are summarized in the following table

Table 3.3: Stream property and composition at the inlet and outlet of the two interesting reactors per 1 t/h of DRI produced

System	# of stream	Mass flow rate [kg/h]	Molar flow eate [kmol/h]	Temperature [°C]	Pressure [bar]	Average mol wt	y H2	y CH4
In Carbonator	41	872,4	28,9	630	1,2	30,2	0	0
		y H2O	y CaCO3	y CaO	y CO	y CO2	y O2	y N2
		0,16	0	0,0865	0	0,079	0,016	0,66
System	# of stream	Mass flow rate [kg/h]	Molar flow eate [kmol/h]	Temperature [°C]	Pressure [bar]	Average mol wt	y H2	y CH4
Out Carbonator	42	872,4	27,2	650	1,2	32	0	0
		y H2O	y CaCO3	y CaO	y CO	y CO2	y O2	y N2
		0,17	0,061	0,03	0	0,02	0,016	0,7
System	# of stream	Mass flow rate [kg/h]	Molar flow eate [kmol/h]	Temperature [°C]	Pressure [bar]	Average mol wt	y H2	y CH4
In SE-WGS	7	1511,2	66,5	409	5	22,7	0,336	0,002
		y H2O	y CaCO3	y CaO	y CO	y CO2	y O2	y N2
		0,32	0	0,2	0,07	0,07	0	0
System	# of stream	Mass flow rate [kg/h]	Molar flow eate [kmol/h]	Temperature [°C]	Pressure [bar]	Average mol wt	y H2	y CH4
Out SE-WGS	8	1511	56,6	650	5	26,7	0,434	0,013
		y H2O	y CaCO3	y CaO	y CO	y CO2	y O2	y N2
		0,31	0,15	0,075	0,003	0,004	0	0

The solids accumulated in the storage site, when there is availability of solar energy, ( $\dot{n}_{solids,calciner}$ ) are directed to the solar calciner where regeneration of the sorbent takes place. The size of the storage sizing was evaluated according to the different operational time of the two reactors described above and calciner reactor. The ISCal iron and steel plant operates for all day, while 8 hours is the daylight time settled. Thus, the follow molar-balance equation has to be satisfied:

$$\int_{24h} \dot{n}_{solids}(t) dt = \int_{24h} \dot{n}_{CaO_{calciner}}(t) dt \quad (3.8)$$

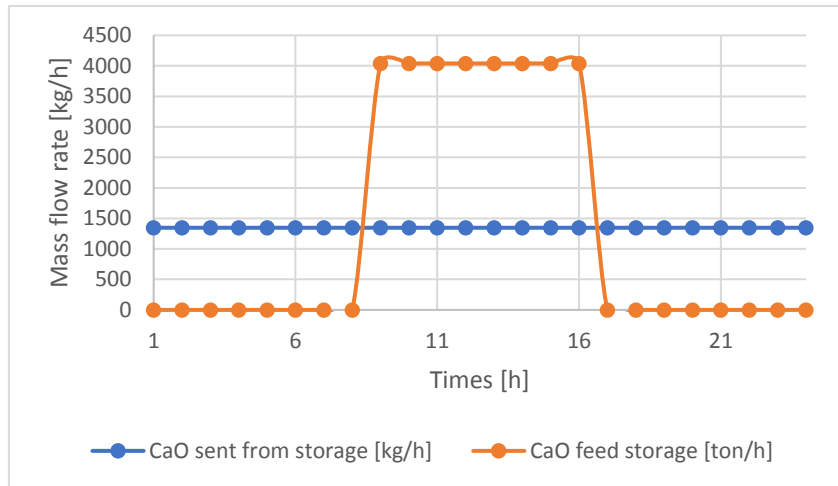


Figure 3.6: Mass flow rate of Calcium oxide to iron plant in blue and from calciner in red

### 3.3. Energy assessment

In this section an analysis of two different plants (Benchmark and IS Cal iron plant) is carried out by solving the material and energy balances. As benchmark case, a conventional iron and steel Midrex plant without carbon capture was considered to assess the energy penalty involved by the carbon capture feature.

CO<sub>2</sub> emitted for power production depends on the energy mix used in the country based on the different ratios of thermal, nuclear and renewable power generation accounted. To calculate the total CO<sub>2</sub> specific emissions relating to the power import/export, the average emission factor for the Italian thermoelectric park was considered: 406 kg CO<sub>2</sub>/MWh [7].

The two type of plants have been designed to produce 100 t/h and about 0.87 Mt/y. No changes in the operating conditions and reaction atmosphere are envisaged with respect to the standard operation of the Midrex process in the state of the art of the commercial solutions. The shaft furnace and EAF work at (900°C, 5 bar) and (1600°C, 1 bar) respectively. The electricity consumption in EAF is the same for both models while the heat provides at the shaft furnace change due to different inlet streams.

As it was summarized in table 3.2, the heat provided by flue gas from reformer, gas and solid at exit of carbonator reactor, and the heat of reaction from SE-WGS reactor is used to generate electricity in a Rankin cycle.

The electric power consumed in a modern steel plant with EAF is assumed equal to 0.575 MWhe/t ls as reported in [8],

Four main factors have been considered to compute the electricity consumption in CO<sub>2</sub> capture plant:

- The electricity demand of the conventional EAF;
- the electricity demand to CO<sub>2</sub> compression;
- The energy penalty of the air separation unit (ASU: 160 kWh/t O<sub>2</sub>[9]);
- The electricity consumed by the new auxiliary equipment (2% of the generated gross power [10]);

To compute thermal consumption of the plant it is necessary to consider the heat provides by the fuel combustion of methane (LHV: 50 MJ/kg) and anthracite (LHV: 29 MJ/kg) and the heat provide by the CSP plant to regenerate sorbent (thermal efficiency: 41%). All the assumption used in this chapter are summarized in the following table.

Table 3.4: Assumption adopted for the calculation of the environmental and energetic performances

<b>Electricity demand from EAF</b>	[MWhe/t ls]	0,575
<b>Energy penalty to Air Separation Unit</b>	[kWhe/t O <sub>2</sub> ]	160
<b>Electricity consumed by auxiliary equipment</b>	[% og generated gros power]	2
<b>Emission factor</b>	[kg CO <sub>2</sub> /Mwhe]	406
<b>LHV of anthracite</b>	[MJ/kg]	29
<b>LHV of methane</b>	[MJ/kg]	50
<b>Steam cycle efficiency</b>	[%]	33
<b>Thermodynamic efficiency of Concentrated Solar Power</b>	[%]	41
<b>Italian electric park efficiency</b>	[%]	40,2

#### Reference iron and steel plant

Manufacturing steel is an energy and carbon-intensive and therefore one of the major contributors to global anthropogenic CO<sub>2</sub> emissions. The reference iron and steel industry consume about 17 GJ/t liquid steel (ls): 64% to produce DRI (i.e. reformer and shaft furnace), while about the remaining part is consumed into the EAF. From the total energy required, 11.3 GJ/t ls is supplied via fossil fuel and 5.7 GJ/t ls in electricity form used for around 90% into EAF.

#### Integrated solar calcium looping iron and steel plant

Due to the SE-WGS reactor, about 40 kg /t ls of methane was saved, and heat at 650°C was also produced. The additional heat at 650°C is also produced inside the carbonator reactor in which the CO<sub>2</sub> contained in the combustion fumes is captured. These two processes involve the conversion of CaO into calcium carbonate. One of the most studied methods for calcium oxide regeneration is oxy-Cal process where methane is combusted with oxygen.

In the proposed plant the oxy-Cal is replaced with a solar calciner. The saving of methane is therefore due to the use of solar energy to regenerate the sorbents exhausted. A thermodynamic efficiency of 41% is considered [11] for CSP which operates at 900°C. Calcium carbonate produced into decarbonised iron and steel plant during the day is stored at ambient temperature. The calcination of the material happens only 8/24h per day.

The energy consumed by the decarbonised industrial system rises to about 20 GJ/t ls, of which more than 20% is used for the regeneration of the material. The energy consumed into EAF is as the same as the benchmark configuration (5 GJ/t ls) while that consumed during the production of reducing gas is decreased by about 2 GJ/t ls due to less consumption of methane during the process. The electricity consumption increases to 0.5 GJ/t ls due to the high compression of CO<sub>2</sub> regenerated.

It is possible to recover up to 2 GJ of heat from the processes described in Table 3.2. The SE-WGS reactor, the flue gas and the solids at the carbonator outlet provide approximately 0.7 GJ, 0.45 GJ and 0.4 GJ respectively. The rest comes from the post capture fumes and from the off-gases of the electric arc furnace.

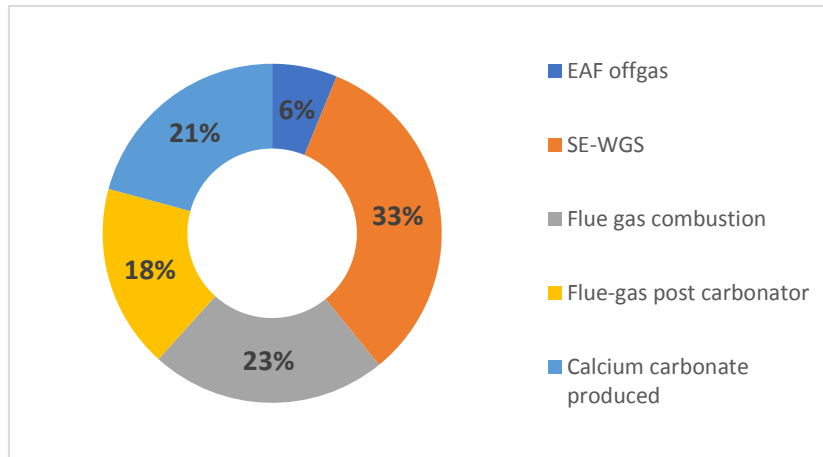


Figure 3.7: Heat recovery in integrates solar CaL Iron and Steel plant

The electricity consumed into the plant is about 0.66 MWhe/t ls and we can generate from the heat recovery into Rankine cycle with 33% efficiency until 0.18 MWhe/t ls.

The comparison between the energy requirements of the two plants is shown in the following two graphs. The comparison is based on HR (heat requirements), that is the heat requirements of the processes considered in terms of primary energy. Conversion of electrical energy into thermal energy is instead carried out considering an average efficiency of the Italian electric park equal to 39.5% at December 2017 [12].

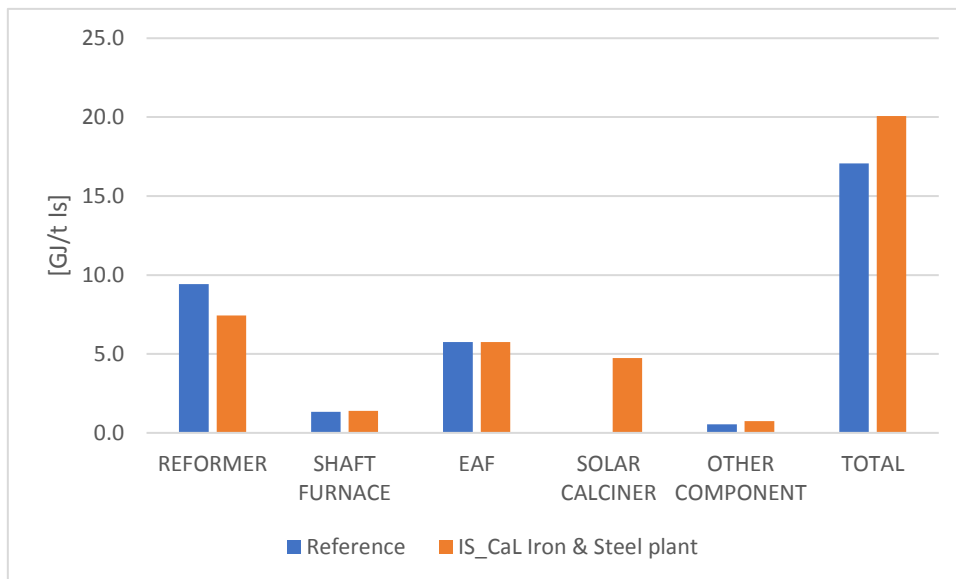


Figure 3.8: Thermal energy requirement for both plants considered

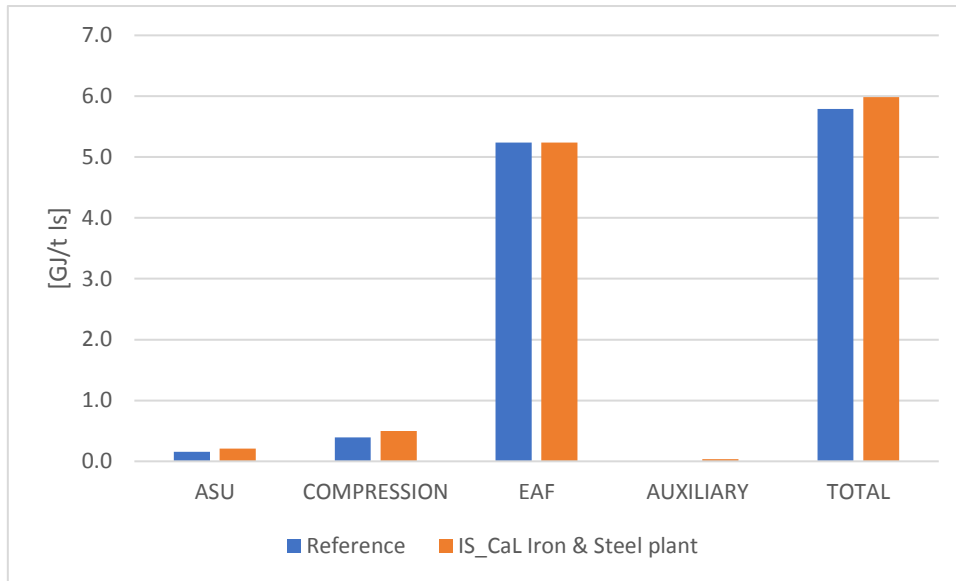


Figure 3.9: Heat requirement due to electricity consumption for both plants

### 3.4. Avoided emissions and environmental performance

The CO<sub>2</sub> is emitted in several processes in iron and steel industry, including:

- Direct emission from combustion of conventional fuels on-site;
- Direct emission from industrial process (non-energy process);
- Indirect emissions from electricity consumption

In 2005, the iron and steel industry released 1.99 Gt of CO<sub>2</sub>, whilst producing 1144 Mt of steel [2].

The reference steel mill that uses the Midrex-NG technology combined with EAF emits about 0.9 t CO<sub>2</sub>/t ls of which 30% due to electricity consumption.

The new concept of iron and steel plant proposed reduce drastically the direct CO<sub>2</sub> emission of 85%, while a reduction of 26% of indirect emission is obtained due to the in-situ production of electricity from thermal waste.

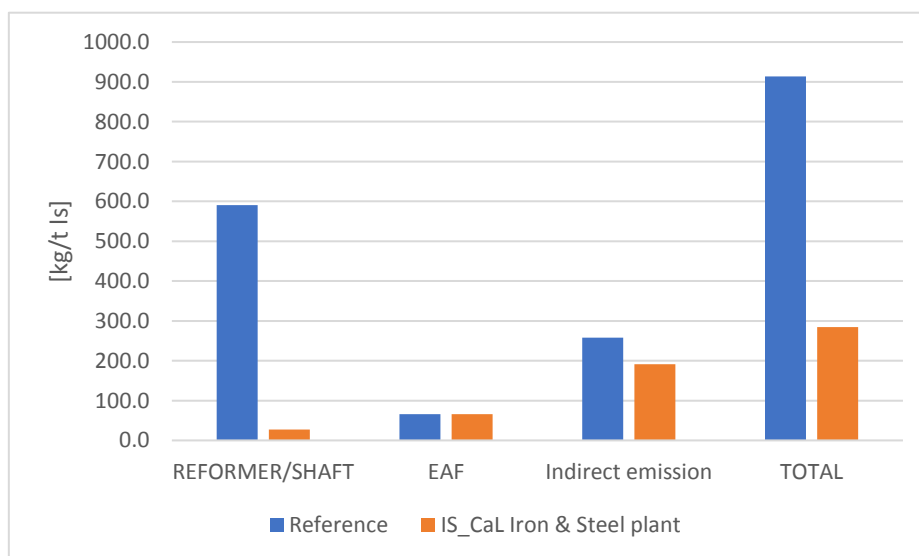


Figure 3.10: Direct and indirect CO<sub>2</sub> emission for both plants considered

From the figure above, almost all CO<sub>2</sub> emitted during the DRI production process is captured. A further reduction of direct emissions could be achieved in the EAF avoiding the use of conventional

fuels. Another share of CO<sub>2</sub> is instead produced by the oxidation of the carbon electrodes of the arc furnace and cannot be avoided. The equivalent CO<sub>2</sub> emission is reduced by 68%.

As it can be seen, the share of emissions due to electricity consumption is significant. The design and installation of a renewable power plant that directly assists the industrial site could be a sustainable solution.

### 3.5. SPECCA AND SPECCA\*

An important parameter for the evaluation of energy penalty is the SPECCA (Specific Primary Energy Consumption for CO<sub>2</sub> avoided) index [12] defined as:

$$SPECCA = \frac{HR - HR_{ref}}{e_{ref} - e} \left[ \frac{GJ}{t_{CO_2}} \right] \quad (3.9)$$

For the calculation of this parameter the following parameters are required:

- Difference heat requirement in terms of fossil fuels between with and without CCS plant;
- Difference CO<sub>2</sub> emission between with and without CCS plant;

The HR represents the primary energy input provided to the system per unit of liquid steel necessary in form of heat or electricity (17 GJ/t ls for the benchmark and 20 GJ/t ls for integrated solar CaL iron and steel plant).

The denominator instead represents the net emission avoided in atmosphere expressed in tCO<sub>2</sub>/t ls. Usually only the direct CO<sub>2</sub> emission is considered. In order to take into consideration, the power produced in the decarbonised plant and the abatement of the indirect CO<sub>2</sub> emission, a new definition of SPECCA is introduced:

$$SPECCA^* = \frac{HR^* - HR_{ref}^*}{e_{ref}^* - e^*} \left[ \frac{GJ}{t_{CO_2}} \right] \quad (3.10)$$

Where:

- HR\* is the new heat requirement calculated as the difference of the total primary energy consumption and the heat recovered to generate electricity in Rankine cycle;
- $$HR^* = HR_{fuel} - HR_{NEP} \quad (3.11)$$
- HR<sub>fuel</sub> is the total primary energy consumption;
  - HR<sub>NEP</sub> is the net electricity produced by the plant. The electricity consumed and produced are both divided by Italian park electric efficiency (39.5%) to obtain a primary energy;
  - e\* represent the equivalent CO<sub>2</sub> emission calculated as the sum of direct and indirect emission;

The values of the SPECCA and SPECCA\* are reported below.

Table 3.5: Comparison between the two plants considered in terms of energy consumption and CO2 emission

Parameter	Unit	Reference	IS_CaL Iron & Steel plant
<b>HRfuel (Total fuel consumption)</b>	[GJ/t ls]	11,28	14,08
<b>HRec (Electricity Consumed)</b>	[GJ/t ls]	5,79	5,98
<b>HRep (Electricity Produced)</b>	[GJ/t ls]	0,00	-1,69
<b>HR</b>	[GJ/t ls]	17,07	20,07
<b>HR*</b>	[GJ/t ls]	17,07	18,37
<b>Direct CO2emissions</b>	[t CO2/t ls]	0,66	0,09
<b>Indirect CO2 emissions</b>	[t CO2/t ls]	0,26	0,19
<b>Equivalent CO2 emissions</b>	[t CO2/t ls]	0,91	0,28
<b>CO2 avoided</b>	-		0,63
<b>CO2 captured</b>	-		0,46
<b>Direct emission reduction</b>	[%]		86%
<b>Eq. CO2 emission reduction</b>	[%]		69%
<b>SPECCA</b>	[GJ/t CO2]		<b>5,32</b>
<b>SPECCA*</b>	[GJ/t CO2]		<b>2,07</b>

With the new formulation, the SPECCA (2.01 GJ/ t CO2] has a value that is certainly more comparable than the previous one and can certainly compete with the reference industries. above all considering that these 2 GJ/t ls will come from solar sources and not from the combustion of fossil fuels.

## References

- [1] B.R. Stanmore and P. Gilot, « Review—calcination and carbonation of limestone during thermal cycling for CO<sub>2</sub> sequestration », ELSEVIER, 2005
- [2] A. Carpenter, «CO<sub>2</sub> abatement in the iron and steel industry,» IEA: International Energy Agency, 2012
- [3] R.Perry and D. Green; « Perry's chemical engineers' handbook »; McGraw-Hill Book Company; 1984
- [4] Midrex Technology Inc , «The Midrex Process,» technical paper, 2019
- [5] S.K. Dutta « Direct reduction iron; production » ReserchGate, 2009.
- [6] R. Cheeley, et al; « Coal gasification based DRI solution for Indian ironmaking »; International Steel Seminar and exhibition; Kolkata; 2010
- [7] <https://www.sunearthtools.com/it/tools/CO2-emissions-calculator.php> (data from International Energy Agency, IEA, 2010)
- [8] A. Otto, et al; « Integration of Renewable Energy and Hydrogen into the German Steel Industry »energies; 2017
- [9] Sandeep Alavandi, et al, «Emerging and Existing Oxygen Production Technology Scan and Evaluation », 2018
- [10] M. Homberger, et al; « Calcium looping for CO<sub>2</sub> capture in cement plants – pilot scale test »; ELSEVIER; 2017
- [11] M. Binotti, et al; « Preliminary assessment of sCO<sub>2</sub> power cycles for application to CSP Solar Tower plants »; ELSEVIER; 2017
- [12] X. Zhu, et al; « Integrated gasification combined cycle with carbon dioxide capture by elevated temperature pressure swing adsorption »; ELSEVIER; 2016

## 4. Implementation of a storage system and Rankine power production in IS-CaL

A climate change represents a critical issue for all people in the world and now it is time to intensify our efforts to counter it. Power production emits the two-thirds of all green-house gas emission and almost the 80% of CO<sub>2</sub> produced in the world. It is necessary to improve renewable energy technology which produces heat or power avoiding CO<sub>2</sub> emissions [1].

As mentioned in the inductor chapter, the renewable energy share will go up and concentrated solar power will have an important role. Concentrated solar power depends on the availability of direct sunlight: storage system and more widely flexibility needs to be improved in order to increase the energy production capacity and correct the mismatch between the discontinuous renewable energy supply and demand.

The Calcium Looping storage system is studied in this Thesis. It uses the heat at temperature above 900°C obtained from CSP to drive the calcination endothermic reaction producing CaO and CO<sub>2</sub>. When energy is needed, the separately stored products (i.e. CaO and CO<sub>2</sub>) are sent into the carbonator reactor for the reverse exothermic reaction (i.e. carbonation), which releases the heat of reaction to power production.

The main drawback is the deactivation of the sorbent during the different cycle of CO<sub>2</sub> capture. However, accordingly to recently thermogravimetric analysis, a high chemical stability is obtained with CaO-based aluminate materials [2]. These considerations justify the use of this process reducing the material that will be sent to landfill.

In this chapter a detailed analysis of the CSP-CaL-Power system integration is carried out. A reheat power Rankine cycle plant according to the ENEL standard for 320 MW groups is modelled. It was considered that the heat requirement from the plants was provided only by the storage system.

### 4.1. Integrated Solar Calcium Looping

In this section the main aspects of the CSP-CaL process integration is described. Fig 4.1 shows a schematic representation of the CSP-CaL integration for thermo-chemical energy storage. The main concept is to separate the energy storage and power generation. The energy storage takes place into calcination reactor in which decomposition of CaCO<sub>3</sub> into CaO and CO<sub>2</sub> occurs at high temperature by solar energy.

The solar radiance coming from the field of the heliostats are concentrated in a single point of the reactor by means of a secondary receiver. The two products of calcination reaction (CO<sub>2</sub> and CaO) are cooled and stored. The CO<sub>2</sub> is stored at 74 bar and the heat collected by the cooling system of the compression is used to feed a district heating network.

Inside each individual intercooler water enters at 60°C and exits at 90°C at a pressure of 4 bar. Subsequently it is pumped up to 10.3 bar and sent to the district heating network as is common to do [3]. Thanks to the use of heat at low temperatures, high performance can be achieved with greater efficiency than simply cooling CO<sub>2</sub> leaving the calciner. The greater the CO<sub>2</sub> flow rate to compress and cool, the more power it is possible to send to the district heating network. This network is discontinued and works only during the charge of storage.

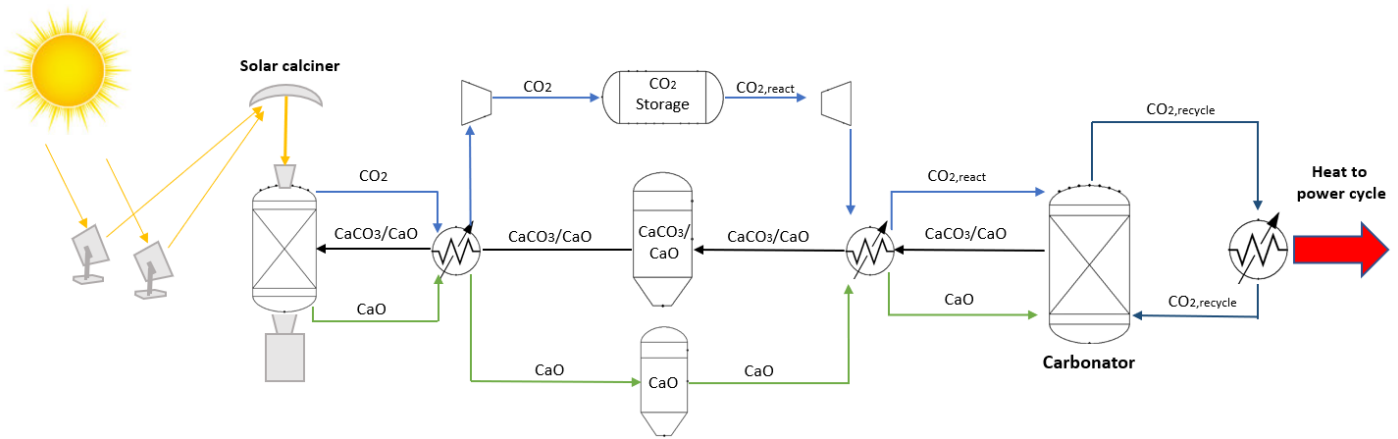


Figure 4.1: Integrated solar CaL for power production

From CO<sub>2</sub> storage is existing the molar rate that will react with calcium oxide into carbonator reactor. The expansion of previously stored CO<sub>2</sub> supplies useful work and provide efficiently cooling power. In fact, the expansion from 74 to 2 bar require the use of inter-heating expansion to avoid the condensation of CO<sub>2</sub> and protect the turbine blades. This heating system provides water at 6 °C and the same return into inter-heating at 12 °C.

During heat release, CO<sub>2</sub> expanded before, CaO from reservoir and the CO<sub>2</sub> used as heat transfer fluid are heated and then come into carbonator reactor where the realise of energy can occurs. Under favourable conditions in the carbonator, CO<sub>2</sub> and part of CaO react in an exothermic reaction and the heat produced at higher temperature, to increase the efficiency of the power cycle, is used to increase the temperature of the heat transfer fluid. The solids stream composed of CaCO<sub>3</sub> and un-reacted CaO, is cooled and stored inside tank almost at ambient condition.

The carbonator reactor is connected to power cycles indirectly by CO<sub>2</sub> which acts both as fluidising agent and heat transfer fluid. This means that increasing the carbonator pressure, it does not take advantage of the possible expansion of the CO<sub>2, recirculate</sub> in the turbine to protect it. Therefore, the graph in Fig 4.2 shows how the efficiency of the storage system is reduced with higher pressure. Instead, increasing the carbonator temperature, leads to higher power cycle efficiency.

$$\eta_{Storage} = \frac{\text{Heat to power cycle}}{\text{Heat to regenerate sorbent}} \quad (4.1)$$

In calculating the efficiency of the storage system, the thermal and optical efficiencies of the CSP were not considered.

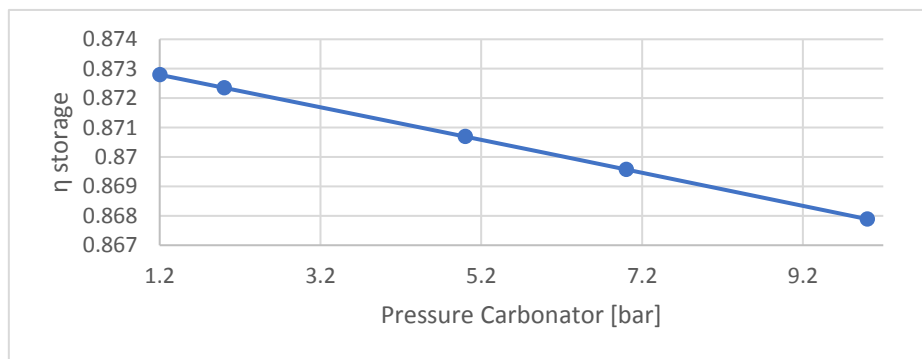


Figure 4.2: Efficiency of the storage system at several carbonator pressure

The pressure of the carbonator reactor is set a 2 bar to overcome the pressure drops in the reactor and in the various heat exchangers.

Both carbonator and calciner reactor work under an atmosphere composed only of CO<sub>2</sub>, on the contrary, while carbonator reactor is a pressurized fluidized bed that work at 2 bar, the calciner reactor operate at atmospheric pressure. Thermodynamic condition of the two reactors are limited by the thermodynamic equilibrium. Thus, for a given CO<sub>2</sub> partial pressure, into both reactor, there is a maximum carbonator temperature above which carbonation reaction cannot occurs and a minimum calcinations temperature under which regeneration of CaCO<sub>3</sub> cannot happen. A typical expression of CO<sub>2</sub> molar fraction uses the equilibrium decomposition pressure see before at Eq. 2.3 over the carbonator or calciner pressure:

$$y_{eq} = \frac{P_{eq}}{P} = \frac{\left(4.137 \cdot 10^7 \exp\left(-\frac{20474}{T}\right)\right)}{P} \quad (4.2)$$

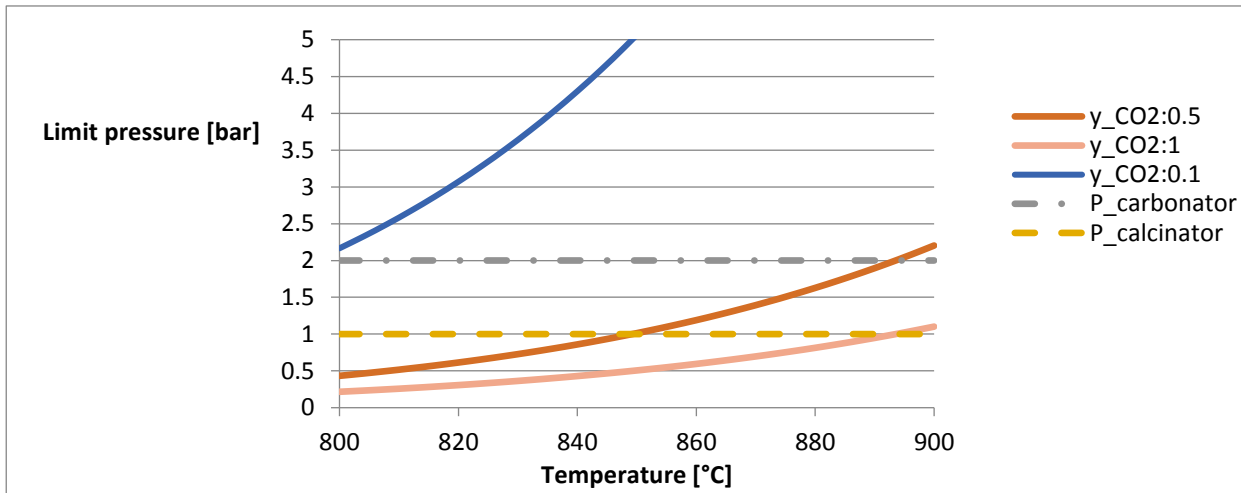


Figure 4.3: Equilibrium condition at vary CO<sub>2</sub> molar fraction

#### 4.1.1. Balance equation

The fig 4.4 illustrates the molar streams scheme in CaL storage. Into carbonator reactor, a carbonation reaction at high temperature and 2 bar occurs. Here the CO<sub>2</sub> that coming out from pressurize storage ( $\dot{n}_{CO_2 r,carb}$ ) react with the CaO ( $\dot{n}_{CaO_{carb}}$ ). Into the reactor flow also CO<sub>2</sub> as heat transfer fluid ( $\dot{n}_{CO_2_{HTF}}$ ) that not participate at the reaction. Calcium oxide not react all with the CO<sub>2</sub> due to loss of reactivity during different cycles and depending on the thermodynamic condition and residence time. Thus only part of the CaO react to produce CaCO<sub>3</sub> ( $\dot{n}_{CaCO_3_{carb}}$ ) and therefore solids ( $\dot{n}_{solids_{carb}}$ ) at the carbonator outlet consist in CaCO<sub>3</sub> and unreacted CaO ( $\dot{n}_{CaO_{un-reacted}}$ ). In the model they are considered as two different streams but, in reality, consists of partially carbonated particles in which a core of unreacted CaO is surrounded by a layer of CaCO<sub>3</sub> [4].

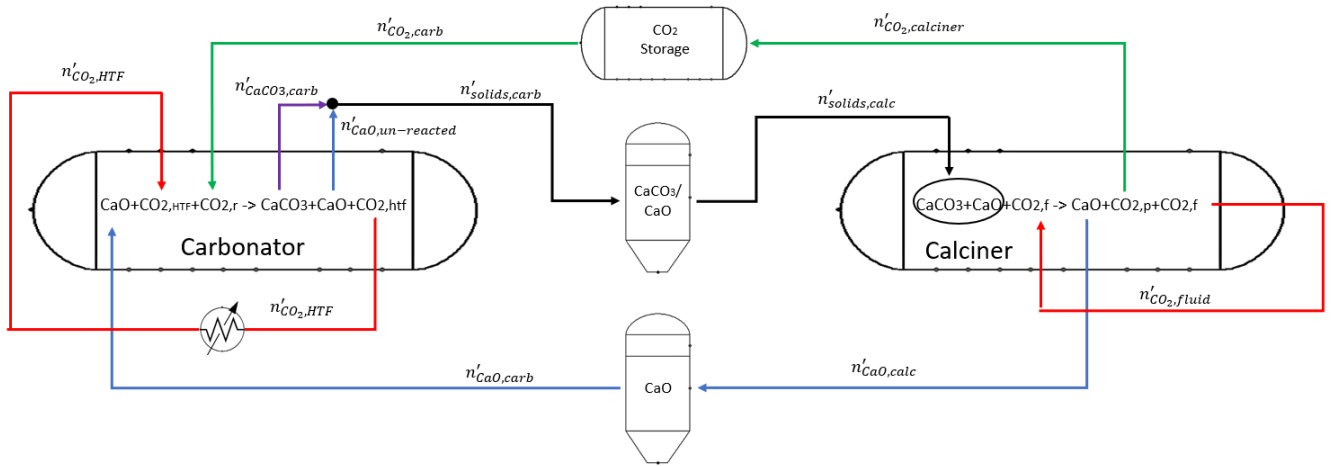


Figure 4.4: Molar balance of storage system

On the other side, the  $\text{CaCO}_3$  phase contained in the solids stream ( $\dot{n}_{\text{solids,calc}}$ ) entering the calciner will be completely regenerated to produce calcium oxide ( $\dot{n}_{\text{CaO,calc}}$ ) and carbon dioxide ( $\dot{n}_{\text{CO}_2,calc}$ ) that will be compressed and stored.

One of the most important parameters for this technology is the average CaO conversion ( $X$ ) useful to quantify the amount of CaO converted to  $\text{CaCO}_3$  during carbonation reaction. This reaction extent is defined as follows:

$$X = \frac{\dot{n}_{\text{CaCO}_3 \text{ carb}}}{\dot{n}_{\text{CaO carb}}} \quad (4.3)$$

In order to guarantee a steady state condition during the storage and release of energy, the solid material regenerated into calciner reactor has to be enough to produce the required heat during carbonation. In fact, the carbonator has to release the required energy for all day long whereas the calciner is able to regenerate the solid material for eight hours approximately. As a consequence, an adequate storage volume is required to store solids (i.e CaO and  $\text{CaCO}_3$ ) and  $\text{CO}_2$  to continuously feed carbonator during the energy demand. Thus, the follow molar-balance equation has to be satisfied:

$$\int_{24 \text{ h}} \dot{n}_{\text{CaCO}_3 \text{ carb}}(t) dt = \int_{24 \text{ h}} \dot{n}_{\text{CaO calc}}(t) dt \quad (4.4)$$

The left-hand side represent the mole of  $\text{CaCO}_3$  producing into the carbonator reactor during the day. This term has to be equal to the mole of CaO regenerated into the calciner.

As for the energy balance, the same equations applied to chapter 3.2.2.1 can be considered. Energy balance is explained in the following figure.

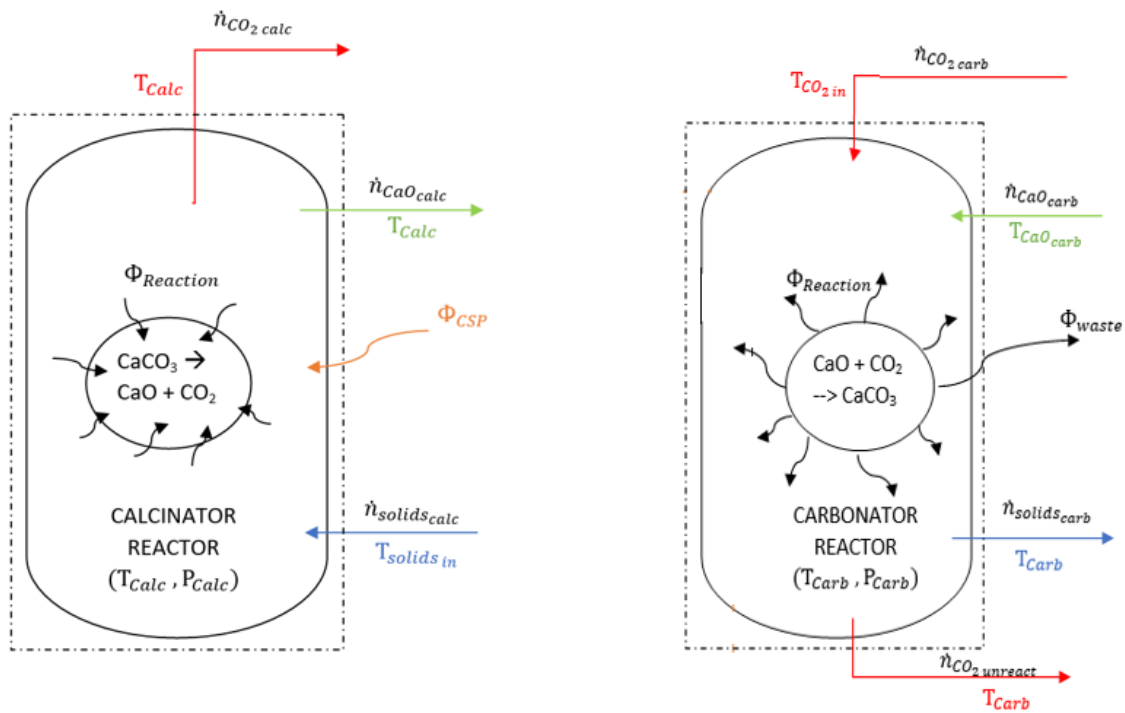


Figure 4.5: Energy balance of storage system into the two critical reactors

## 4.2. Rankine power cycle

A reheat power Rankine cycle plant with seven extraction streams according to the ENEL standard for 320 MW groups with 43.7% efficiency is used to produce electricity. Within the power plant, 1023.3 tonne per hour of water circulates, which must be heated by the heat transfer fluid leaving the carbonator. Turbine and pump efficiencies values of 83% have been considered as well as a heat exchangers minimum temperature difference of 20°C. On the other hand, non-pressure drops are assumed.

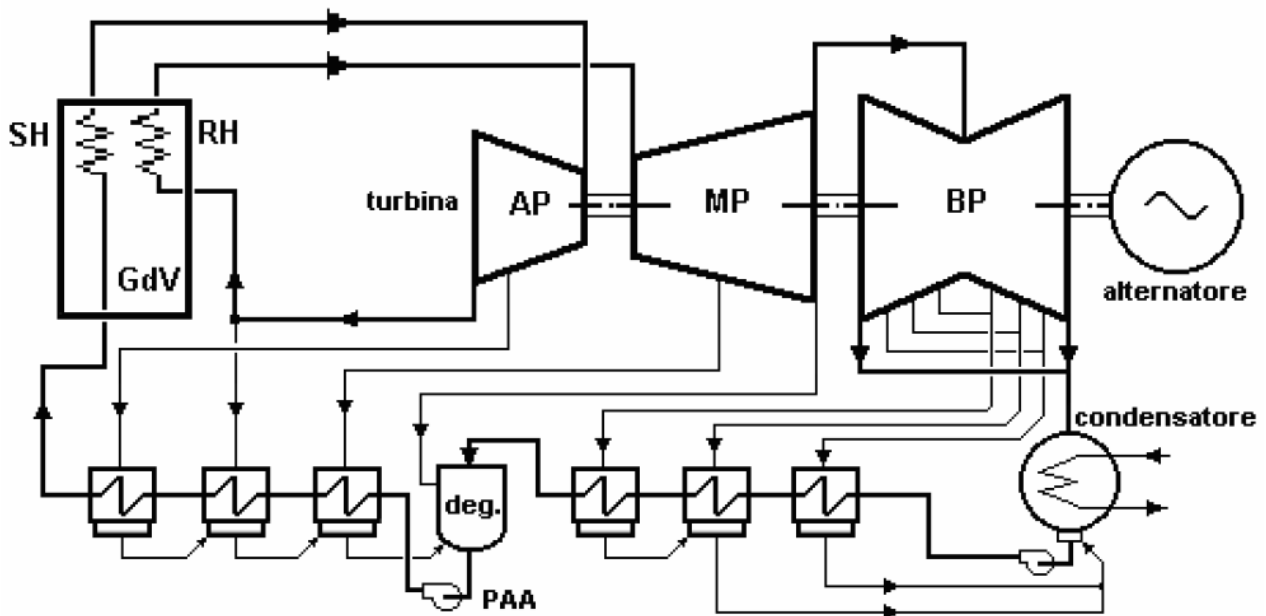


Figure 4.6: Scheme of reheat Rankine cycle plant with 7 streams extraction for 320 MW

The discharge of water condensation (drains) from the recovery heaters (showed in fig. 4.6) is carried out in cascade, i.e. the drains of the higher tapping pressure heater will discharge into the immediately lower pressure heater. This process continues until the last drain is recovered.

For a given power rate, with the increase of steam extraction, the water steam produced in the boiler and used as working fluid will increase.

Nevertheless, the heat required by the boiler goes down due to the greater water inlet temperature..

With regards to the turbine, the several spills have the advantage of reducing the steam flow rate in the last stages. Indeed, for constructive reasons, it is difficult to dispose of large vapor capacities in the last stages (blades of considerable length, subject to high centrifugal forces). Furthermore, the greater flow rate in the high-pressure stages allows the use of efficiency rotor blades of greater dimensions.

The plant considered was designed in the 1960s in order to increase the efficiency of the Rankine cycle by increasing pressures and temperatures. The HP turbine of the investigated Rankine cycle plant operates at a pressure of 165 bar and super-heated and re-super-heated temperature of 538°C.

In Italy, these plants represent the bas-load for power production, some of these are located in coastal areas fed by coal. The plants located in the internal areas are generally built for operation with oil fuel that with natural gas. Fuel oil is supplied by pipelines or by tankers or rail tankers. Natural gas is supplied through methane pipelines. In this paper, the only case of operation with the CaL technology was analysed.

The main circuits of a Rankine power cycle are the following:

- Condensate-admission circuit;
- Water-steam circuit in the boiler;
- Condenser water circuit;
- Heat transfer fluid circuit;
- Reactants-solids product circuit;

In the **condensate-admission circuit**, the water is extracted from the condenser hot well by means of the condensed extraction pumps (PEC) and, after passing through the treatment plant, increases its temperature in the low-pressure heaters (HLP). It takes place to the degasser and from there, taken from the admission water pumps, it goes through the high-pressure heaters (HHP) and enters the new vapour generate.

In the boiler **water-steam circuit**, the temperature of the feed water at the outlet of high-pressure heaters is fixed at 266°C and passes first through the economizer in which it is heated up until 350°C. The pre-heated water feed the wall evaporator into the bubbling fluidised bed reactor (Carbonator) in which the heat of reaction provides the heat required to evaporate the inlet water. At the evaporator outlet the steam overheats to 538°C in the superheaters. The superheated steam exits the steam generator and is sent to the high-pressure turbine, where a first expansion takes place from 170 to 37.7 bar. Subsequently the steam, which has decreased its pressure and temperature, returns to the boiler to re-heat itself to 538°C. The steam re-heated by the boiler returns to the turbine to expand into the remaining medium and low-pressure turbine reaching the pressure of 0.05 bar. At the end of the expansion the steam is discharged into the condenser, where it condenses by exchanging heat with the condenser water and accumulates in the liquid state in the hot well. Part of the steam generated is sent at the heat recovery and it not expand in each turbine.

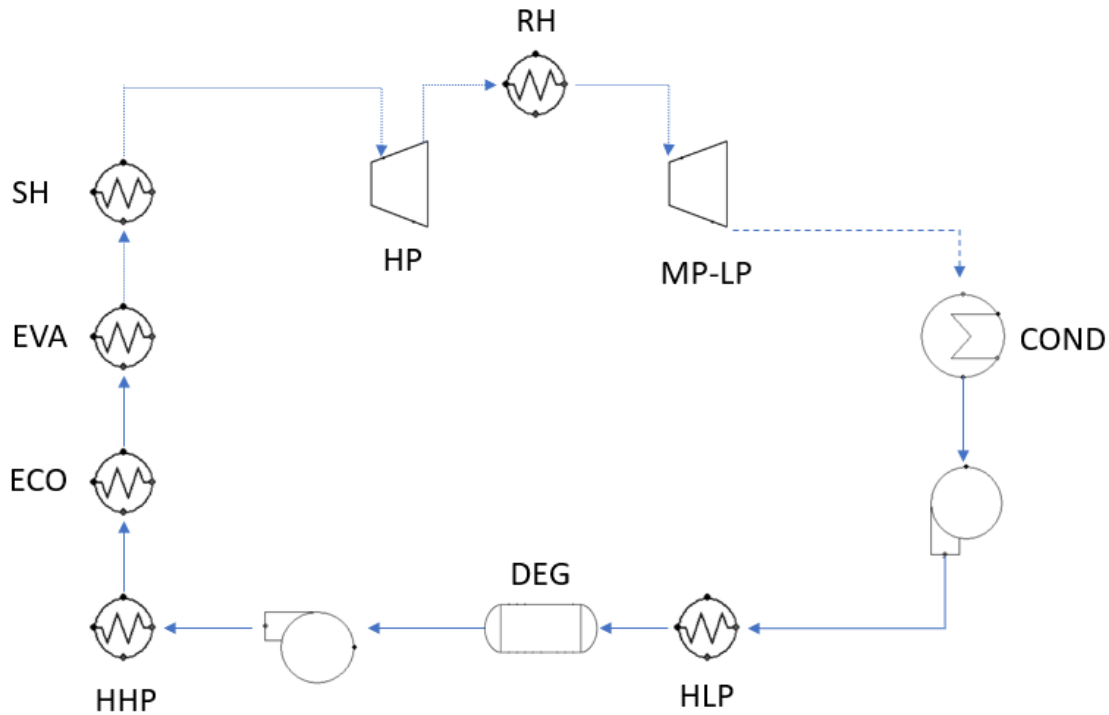


Figure 4.7: Condensate-steam circuit of the Rankine power cycle. Whole line indicates the liquid. Line with dots indicate only vapor. Line mixed indicate the bi-phase fluid.

The **circuit of the condensing water**, open cycle with river or sea water, includes the intake work with the fixed and rotating grids, the condenser water pumps, the pipes up to the condenser inlet, the pipes from the outlet of the condenser up to the discharge work. In the case of a closed cycle, when enough quantities of water are not available, cooling towers are used which transfer the condensation heat of the steam discharged into the condenser to the air.

The **heat transfer fluid circuit** start in the pre-heater in which it is heated by the product of the reaction that occur in the carbonator reactor. The preheating of the fluid at the inlet of the reactor allows a reduction in the consumption of the stored materials and a more homogeneous temperature inside the fluidized bed reactor. The  $\text{CO}_2$  used as HTF transfer the heat of exothermic reaction. The reaction occurs at  $830^\circ\text{C}$  and the reactor have to be cooled. The same technology of combustion chamber can be adopted in which a bi-phase water receives the heat flowing through walls membranate. The outlet  $\text{CO}_2$  is sent subsequently at the pre-heat of the HTF, super-heater, re-heater and economizer. The HTF flows through a closed cycle and then returns to the pre-heater. It operates at 2 bar to overcome eventually pressure lost.

The conventional thermoelectric plants emit the product of combustion in the atmosphere and heat the sea or river water used for the condensation of the steam at the outlet of the low-pressure turbine. Concerning the atmosphere pollution, the most harmful emission are sulphur dioxide and nitrogen oxides which they have to be avoided using electrostatic precipitators or through a desulphurisation of the fuel combustion. However, the flue gas is composed mainly of carbon dioxide that cause a temperature increase of the world.

To safeguard the environment a reconversion of this power plant is necessary and, in this work, an integration with CaL and CSP is analysed.

#### 4.2.1. Rankine Power cycle integrated CaL technology

The use of the calcium looping integrated in a CSP (ISCaL) allows storing the excesses of renewable energy by producing chemical compounds. An indirect coupling of CaL to a Rankine cycle for generating power was analysed. As it was previously stated, the size of the modelled Rankine cycle is 320 MW working for 24 hours a day. Thermochemical storage must provide the necessary reagents so that the exothermic reaction supplies the heat requirement to the steam.

The heat is mainly supplied in four components (see fig. 4.8):

- Water evaporation occurs inside the water-tube walls (EVA) that absorb part of the heat of reaction;
- At the exit of fluidized bed, the CO<sub>2</sub> used as a heat transfer fluid (HTF) enters the superheater (SH), heating the steam at high pressure up to 538°C;
- then it enters the re-heater (RH), heating the medium pressure steam (about 37 bar) up to 538°C;
- Finally, the CO<sub>2</sub>-HTF enters the economizer, heating the liquid water up to approximately 270 °C coming back to the carbonator;

Fig 4.8 illustrates the integration between the two systems.

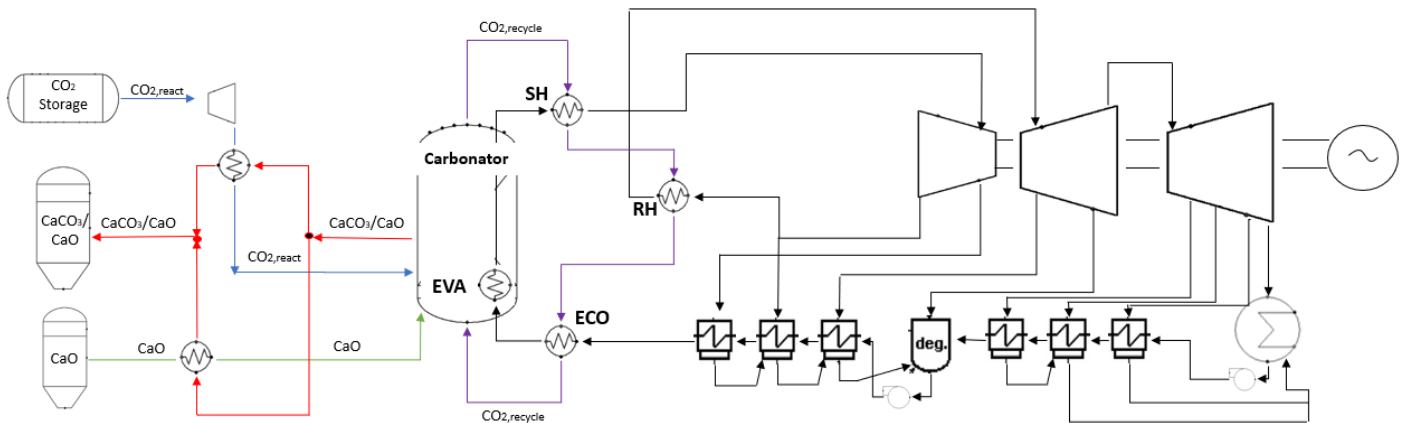


Figure 4.8: Rankine Power cycle integrated with Solare Calcium Looping

To optimize the network of heat exchangers, a pinch analysis of the storage system integrated with the Rankine cycle is performed.

#### 4.2.2. Pinch analysis: design with minimal energy requirements.

Pinch analysis is a useful technique to optimise the heat exchanged in energy systems minimising external supply of heat and cold. The easiest and often most expensive way is to use external hot or cold resources. The most efficient way is to couple the different fluids through heat exchangers where simultaneous heating and cooling among the streams happens. To achieve this purpose, it is necessary to provide a heat recovery system thus building a network of heat exchangers. However, this analysis must always take into account the constraint of the second law of thermodynamics, while the difference in temperature between the cold and hot fluids must be sufficiently high to not result in excessive heat exchange surfaces.

The analysis will be carried out separately for the two sides of the storage system (i.e heat storage side and heat release side). The two parts communicate only through the storage area to be able to separate not only temporally but also physically the storage (calciner) from the release (carbonator) of energy.

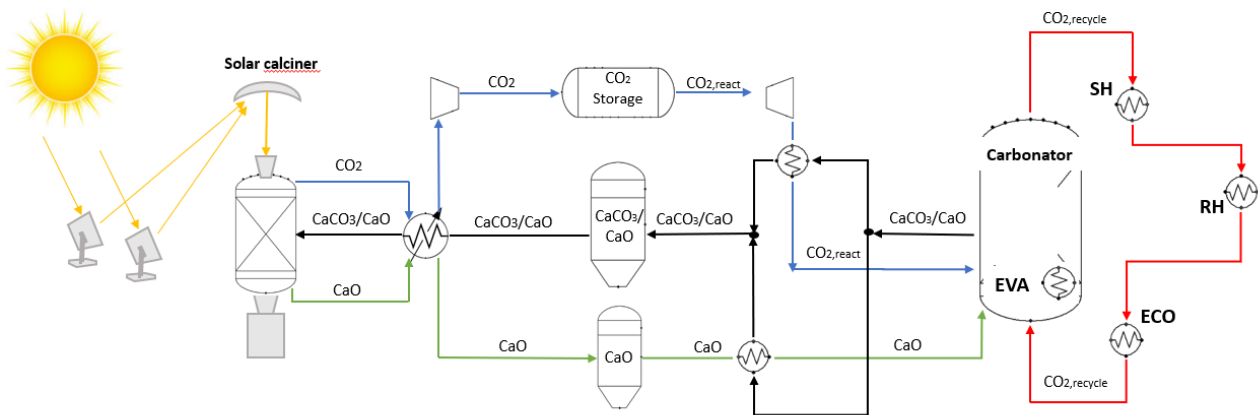


Figure 4.9: Part of plant subject to the Pinch analysis

#### 4.2.2.1. Pinch analysis of calciner side

The pinch analysis will be used for the optimal synthesis of the heat exchanger network with the aim of minimizing the energy requirement with external resources.

##### Identification and characterization of flows

The first step of the analysis consists in identifying the components of the system and the related entering or exiting fluids.

In the case of energy storage, the system is composed of the reactor itself in which the calcination reaction occurs and the CO<sub>2</sub> compression system. Although the latter consists of five compressors with the relative intercooler that exchange heat with water that supplies a district heating network, the compressor area is represented in fig 4.9 as a single component in which CO<sub>2</sub> enters at ambient pressure and exits at supercritical conditions.

As a consequence, four fluids are identified (see fig. 4.9), three of which are hot streams ((i) CO<sub>2</sub> leaving the calciner; (ii) CO<sub>2</sub> leaving the compressor; (iii) CaO leaving the calciner) and one cold stream (solids stream entering the calciner). Details of these streams are reported in table 4.1. The only cold fluid is made up of solids (i.e. X CaCO<sub>3</sub> and (1-X) CaO) that will be sent into the calciner in which complete regeneration of the sorbent takes place. The hot fluids are the low-pressure carbon dioxide emitted from the reactor, the regenerated calcium oxide leaving the reactor and finally the high-pressure carbon dioxide coming out of the compression train respectively. A fixed value of CaO conversion (X=0.7) has been employed.

Table 4.1: Stream identification in Calciner side

# of stream pynch	# of stream	Component	Type of stream	T <sub>in</sub> [°C]	T <sub>out</sub> [°C]	Mass rate [kg/s]	G x cp [MW/K]	Power Heat [MW]
1	97	Solids	COLD	20	900	1540,4	1,78	-1566,5
2	110	CO <sub>2</sub>	HOT	900	20	594,13	0,66	582,4
3	122	CO <sub>2</sub>	HOT	70	20	594,13	2,67	133,4
4	108	CaO	HOT	900	20	946,3	0,88	770,6

##### Definition of constraints and boundary conditions

Before performing the pinch analysis, it is necessary to define the technical constraints and the boundary conditions.

The constraints to be respected are:

- Temperature of hot fluids have to be higher than cold fluids
- In each coupling of hot and cold fluids, a minimum temperature difference of 20 ° C must be respected
- the temperature of the CO<sub>2</sub> at the compression train inlet must be as low as possible to reduce the compression work

The boundary conditions are:

- The ambient temperature is 20 ° C
- The reactor is at a temperature of 900 ° C and ambient pressure
- The containers are all at ambient temperature
- The carbon dioxide at the exit of the compression train will be about 74 bar and 70°C

Calculation of energy requirements

At the beginning of this methodology it is necessary to determine the external maximum heat and cold requirements obtained.

Then the minimum requirements will be calculated starting from the composite curves, obtained separately for the cold and hot fluids.

Initially both curves are started at zero abscissa. For the constraint of the second law, The cold fluids curve (blue line reported in fig. 4.10) must always be below that of the hot fluids (red line reported in fig. 4.10) . To make the result acceptable, the cold fluid curve is translated horizontally until the difference of minimum temperature is 20 °C.

Between the two dashed lines reported in fig. 4.10 (area (B)), the available thermal flow of the hot fluids can be transferred to heat the cold fluids. In the right-hand section (area (C)), the thermal requirement of the cold fluids will be provided by an external resource, while in the left-hand section (area (A)) the heat contained by the hot fluids cannot be recovered and will be transferred to the environment. Finally, the point at which there is the minimum difference in temperature is the pinch point. The proposed heat exchanger network (HEN) is showed in fig. 4.11. As you can see, in this case incoming stream (CaCO<sub>3</sub>) into calciner reached a temperature of 767 °C due to the HEN. The remaining sensible energy to heat the spent solids up to 900 °C is provided by the heat exchanger H1 which represents part of the energy gathered by CSP. The remaining energy necessary to drive the calcination and decompose CaCO<sub>3</sub> into the respective CaO and CO<sub>2</sub> will be provided by the CSP.

Fluid coupling and representation of the exchanger network

The network heat exchangers have been designed following the basic rules of pinch-analysis [5-6] and including some technical suggestions:

- If possible, avoid dividing a solid flow.
- Prefer fluid-fluid or fluid-solid thermal exchange avoiding the use of less efficient solid-solid exchangers if it is possible.

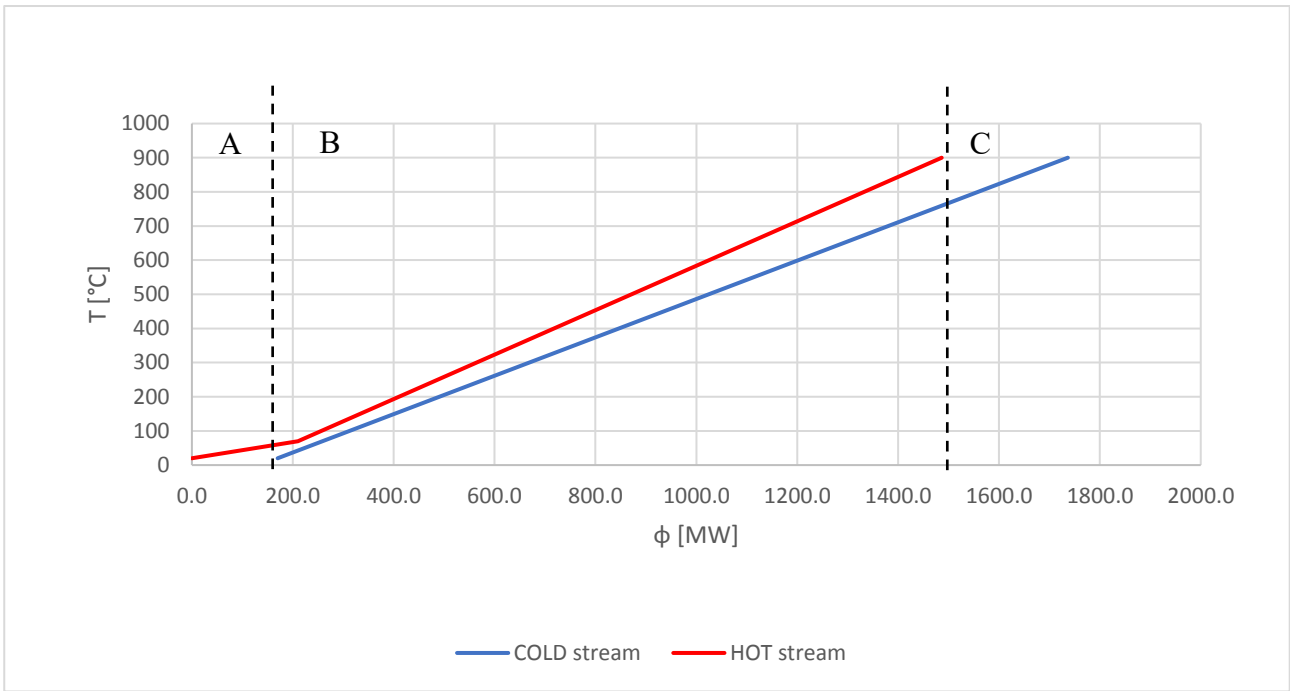


Figure 4.10: Composite curve of the solar calciner side

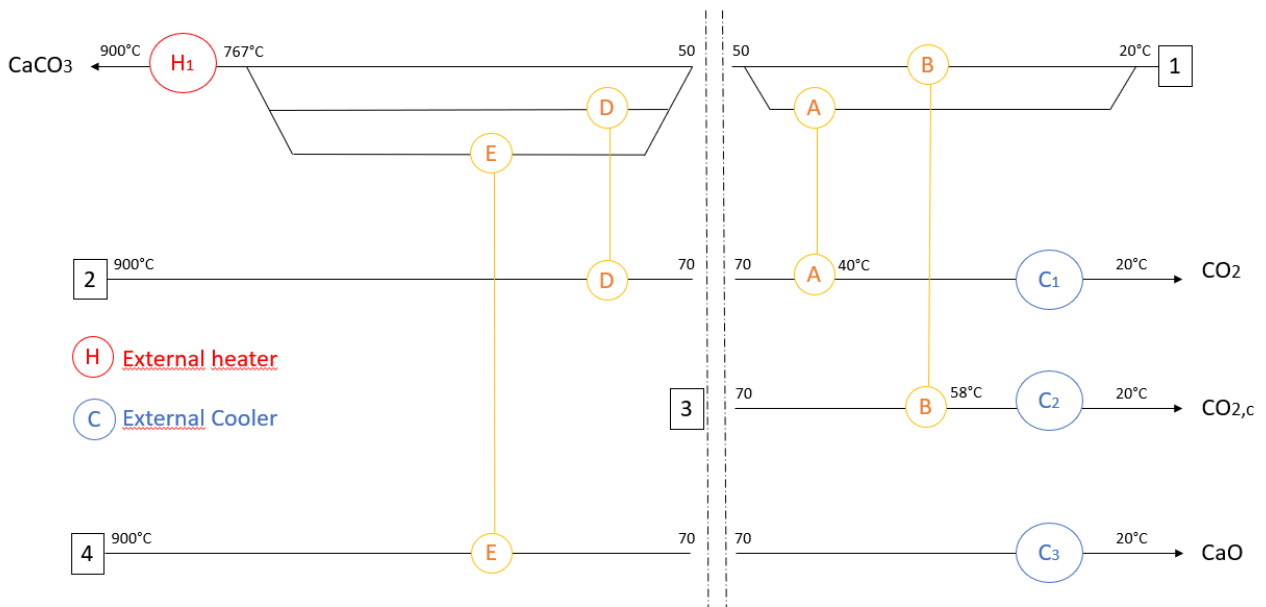


Figure 4.11: Minimum energy consumption network inferred from the pinch analysis in the calciner side

Table 4.2: Heat exchange in each exchanger

Heat exchanger	# of stream pynch	$\phi$ [MW]
A	1-2	19,86
B	1-3	33,55
D	1-2	549,34
E	1-4	726,82
H	1	238,54

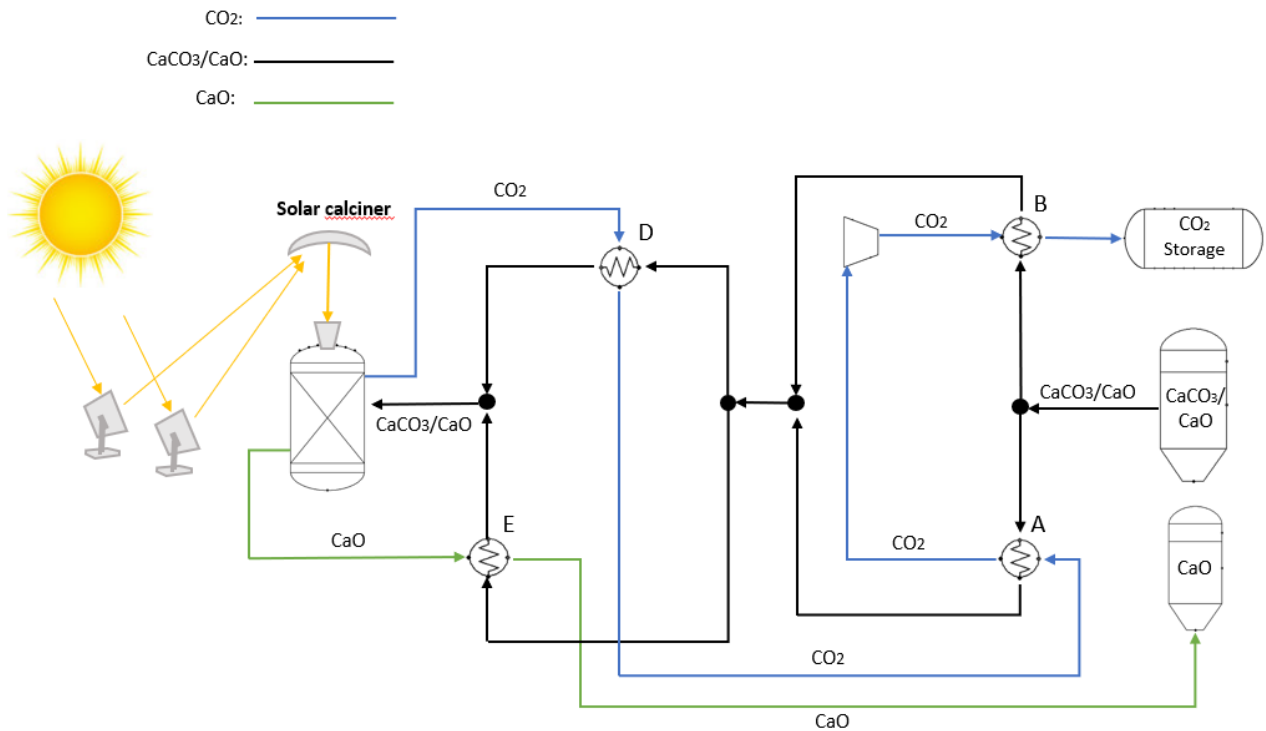


Figure 4.12: Plant configuration (calciner-side) resulting from the pinch analysis.

#### 4.2.2.2. Pinch analysis of carbonator side

Following the analysis thoroughly performed for the calciner side (energy storage), this section is devoted to the carbonator (energy release). Here, the stored solar energy is used to provide the heat required by a Rankine cycle.

The energy release area is mainly composed of two devices: one of these is the carbonator in which the carbonation reaction occurs, and the other one is the turbine train in which compressed CO<sub>2</sub> is expanded from 74 to 2 bar. Through the expansion of CO<sub>2</sub>, it is possible to produce both power and cooling. After each expansion stage, the carbon dioxide is at the temperature of about -30 °C and must be heated in order to avoid condensation and the consequent breakage of the blades. The heat released by the refrigerant fluid (water) in a refrigerant cycle (see fig. XXX) is transferred to the CO<sub>2</sub> which is heated from -30 °C to 7 °C. The refrigerant fluid is sent to a second heat exchanger in order to increase its temperature from 12 to 6 °C and continuously cooling external environment (e.g. hospital). the size of the power chiller is approximately 29 MW.

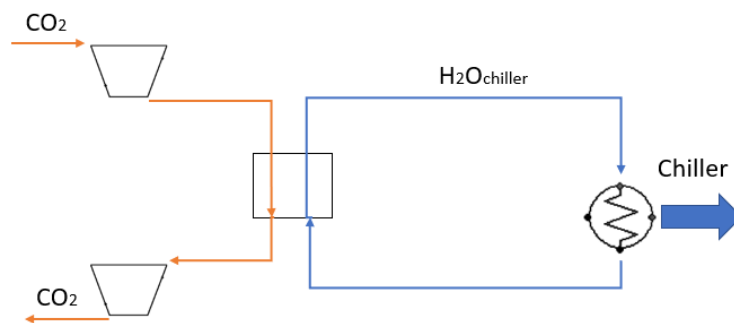


Figure 4.13: Refrigerant cycle coupled with expanded CO<sub>2</sub>

As table 4.3 the pinch analysis accounts for ten fluids, two of which were hot streams leaving the carbonator at a temperature of 830 °C and the remaining are cold streams to be heated as reported in

Figure 4.16. The cold fluids are: (i) the compressed CO<sub>2</sub>, which is heated before entering the turbine in order to produce more power, (ii) the CO<sub>2</sub> at the end of expansion, which temperature between 7 °C to 287 °C (minimum temperature of recirculation CO<sub>2</sub>), (iii) the CO<sub>2</sub> entering the reactor ranging from 287 °C to the carbonation temperature, (iv) CaO heated from ambient temperature to carbonation temperature, and finally (v) the working fluid of a conventional Rankine cycle, which is subjected to preheating, evaporation, overheating and re-heating.

Table 4.3 Stream identification in Carbonator side

# of stream pynch	# of stream	Component	Type of stream	T <sub>in</sub> [°C]	T <sub>out</sub> [°C]	Mass rate [kg/s]	G x cp [MW/K]	Power Heat [MW]
1	63	CO <sub>2</sub>	HOT	830	287	1173,6	1,3721	745,1
2	75	Solids	HOT	830	20	513,48	0,6489	525,6
3	1	H <sub>2</sub> O(l)	COLD	267	352	284,25	1,6263	-138,24
4	3	H <sub>2</sub> O	COLD	352	353	284,25	97,7600	-97,76
5	4	H <sub>2</sub> O(v)	COLD	353	538	284,25	1,2078	-223,45
6	9	H <sub>2</sub> O(v)	COLD	325,9	538	232,064	0,5402	-114,57
7	48	CO <sub>2</sub>	COLD	20	60	198,045	1,0353	-41,41
8	59	CO <sub>2</sub>	COLD	7	287	198,045	0,1900	-53,20
9	61	CO <sub>2</sub>	COLD	287	830	1371,645	1,6035	-870,68
10	64	CaO	COLD	20	830	315,43	0,2908	-235,55

Many constrains and boundary condition are similar to calciner side and can be summarized below:

- Temperature of hot fluids have to be higher than cold fluids;
- In each coupling of hot and cold fluids, a minimum temperature difference of 20 °C must be respected;
- the temperature of the CO<sub>2</sub> at the inlet of turbine train must be as high as possible to increase electricity production;
- The ambient temperature is 20°C;
- The reactor is at a temperature of 830°C and 2 bar;
- The containers are all at ambient temperature;
- The carbon dioxide at the exit of the turbine train will be 2 bar and 7°C;
- Minimum temperature of recirculating CO<sub>2</sub> is equal to temperature of water coming into economizer plus minimum difference temperature (267 + 20 °C);
- Water temperature at the superheater and re-heater outlet must be 538°C;

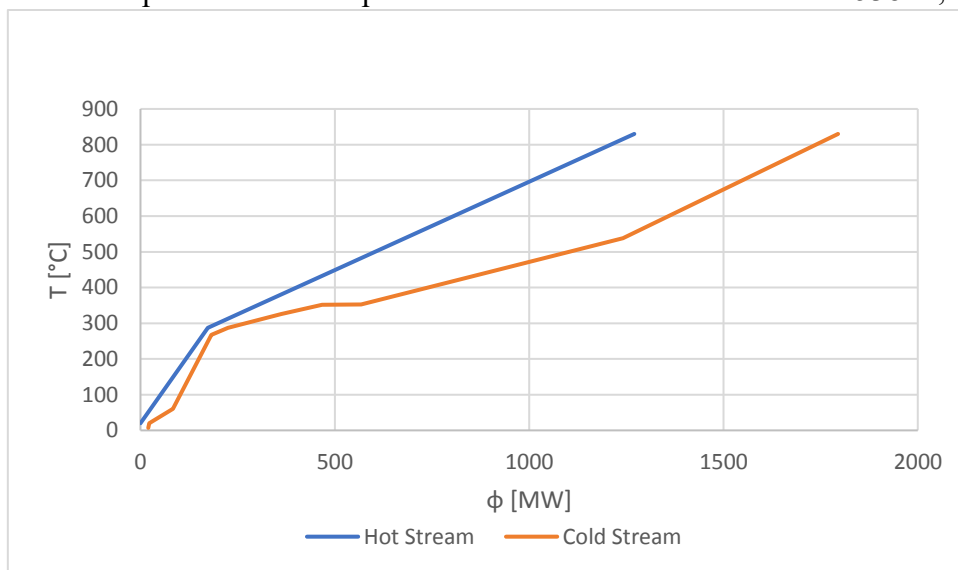


Figure 4.14: Composite curve of the carbonator side

As mentioned previously, part of the heat contained in the hot fluids is dispersed in the environment (cold sink) whereas a large part of the heat needed for the cold fluids is supplied by an external source (hot sink) and, finally, the remaining part of the heat needed for the cold is provided by the exothermic carbonation reaction that it takes place inside the carbonator. In the study of the pinch analysis, the heat given by the reaction is considered as an external source, while the enthalpy of carbonation reaction which was used for the vaporisation of the water was not considered in the pinch analysis. The heat exchanger network (HEN) for the release energy is proposed in fig. 4.14.

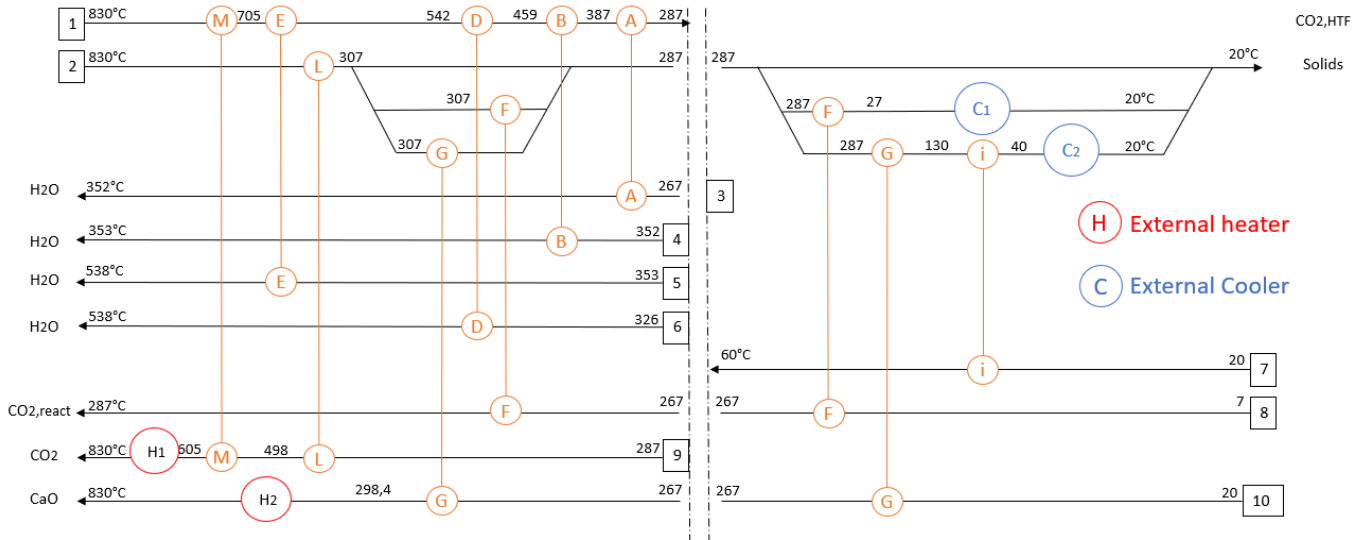


Figure 4.15: Minimum energy consumption network inferred from the pinch analysis in the carbonator side

Table 4.4: Heat exchange in each exchanger

Heat exchanger	# of stream pynch	$\phi$ [MW]
A	1-3	138,24
B	1-4	97,76
D	1-6	114,57
E	1-5	223,45
F	2-8	53,2
G	2-10	71,83
I	2-7	41,41
L	2-9	352,33
M	1-9	171,05
H1	9	379,37
H2	10	163,72

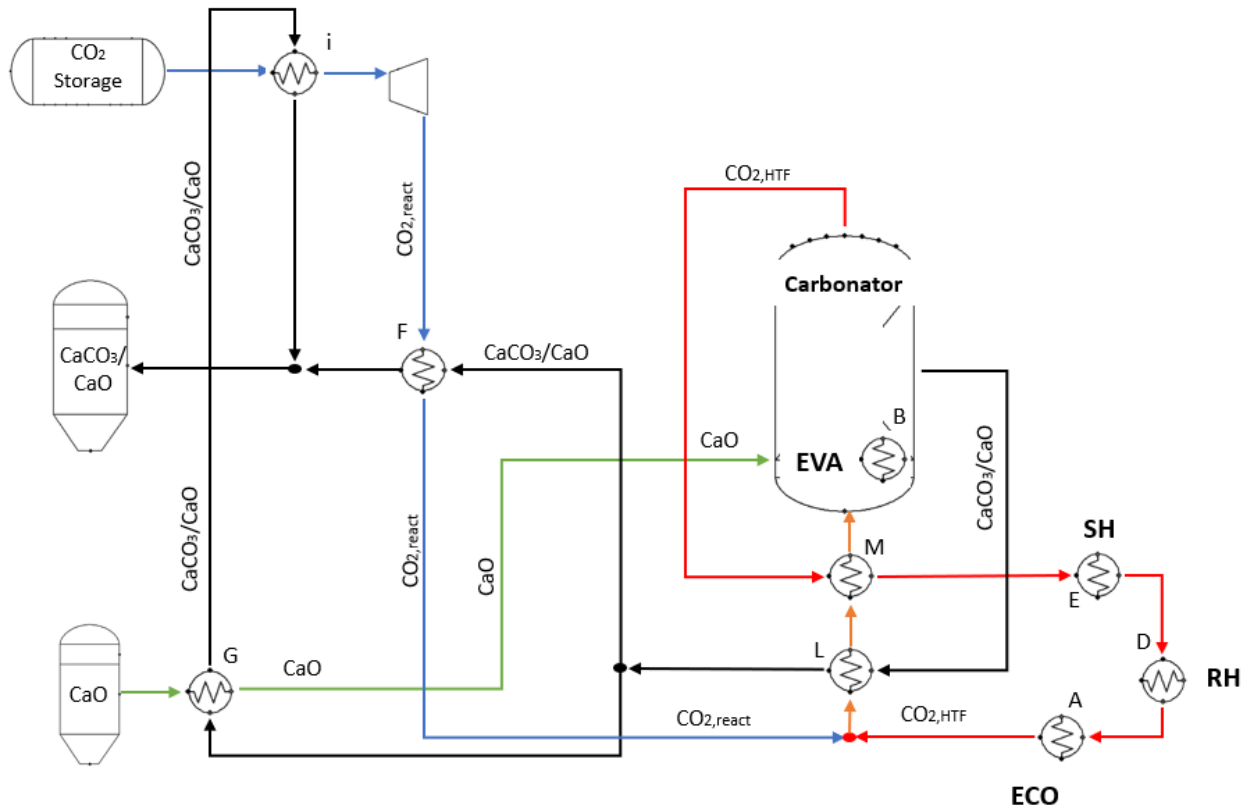


Figure 4.16: Plant configuration (carbonator-side) resulting from the pinch analysis.

The final goal of the analysis is to configure a heat exchanger network which can be used in parametric analysis with regards to key operating parameters (e.g.  $X$ , operating temperature and pressure). This is achieved by dividing the hot stream (solids leaving carbonator) and changing the mass flow rate at each single simulation. The configurations obtained in Fig 4.16 and 4.12, indeed, provide a good flexibility by splitting the hot stream and cold stream respectively. In this way it is possible to regulate the mass fraction in each branch for several values of CaO conversion  $X$ .

#### 4.2.3. Modelling

As it was done for the modelling of steel plants, the commercial software Chemcad<sup>TM</sup> was used for the modelling and simulation of the Rankine cycle power plant integrated with calcium looping technology. This is used to solve mass and energy balances of complex systems providing a large database of chemical components. It is specifically designed to simulate chemical reactions with regards to the power production in a steady-state environment.

Both the Rankine cycle plant and the CaL unit were simulated through several components such as reactors, flow mergers/splitter, heat exchangers. Due to the large amount of sub-processes taking place and to their complexity, some simplifying assumptions had to be made:

- Operation of all components is at steady state;
- Only thermodynamic equilibrium has been considered neglecting the kinetic of reactions;
- The ambient temperature and pressure are constant and equal to 20°C and 1 bar, respectively;
- The pressure losses were neglected;
- The heat losses in the piping and in the rest of the system were neglected with the exception of the carbonator reactor in which about 4% of heat produced is lost.

- The performance of the main reactors e.g. Carbonator and Calciner were represented using the chemical and phase equilibrium through the free energy minimization at the operating temperature;
- A complete calcination of calcium carbonate takes place into solar calciner;
- Minimum temperature difference (pinch temperature) is 20°C for all main heat exchangers and 10°C for intercooler;
- The plant is equipped with a solid-solid heat exchanger, gas-solid heat exchanger and with gas-gas regenerator.

Several of this assumption are summarized in the follow table:

*Table 4.5: Assumptions for the Solar CaL Rankine power plant*

Reference case		
Solar heat provided to Calciner	2431,58	MWth
Termal dispersion in Carbonator	3,85%	%
Calciner Temperature	900	°C
Calciner Pressure	1	bar
Ambient Temperature	20	°C
CaO average conversion	70%	%
Carbonator Temperature	830	°C
Carbonator Pressure	2	bar
CO2 storage conditions	74	bar
Daylight hours	8	h
Isentropic efficiencies	83%	%

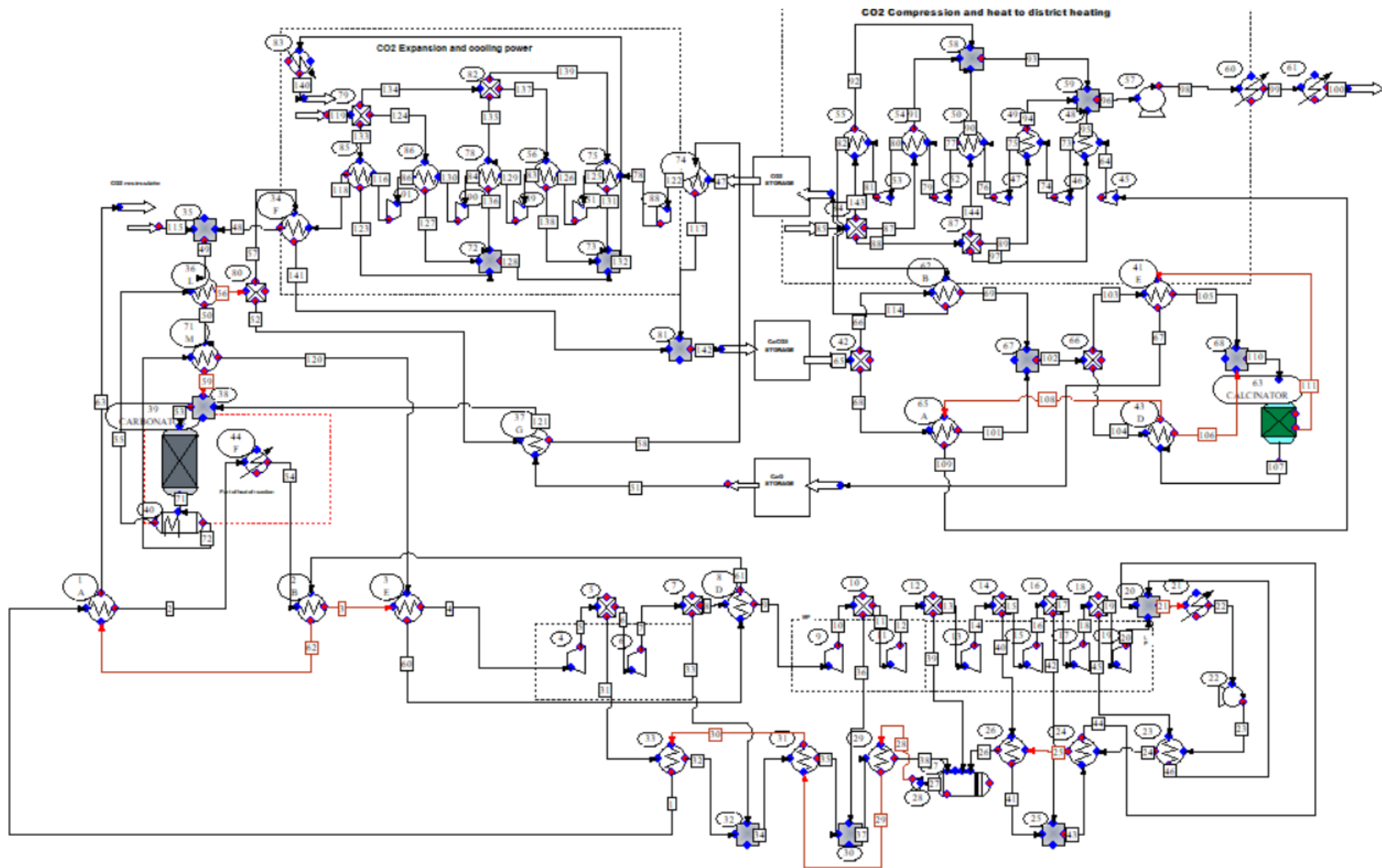


Figure 4.17: ChemCad model for Solar CaL integrated Rankine cycle power plant

Figure 4.17 displays the ISCaL Rankine power plant. As for the calcium looping, it was assumed that the carbonation reaction reached chemical equilibrium, sorbent conversion was represented by an isothermal GIBBS reactor (a Chemcad™ model based on the free energy minimization).

The thermodynamic equilibrium is supposed to be reached in both carbonator and calciner reactors: the molar flow of calcium oxide feeding the system was set to react with the CO<sub>2</sub> expanded providing the heat enough to run the Rankine cycle. According to experimental results () an average CaO conversion of 0.7 was selected.

As it was previously performed, the average conversion  $X$  is considered by introducing an element with the same chemical property of the CaO but inert in presence of the carbon dioxide and thus does not produce calcium carbonate. It was introduced in the simulation of the plant in to properly solve the energy balance of the CaL system. It is known that the thermal energy input required by the calciner is mainly due to the decomposition of calcium carbonate. Consequently, the calciner energy consumption is estimated based on the average possible amount of solids sent into the regeneration/storage step

In addition, a complete conversion of CaCO<sub>3</sub> to CaO into the calciner operating at 900°C has been supposed. The performance of the calciner as well as the carbonator were analysed using the Gibbs free energy minimization model (GIBBS reactor).

The CaL process requires a continuous make-up flow of fresh limestone to counteract the deactivation of lime with the number of carbonation/calcination cycles while a corresponding purge is also extracted from the calciner. The calcined purge is obviously a potential material to be fed to the cement plant and other industrial process (e.g. steel, glass and pulp). Due to the high resistance of the new sorbents at higher number of cycles, a continuous make-up flow is not simulated.

#### 4.2.4. Optimum configuration and parametric analysis

Being evaluated the optimal configuration of the HEN for the storage and release system, a parametric analysis was carried out by varying the CaO conversion. This parameter has an important influence on the system as whole (e.g. (i) size of storage vessels, (ii) solids flow rates and (iii) heat requirements).

During this analysis, the power production of the Rankine cycle is fixed. Therefore, the thermal energy produced by carbonator reactor has to meet the Rankine cycle and heat the inert materials entering with the active CaO. The same amounts of reagents participate in the carbonation reaction, however, decreasing the  $X$  parameters, the CaO flow rate that does not participate in the reaction will increase. The obtained results are illustrated in the Figure below.

The Figures 4.17 and 4.18 show the effect of the CaO conversion on the thermal power in both main reactors in which the carbonation and calcination reaction occur. By fixing the quantities of the compounds that must react in the reactors (4.5 kmol/s of CO<sub>2</sub> and 5.85 kmol/s CaO), the necessary thermal power produced respectively in the calciner ( $\Phi_{calcination} = 2409 MW$ ) and carbonator ( $\Phi_{carbonation} = 803 MW$ ) reactors remain constant. However, the sensible heat necessary to heat up the reactants to the temperature of the respective reactor, slumped significantly at high CaO conversion.

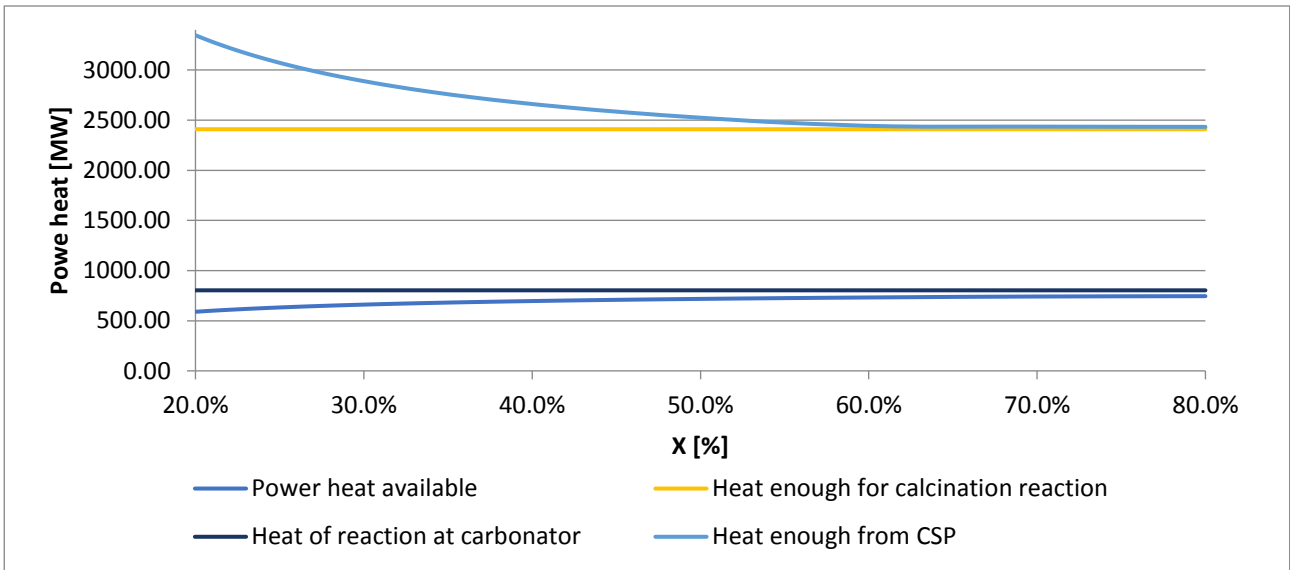


Figure 4.18: Thermal power fluxes of main reactors to vary CaO conversion

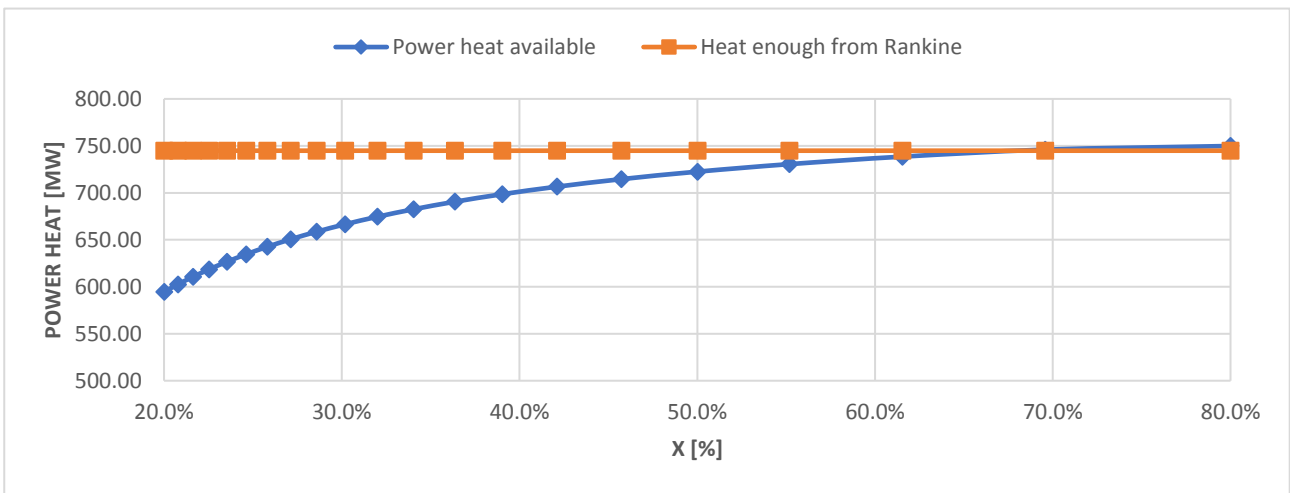


Figure 4.19: The heat enough from Rankine cycle is fixed, while change the heat provides by the storage system.

Therefore, in case of loss of performance of the sorbent (low X), it may be necessary:

- Reduce the power produced, thus requiring less energy to the carbonator;
- Use an external resource that provides the remaining power;
- Increase the flow rate of the reagents (CaO and CO<sub>2</sub>), making the system operating at nominal power with less hours per day;

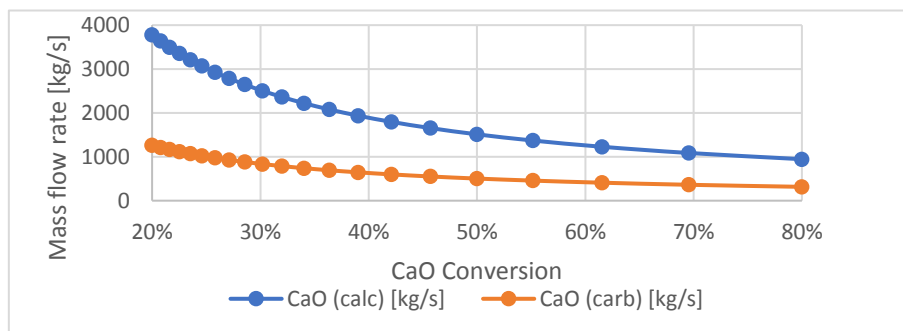


Figure 4.20: Solids mass flow rate at different CaO conversion

At fixed heat requirement of Rankine cycle, it is possible to evaluate the mass rate (see fig 4.20) and storage volume (see fig. 4.21) of each component by changing X.

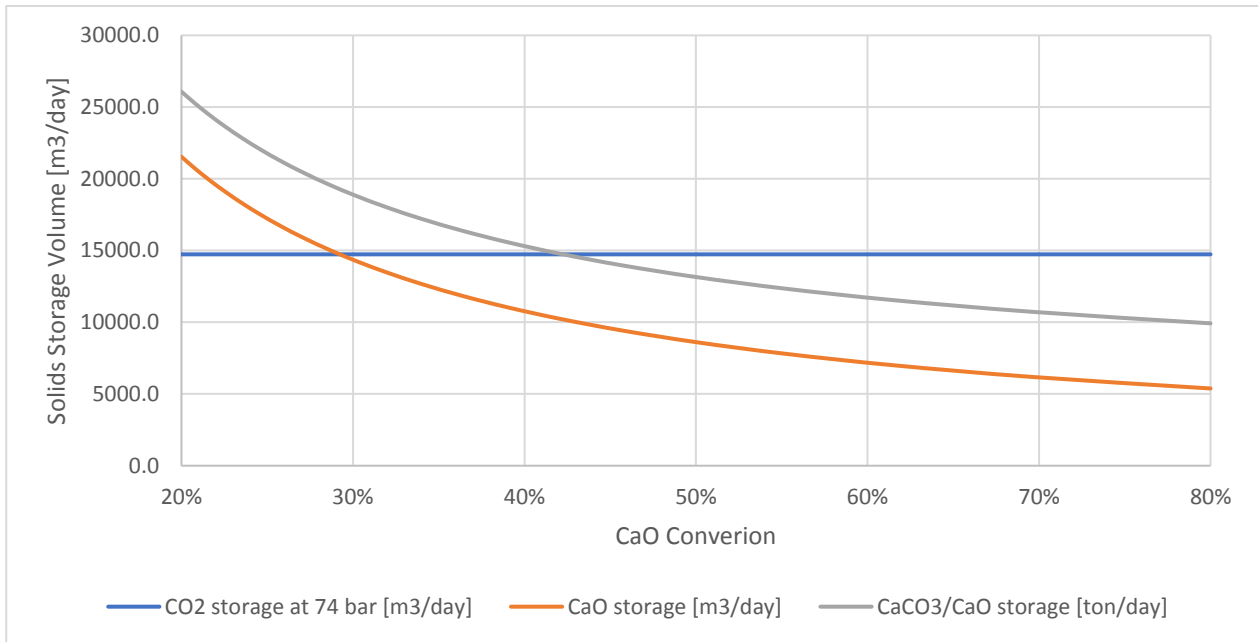


Figure 4.21: Storage volume as a function of average CaO conversion of the solids and CO2 at 74 bar and 20°C

Figure 4.21 shows that increasing the CaO conversion, storage volume of the solid streams decreases while the CO2 storage is not affected. This last observation is due to the fact that the CO2 required for the carbonation reaction has not changed. The CO2 storage volume is strongly depends (chapter 2.3) on the thermodynamic storage conditions.

In the following table are summarized the parameter used to compute the storage volume of components:

Table 4.6: Parameters used to compute storage volume

<b>MM CO2 [kg/kmol]</b>	44
<b>MM CaO [kg/kmol]</b>	56
<b>MM CaCO3 [kg/kmol]</b>	100
<b><math>\rho</math> CO2 (P=74 bar T=20°C) [kg/m<sup>3</sup>]</b>	773,99
<b><math>\rho</math> CaO [t/m<sup>3</sup>]</b>	3,37
<b><math>\rho</math> CaCO3 [t/m<sup>3</sup>]</b>	2,93
<b>Daylight hours [h]</b>	8
<b>hours of storage [h]</b>	16

In order to guarantee a steady state condition during operation, the sorbent regenerated into calciner reactor has to be enough to produce heat into carbonator side. Therefore, the follow molar-balance equation has to be satisfied:

$$\int_{24\text{ h}} \dot{n}_{CaCO_3\text{ carb}}(t) dt = \int_{24\text{ h}} \dot{n}_{CaO\text{ calc}}(t) dt \quad (4.4)$$

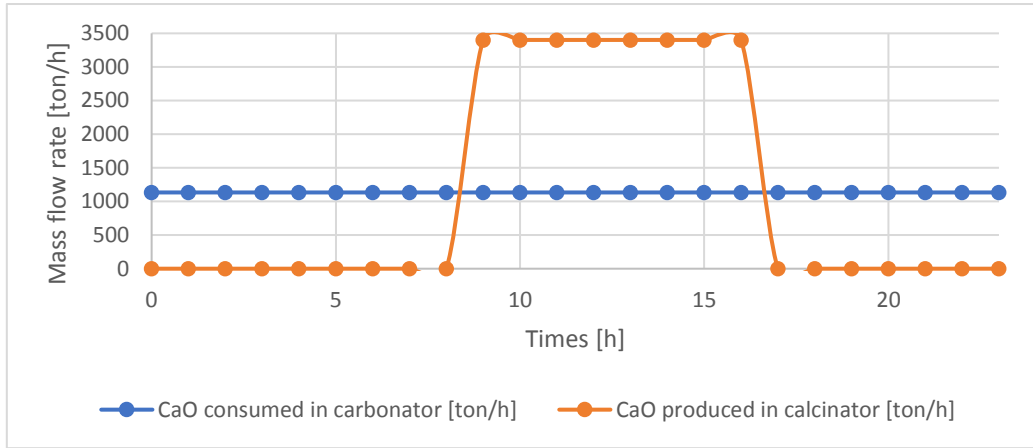


Figure 4.22: Mass flow rate of calcium oxide consumed and produced respectively in different operational times

A key performance indicator to evaluate the effectiveness of the storage and release system is the *storage efficiency* defined as the ratio of the heat released during carbonation and expansion of CO<sub>2</sub> to the heat gathered by the CSP and required during CO<sub>2</sub> compression.

Figure 4.23 shows the comparison of the storage efficiency (right axis) with the heat stored (blue line) and release (orange line) both as a function of the CaO conversion. The efficiency of the storage system increases with high values of released energy and low values of stored energy.

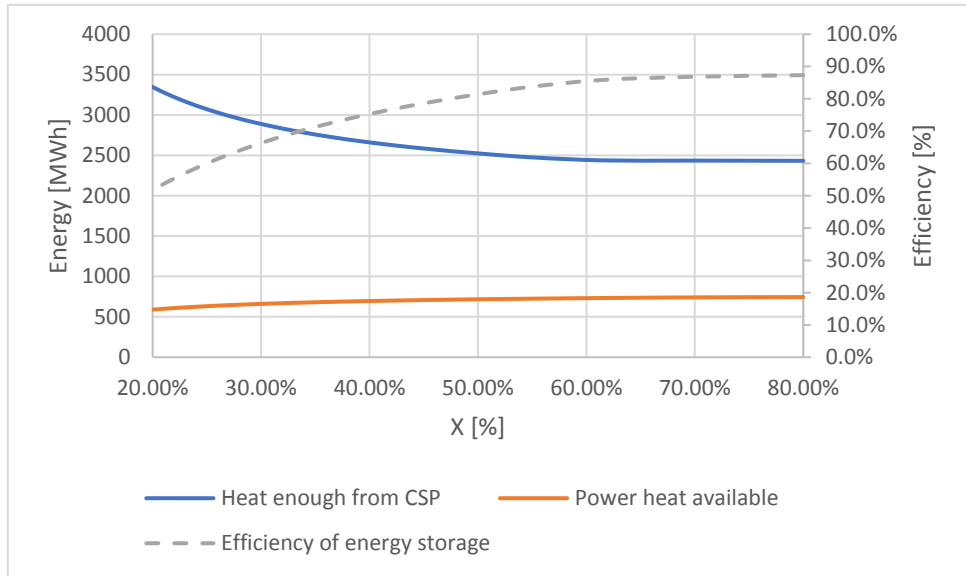


Figure 4.23: Thermal power fluxes (left axis) and energy storage efficiency (right axis) function of CaO conversion

Two different efficiencies were assessed, one takes into account the thermal recovery by refrigerant cycle (red line).

- Storage Efficiency

$$\frac{Q_{\text{carbonator}} + L_{\text{CO}_2, \text{expansion}}}{Q_{\text{CSP}} + L_{\text{CO}_2, \text{compression}}} \quad (4.5)$$

- Storage and Recovery efficiency:

$$\frac{Q_{\text{carbonator}} + L_{\text{CO}_2, \text{expansion}} + Q_{\text{chiller}} + Q_{\text{district heating}}}{Q_{\text{CSP}} + L_{\text{CO}_2, \text{compression}} + L_{\text{pump}}} \quad (4.6)$$

Each term of the efficiency represents an energy and it is calculated by multiplying the thermal or mechanical power by the respective operating time.

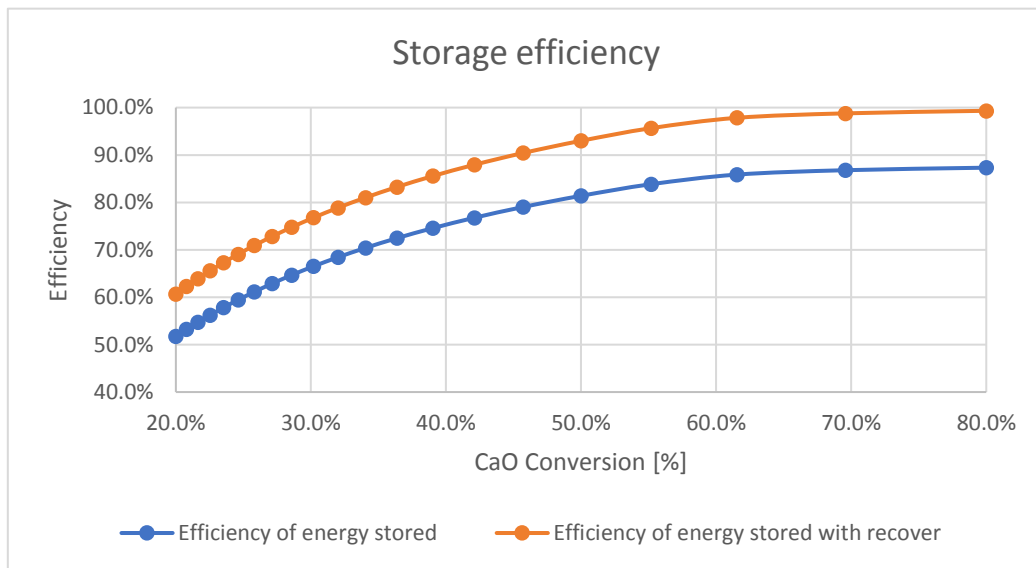


Figure 4.24: Storage efficiency (blue line) and Storage and recovery efficiency (orange line)

The two efficiencies increase significantly with the increasing of  $X$  and they reach a good peak of 87.3% and 99.3% respectively. Therefore, it is better to work with a material having excellent conversion performance and recover the various energies available at low temperature to achieve very high levels of efficiency for a storage system.

The optical and thermodynamic efficiencies of the CSP were not considered in this analysis. Figure 4.24 report: (i) the *net efficiency* (blue line) defined as the ratio of produced power by Rankine and CO<sub>2</sub> expansion to the heat gathered by the CSP and required during CO<sub>2</sub> compression; (ii) the net recovery efficiency (orange line) defined as the ratio of produced power by Rankine, CO<sub>2</sub> expansion and heat and cooling systems to the heat gathered by the CSP and required during CO<sub>2</sub> compression.

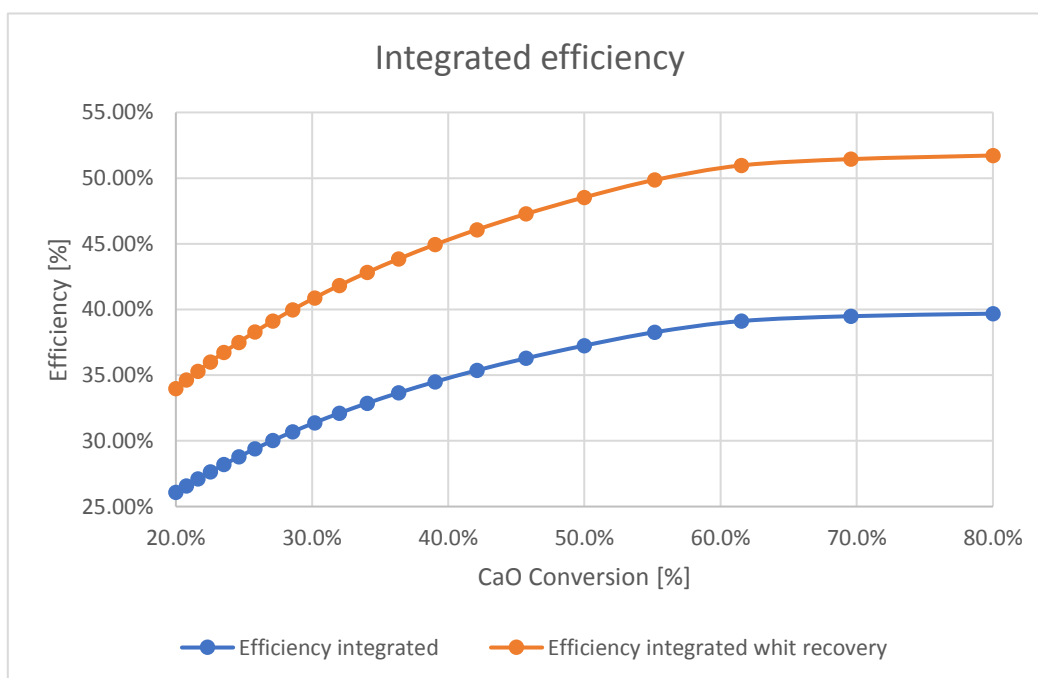


Figure 4.25: Thermodynamic integrated efficiency with and without low thermal energy recovery

The thermodynamic efficiencies at low values of CaO conversion have plummeted. Therefore, when the conversion degree of the sorbent decreases, the material should be changed with fresh material.

At high conversion levels, the system performs well, reaching almost 40% of storage efficiency without low-temperature heat recovery, exceeding 50% in the event we supply a district heating and cooling capacity network.

All the electrical and thermal powers produced and consumed by the various components, and the values of the plant efficiencies at a fixed CaO conversion value set at 0.7 are summarized in the following table.

Table 4.7: Thermal end electrical input and output for each component

Calcinator side	Power Heat from CSP to calciner	-2432,40	MW
	Daylights hours	8,00	h
	Energy heat from CSP	-19459,20	MWh
	Electric power to compress CO2	-208,10	MW
	Electric energy to compress CO2	-1664,80	MWh
	Power pump to water networking	-1,27	MW
	Energy to pump water networking	-10,16	MWh
	Power to district heating	232,00	MW
	Energy to district heating	1856,00	MWh
Carbonator side	Electric power from compressed CO2	23,70	MW
	Electric energy from compressed CO2	568,80	MWh
	Cool power	28,70	MW
	Cool energy	688,80	MWh
	Power to rankine cycle	744,88	MW
	Energy to rankine cycle	17877,12	MWh
Rankine cycle	HP T1	57,64	MW
	HP T2	39,32	MW
	MP T1	53,53	MW
	MP T2	42,92	MW
	LP T1	43,00	MW
	LP T2	37,77	MW
	LP T3	22,72	MW
	LP T4	35,10	MW
	P1	-0,09	MW
	P2	-6,16	MW
	Power output from rankine	325,75	MW
	Daily work	24,00	h
	Energy output from Rankine	7818,10	MWh
Efficiency	Efficiency of energy stored	86,8%	-
	Efficiency of energy stored with recover	98,8%	-
	Efficiency of rankin cycle	43,7%	-
	Efficiency integrated	39,5%	-
	Efficiency integrated whit recovery	51,4%	-

## References

- [1] IEA; «Global Energy & CO2 Status Report 2017 »; International Energy Agency, 2017
- [2] H. Chen, et al «CO2 capture and attrition performance of CaO pellets with aluminate cement under pressurized carbonation,» ELSEVIER; 2011
- [3] US Department of Energy (DOE), «Kemper County Integrated Gasification Combined-Cycle (IGCC) Project, Draft Environmental Impact,» 2009.
- [4] S. Stendardo, P.U. Foscolo « Carbon dioxide capture with dolomite: A model for gas–solid reaction within the grains of aparticulate sorbent » ELSEVIER; 2009
- [5] L. March « Introduction to Pinch Technology» 1998.
- [6] V.Verda, E. Guelpa; « Metodi termodinamici per l'uso efficiente delle risorse energetiche»

## 5. Supercritical Carbon Dioxide Power Cycle

Due to the strong environmental impact of conventional power plants, the reduction of raw material quantities used as fuel which can lead to a crisis of energy shortages, renewable energy has to replace the conventional fossil fuel energy. One of the most promising renewable energy sources certainly is the concentrating solar plant technologies that provide carbon-free and dispatchable electric energy to meet the increasing energy demand. However, the high investment cost and still the contained efficiency does not make it competitive with high conventional power plants (0.25-0.33 €/kWh<sub>e</sub> [1]).

Solar power tower system can reach high temperatures, has the potential to scale up its size and achieve high efficiencies. Solar tower technologies capture the light and convert them into heat. The direct solar irradiation is focused onto a receiver using a ground-based field of mirrors. When the solar receiver is mounted high in a central tower, lights are reflected directly here. Other technologies use a second mirror that further reflects the rays concentrated by the other heliostats in a receiver positioned immediately below. The heat drives a thermo-dynamic cycle, in most cases a water-steam cycle, to generate electric power.

Current CSP plants utilize oil, air or molten salt, as heat transfer fluid to transfer the collected solar energy to the power block. The plant performance is limited by these fluids because of they can't reach higher temperature.

The supercritical carbon dioxide (s-CO<sub>2</sub>) Brayton cycle are proposed to be integrated the solar tower plant system, replacing the conventional water-steam Rankine cycle seen before and air Brayton cycle. The CO<sub>2</sub> has the ability to be both the heat transfer fluid and working fluid. It can potentially lead to high efficiency reaching high temperature operation and a compact system layout, reducing the investment cost. The use of supercritical CO<sub>2</sub> allows us to compress a fluid that is in the incompressible fluid state, thus saving electric power. Supercritical CO<sub>2</sub> has both the advantages of water in compression, and of gas in reaching high temperatures. The CO<sub>2</sub> critical condition is 30.98°C and 7.38 MPa and the fluid become more incompressible near this point.

The compactness of the s-CO<sub>2</sub> Brayton cycle is mainly due to the minimum system pressure set above 7.4 MPa compared to the minimum pressure of the Rankine cycle of a few kPa. Therefore, the fluid density is always high, and the volumetric flow rate is lower. The drawback is that the pressure ratio is low and a large amount of heat must be recovery.

Several s-CO<sub>2</sub> Brayton cycle configurations have been proposed, such as simple recuperation cycle, intercooling cycle, re-heating cycle, pre-compression cycle, recompression cycle, pre-heating cycle [2]. Their performances are evaluated as a function of the Turbine Inlet Temperature (TIT) and optimizing other cycle parameter such as flow ratio of the separator or the turbine inlet pressure setting usually at 250 bar [3].

The s-CO<sub>2</sub> Brayton cycle mainly consists of three components: Heat exchange, compressor and turbine. The different number of those components, the different way to connect them and the number of split and reconnection produce several cycle configurations.

Are used two type of heat exchanger:

- One transfer energy between the working fluid and an external heat hot/cold source;
- The second transfer energy between hot and cold streams of the working fluid;

The first consists of pre-cooler, inter-cooler, heater and possible re-heater. The main goal of the heater and re-heater is heat up the working fluid at the turbine inlet temperature sept. Contrariwise, in pre-cooler and inter-cooler the working fluid reject heat to the sink, to obtain a specified compressor inlet temperature.

The recovery heat exchangers are more delicate. They are essential for achieving high system performance due to the small pressure ration and therefore high outlet turbine temperature. However, great care must be taken because the two fluids often reach pinch point temperatures. In the model, each counterflow heat recovery exchanger heat up to a minimum temperature difference of 20°C.

To calculate the performance of the compressor and turbine component, the isentropic efficiency is used ( $\eta_{is,comp} = 0.89$ ;  $\eta_{is,turb} = 0.93$  [4]).

### 5.1. System configuration

Three s-CO<sub>2</sub> Brayton cycle layouts (Recompression cycle RR, Partial cooling cycle PC, Recompression main compressor inter-cooling RMCI) are analysed to find the best performance cycle. The different s-CO<sub>2</sub> Brayton cycle layout are illustrated in the Fig: 4.26-27-28 respectively. The hot source is simulated as simple heater, but we will see later that this cycle will be integrated to the solar CaL and the heat will be provided by the CO<sub>2</sub> used as heat transfer fluid.

The first s-CO<sub>2</sub> Brayton cycle conceived was very inefficient because a large amount of heat could not be recovered and was lost due to high outlet turbine pressure. Therefore, a first Sample regeneration [5] was evolved. Nonetheless, the great difference in the heat capacity between high-pressure and low-pressure streams cause a limited recovery due to temperature pinch-point problem. The pinch point problem was avoided through the Recompression cycle configuration and the heat recovery was divided in Low temperature heat recovery (LTHR) and High temperature heat recovery (HTHR).

#### Recompression cycle

Decrease the temperature pinch point problem into the low temperature het recovery is the main goal of the recompression cycle. The temperature difference between the two streams must be higher than minimum difference temperature to transfer easily heat. This problem is caused by a large heat capacity difference between high-pressure and low-pressure streams.

The recompression Brayton cycle reduce the mass flow rate of the high-pressure stream in the low-temperature recovery heat. This is normally performed by splitting the low-pressure stream in two fluids. One stream flow onto pre-cooler and in is pressurize onto the main compressor. The second stream enters the re-compressor at higher temperature than usual, compressed until turbine pressure design and mixed with the first stream at the inlet of the high-temperature heat recovery. Obviously, the re-compressor is less efficient because the fluid at the inlet is hot.

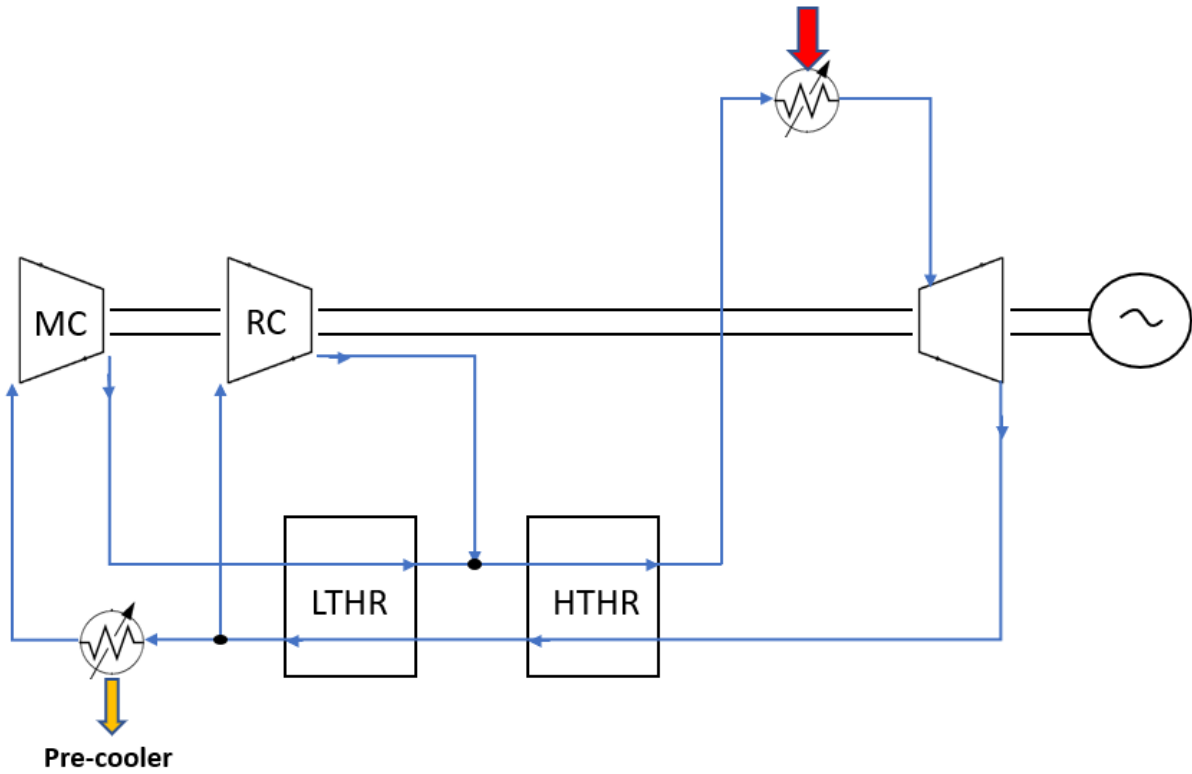


Figure 5.1: Recompression Brayton cycle

#### Partial cooling with recompression cycle

In this cycle an inter-cooling is added to respect the previous one. Usually the inter-cooling is used to reduce the compression work of the cycle. The compression is divided into two stages by inter-cooler. At the first, all the low-pressure exhaust stream is cooled in the pre-cooler and then enters in the low-pressure compressor (pre-compressor), where it is compressed at intermediate pressure.

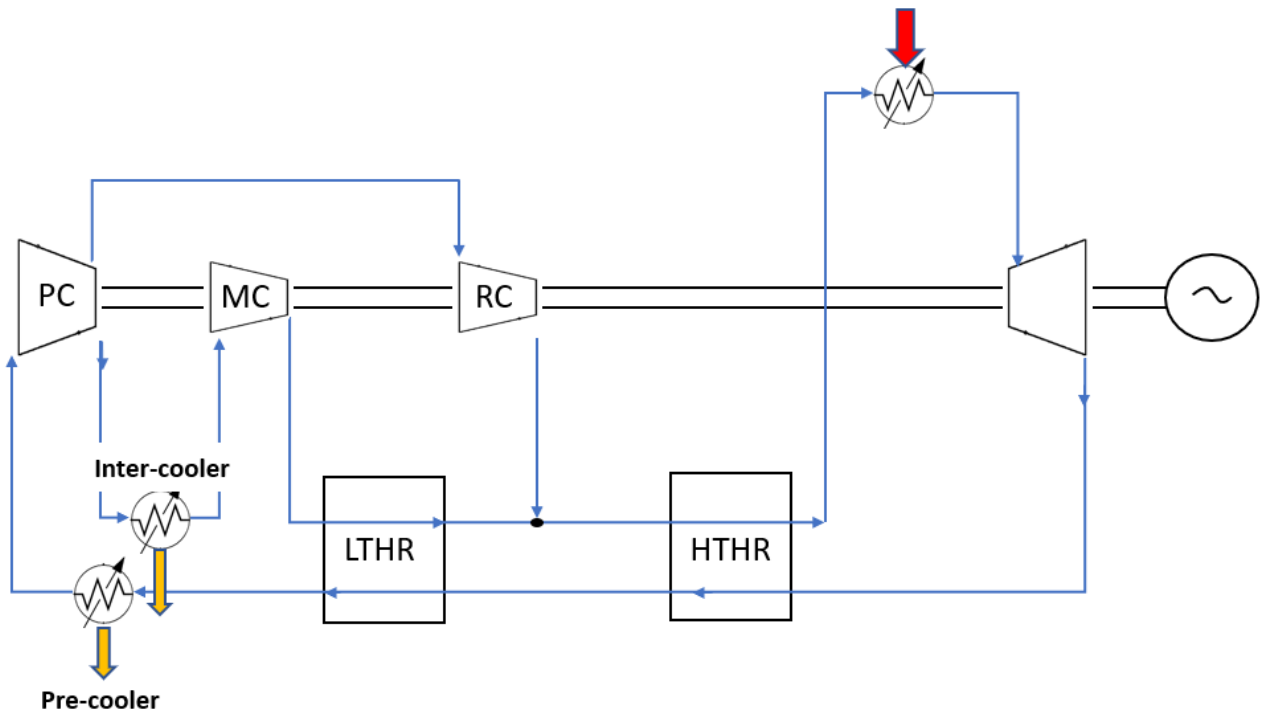


Figure 5.2: Partial cooling with recompression Brayton cycle

At the exit of the pre-compressor (PC), the flow is split. One stream flow into inter-cooler and main compressor, the other flow directly into the re-compressor. In this configuration the electricity consumed by the re-compressor is lower than before, because the fluid flow at first into pre-cooler. The presence of the inter-cooler reduces also the compression work of the main compressor.

#### Recompression with Main-Compression intercooling

In this configuration the pre-cooler unit is after the split. The re-compressor receives a relatively hot fluid and operate at the same pressure ration of the turbine.

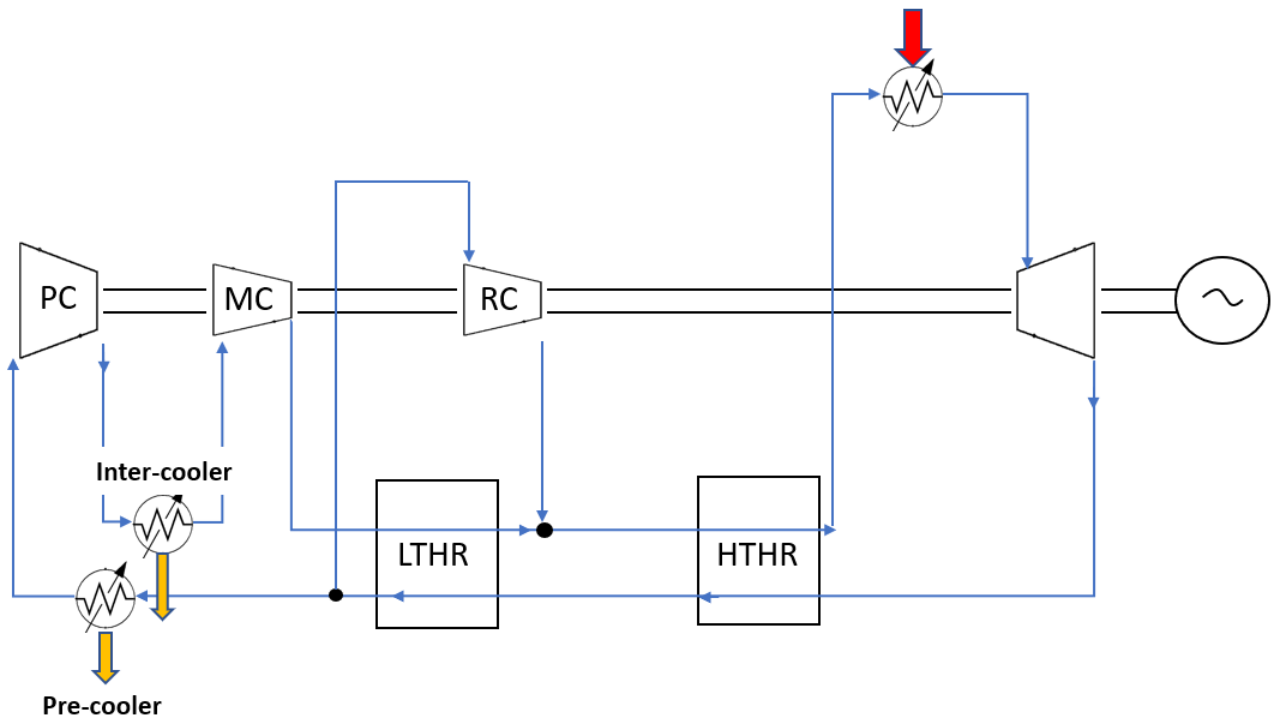


Figure 5.3: Re-compressor with main-compression inter-cooling Brayton cycle

An important parameter valid for the last two cycles described above is the RPR used to optimize the intermediated pressure:

$$RPR = \frac{\left(\frac{P_{max}}{P_{intermediate}} - 1\right)}{\frac{P_{max}}{P_{min}} - 1} \quad (5.1)$$

The simulation results in the following sections show the difference thermal performance varying the two main operating parameters: Turbine Inlet Temperature (TIT) and the Split Ratio (SR) as the main compressor flow rate divided by the total flow rate from the turbine exit. The optimized cycle that will present the best thermodynamic efficiency will subsequently be integrated into the solar CaL CSP power plant.

## 5.2. Modelling approach

The commercial software Chemcad<sup>TM</sup> was used for the modelling and simulation the different configuration of s-CO<sub>2</sub> Brayton cycle. This is used to solve mass and energy balances of complex systems and provides with a large database of chemical components and it is specifically designed to simulate chemical reactions. With regards to the power production, a steady-state Chemcad<sup>TM</sup> model was assembled.

The assumptions are summarized in the Table below:

Table 5.1: Assumption for s-CO<sub>2</sub> Brayton cycle model

Assumption		
Parameters	Value	Unit
Turbine efficiency	0,93	[-]
Compressor efficiency	0,89	[-]
Min $\Delta\tau$	20	[°C]
Mass flow rate	100	[kg/h]
Turbine Inlet temperature	600-700	[°C]
Compressor inlet temperature	51	[°C]
Maximum Pressure	250	[bar]
Pressure Ration	3-4	[-]
RPR	0,35-0,60	[-]

It is important remember that:

- Operation of all components is at steady state;
- The ambient temperature and pressure are constant and equal to 31°C and 1 bar, respectively;
- The pressure losses were neglected;
- The heat losses in the piping and in the rest of the system were neglected;
- The heat exchanger effectiveness is not considered;

The objective of the analysis is to find the best performing cycle among the three mentioned to be able to subsequently integrate it to the solar CaL CSP system. To do this, every single cycle was performed by varying three key parameters: Turbine Inlet Temperature, Split Ratio and RPR.

Another important parameter that can vary but in this simulation is kept constant, is the Compressor Inlet temperature. The Carnot efficiency states that for a cycle operating between two isotherms, the larger the temperature difference between the two isotherms, the greater the cycle efficiency. Therefore, it is obvious that, under the same conditions, reducing the inlet compressor temperature, increases the efficiency of the cycle.

The inlet compressor temperature is strongly conditioned by the temperature of the cold sink. Since, often the solar concentrator plants are positioned in very hot places and with a low quantity of water, it has been assumed that the work fluid cooling is carried out with dry air at 31°C. Therefore, the inlet compressor temperature, due to the minimum temperature difference, can only be set at 51°C.

To optimize the efficiency of the thermodynamic cycle, the three key parameters have been made to vary one at a time.

The first parameter to be optimized is the split ratio, i.e. the flow rate of low-pressure fluid to be sent to the main compressor while the Turbine Inlet Temperature and the RPR (only for the cycles which contain a pre-compressor) are kept constant and equal to 650°C and 0.35 respectively. The following graphs and tables show, for each thermodynamic cycle, how the optimization was performed.

Table 5.2: Higher performance by varying split ratio for the Recompression cycle

Recompression Cycle					
Temperature	[°C]	650			
Split Ratio	W_turbine	W re-compressor	W main compressor	Heat duty	Efficiency
[%]	MJ/h	MJ/h	MJ/h	MJ/h	[%]
0,40	18,06	7,86	2,60	23,00	33,0%
0,50	18,06	7,62	3,25	22,00	32,7%
0,60	18,06	6,23	3,90	22,00	36,0%
0,70	18,06	4,42	4,55	22,30	40,8%
0,80	18,06	2,68	5,20	23,64	43,1%
0,85	18,06	1,81	5,53	24,70	43,4%
0,90	18,06	1,22	5,86	25,70	42,7%

Table 5.3: Higher performance by varying Split Ratio for the Partial Cooling cycle

Partial cooling cycle						
Temperature [°C]	650 RPR			0,35		
Split fraction	W_turbine	W recompression	W Main compressor	W precompressor	Heat duty	Efficiency
[%]	MJ/h	MJ/h	MJ/h	MJ/h	MJ/h	[%]
0,40	18,06	2,23	0,80	2,84	28,00	43,5%
0,50	18,06	1,85	1,00	2,84	28,00	44,2%
0,55	18,06	1,67	1,10	2,84	28,00	44,5%
0,60	18,06	1,48	1,21	2,84	28,00	44,7%
0,65	18,06	1,30	1,30	2,84	28,84	43,8%
0,70	18,06	1,11	1,41	2,84	29,59	42,9%

Table 5.4: Higher performance by varying Split Ratio for the Re-compression Main Compressor Inter-cooling cycle

RMCI- Recompression Main Compressor Intercooling						
Temperature [°C]	650 RPR		0,35			
Split fraction	W_turbine	W_comp_1	W_comp_2	W_comp_3	Heat duty	Efficiency
[%]	MJ/h	MJ/h	MJ/h	MJ/h	MJ/h	[%]
0,40	18,06	8,40	0,81	1,13	22,58	34,2%
0,50	18,06	5,62	1,01	1,41	23,90	41,9%
0,55	18,06	4,65	1,11	1,55	24,48	43,9%
0,60	18,06	3,84	1,21	1,70	25,00	45,2%
0,65	18,06	3,15	1,32	1,83	25,47	46,2%
0,70	18,06	2,70	1,42	1,98	26,74	44,7%

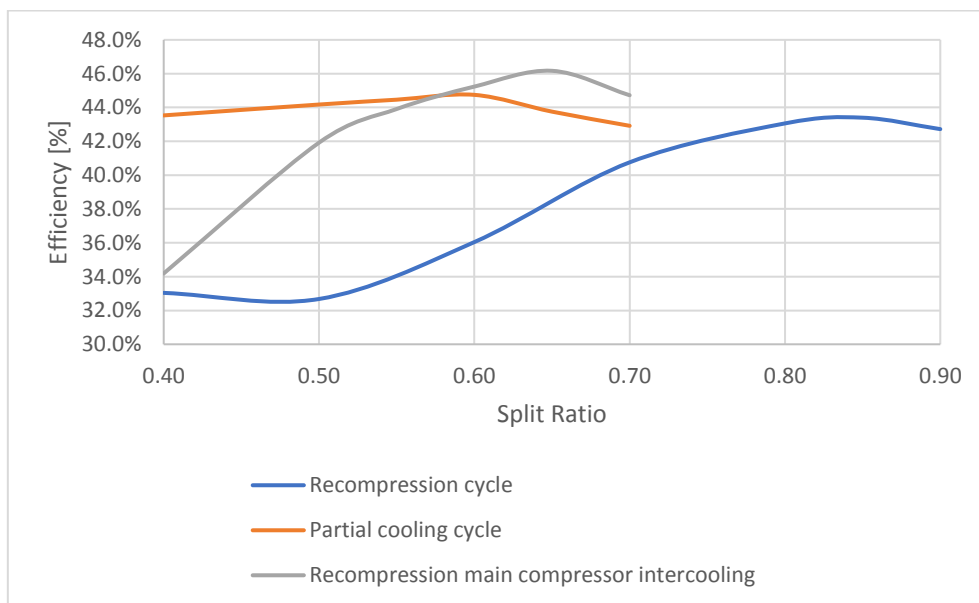


Figure 5.4: Compare the efficiency of the two cycle at the same TIT and RPR by varying the Split Ratio of the Mass flow rate to the Main Compressor

The graphs and tables above obtained, illustrate how the Recompression cycle and RMCI are strongly influenced by the choice of the SR, with a difference of about 10 percentage points between the minimum and the maximum efficiency reached. In contrast, the partial cooling cycle does not seem to change much depending on the split ratio, whose efficiency increases or decreases only by a few percentage points.

The behaviour of the partial cooling cycle is due to cooling to compressor inlet temperature of the totally fluid. The compression work of each compressor does not change much, and the greater amount of energy required is fed by the hot external source.

Once the split ratio that maximizes the thermodynamic efficiency of each cycle is found, a new optimization varying the RPR parameter has been performed for the only two cycles that contain an inter-cooler and therefore divide the compression into two stages keeping constant the temperature and the new value of Split Ratio computed.

Table 5.5: Power production and compression work changing the RPR to maximize the thermodynamic efficiency of the Partial Cooling cycle

Partial cooling cycle							
<b>Pmax [bar]</b>	250	<b>Split fraction</b>	0,6				
<b>Pmin [bar]</b>	78	<b>Temperature [°C]</b>	650				
RPR	P_intermediate bar	W_turbine MJ/h	W recompression MJ/h	W Main compressor MJ/h	W precompressor MJ/h	Heat duty MJ/h	Efficiency [%]
-	-	-	-	-	-	-	-
0,35	140,40	18,06	1,48	1,21	2,84	28,00	44,7%
0,40	132,83	18,06	1,60	1,34	2,54	28,00	44,9%
0,50	118,90	18,06	1,84	1,64	1,96	28,00	45,1%
0,60	107,62	18,06	2,00	2,00	1,46	28,00	45,0%

Table 5.6: Power production and compression work changing the RPR to maximize the thermodynamic efficiency of the RMCI

RMCI- Recompression Main Compressor Intercooling							
<b>Pmax [bar]</b>	250	<b>Split Ratio</b>	0,65				
<b>Pmin [bar]</b>	78	<b>Temperature [°C]</b>	650				
RPR	P_intermediate bar	W_turbine MJ/h	W recompression MJ/h	W Main compressor MJ/h	W precompressor MJ/h	Heat duty MJ/h	Efficiency [%]
-	-	-	-	-	-	-	-
0,35	140,40	18,06	3,15	1,32	1,83	25,47	46,2%
0,40	132,83	18,06	3,22	1,45	1,65	25,30	46,4%
0,50	118,90	18,06	3,43	1,78	1,27	24,87	46,6%
0,6	107,62	18,06	3,7	2,19	0,95	24,34	46,1%

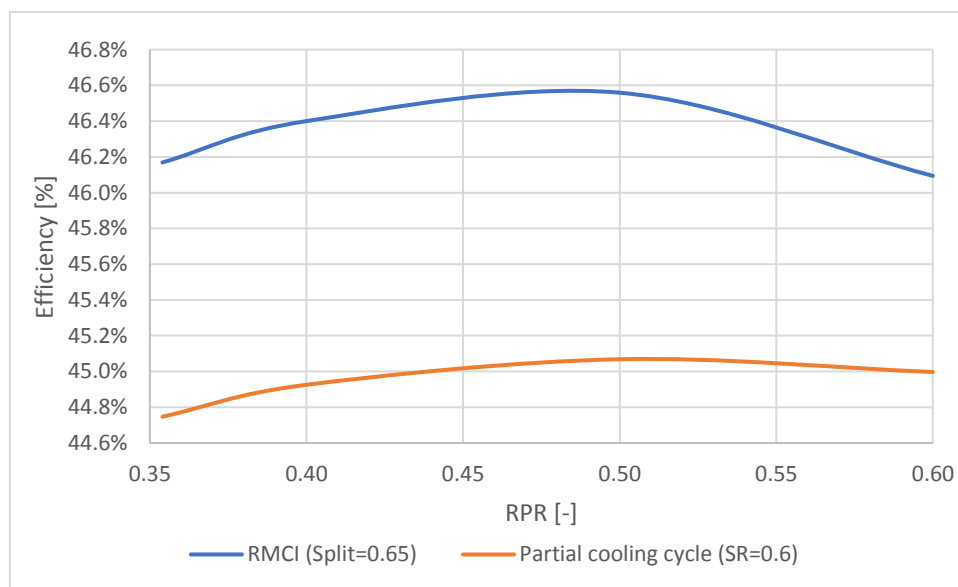


Figure 5.5: Thermodynamic performance of the both cycles that contain intercooler at different value of RPR

For both cycles, the change in efficiency with increasing RPR changes little. Nevertheless, the rise of almost one percentage point for both cycles is not to be overlooked.

A final parameter to consider is obviously the Turbine Inlet Temperature. We expect that the efficiency of the cycle will improve as this parameter increases for the same assumption made on the Carnot efficiency for the Compressor Inlet Temperature.

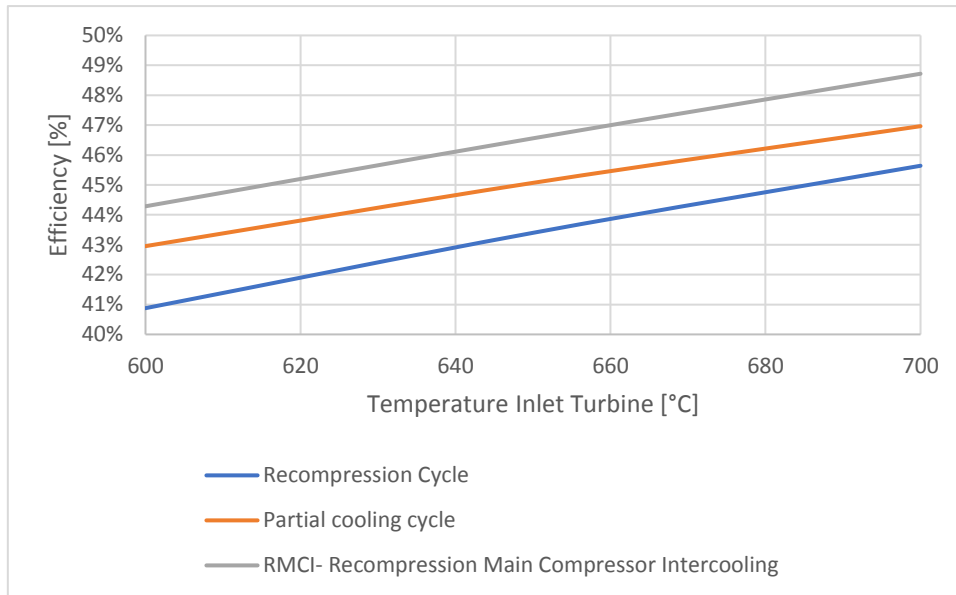


Figure 5.6: Compare of the s-CO2 Brayton cycle at different Turbine Inlet Temperature

Keeping the two parameters previously optimized constant, Fig 5.6 shows the trend of the efficiency of the thermodynamic cycles analysed with the change of TIT. The line of the partial cooling cycle shows a minor slope with respect to the others, but for all the cycles, as the TIT increases, the efficiencies go up significantly. The most efficient cycle was shown to be the RMCI which maintains a higher efficiency of about 2 points on all the temperatures analysed.

Therefore, the choice of a renewable source at high temperature and the use of a heat transfer fluid that allows to reach ever higher temperatures, allows to achieve largely higher efficiencies. Unfortunately, while thermodynamic cycles increase their efficiency with a higher temperature heat source, almost all high temperature technologies lose performance.

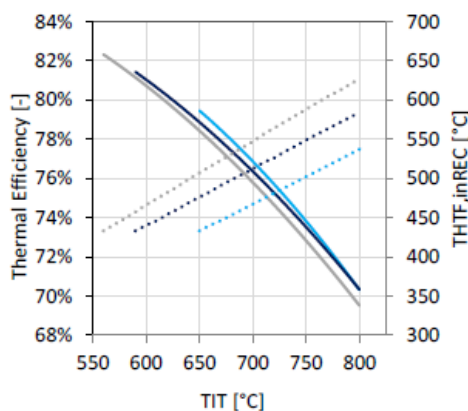


Figure 5.7: Thermal efficiency of the solar receiver at different TIT [3]

An example of performance drops with increasing temperature is shown in the figure above. A solar tower plant, which uses molten salt (KCl-MgCl<sub>2</sub>) consist of about 2500 heliostats and with a capacity

of around 25 MWe, was analysed [3]. The figure shows how the thermodynamic efficiency of the solar receiver decreases rising temperature.

### 5.3. S-CO<sub>2</sub> Brayton power cycle integrated with Solar CaL technology

In this section the main aspects of the CSP-CaL process integrated with s-CO<sub>2</sub> Brayton cycle is described. Fig 5.8 show a schematic representation of the CSP-Brayton-CaL integration for thermochemical energy storage and power production.

The introduction of storage system for CSP plants become mandatory on scenario with high penetration of non-dispatchable renewable energy source as well as the development of a power plants able to follow the electrical demand curve without the use of polluting conventional fuels.

In a concentrating solar tower plant, the sun's rays are reflected onto a receiver, which creates heat that can be used immediately to generate electricity or stored for later use. This enables CSP systems to be flexible, or dispatchable, options for providing clean, renewable energy.

The power block is based on Recompression Main Compression intercooling that can produce 305 MW<sub>e</sub> electrical gross connected to CO<sub>2</sub> solar receiver and CaL storage system. The use of closed Brayton cycle allows to easily regulate the mass flow rate of the supercritical CO<sub>2</sub> that circulates within the cycle in order to control the turbine inlet temperature. As the electricity demand and the availability of solar energy (fluctuating during the day) vary, the TIT variation allows to modulate the electricity production.

When the energy demand is reduced, part of the solar energy can be conveyed into a calciner for the regeneration of the sorbent in Calcium Oxide and Carbon Dioxide and their relative storage at low temperature.

Considering the presence of thermochemical storage, the production of electricity can continue even when there is no availability of solar energy. The carbonation reaction releases heat at high temperature (above 800 ° C) and can be used by the cycle work fluid to achieve high TIT and therefore high performance.

The s-CO<sub>2</sub> Brayton cycle was chosen through the analysis of performance and optimization previously developed with the only addition of an auxiliary compressor and a blade valve for the useful variation of the mass flow which generates a different power production.

The storage system and the exchanger network considered derives from the optimization achieved through the pinch analysis during the study of the coupling between CaL-CSP-Rankine cycle. We have seen how the network optimized by chapter 4.2 is also optimal for the coupling with the Brayton cycle. The only modified components are obviously the heat exchangers between the HTF of the CaL system and the work fluid of the Brayton cycle. The various economizer, evaporator, superheater and re-heater have been replaced with a simple gas-gas exchanger.

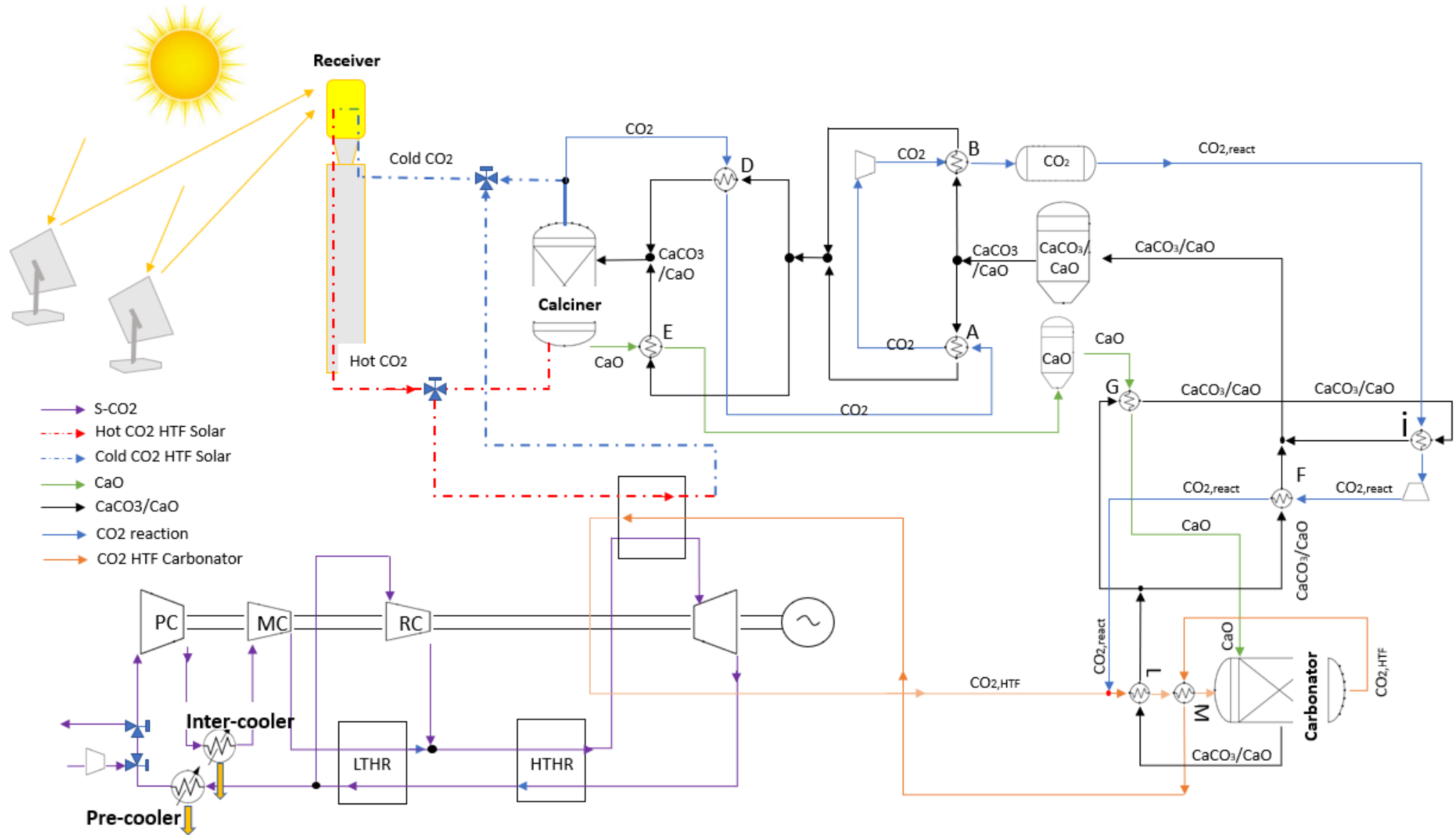


Figure 5.8: Scheme of integrating solar plant with s-CO<sub>2</sub> Brayton cycle and CaL storage system

Figure 5.8 show a conceptual CSP design incorporating a Recompression Main Compressor Cooling cycle and integrated with the Calcium Looping chemical storage system.

As mentioned above, when solar energy is available and there is a large demand for electricity, the solar tower system transfers its thermal power to the thermodynamic power cycle. Inside the gas-gas heat-exchanger, the solar concentrator's heat transfer fluid gave off heat to the super-critical CO<sub>2</sub> of the Brayton cycle. This stage is very important because depending on the turbine inlet temperature, the efficiency of the cycle varies significantly. The higher the TIT, the more performant the cycle is.

The heat transfer fluid used is not composed of molten salts, which limit the maximum achievable temperature, but it is carbon dioxide. The use of the CO<sub>2</sub> also inside the CSP is due both to the high temperature require from Brayton cycle and a high temperature CO<sub>2</sub> required to fluidize the calciner reactor in which the energy storage occurs.

Indeed, when the energy demand decreases, the excessive of solar energy is stored producing chemical compound (TCES). The hot CO<sub>2</sub> provide by the CSP at temperature above 900°C enters onto calciner reactor. The CO<sub>2</sub> provide the heat enough to endothermic calcination reaction and, at the same time, fluidize the reactor. During calcination reaction Calcium Carbonate is regenerated in CaO and CO<sub>2</sub>. The carbon dioxide produced during the reaction is separate by the total CO<sub>2</sub> at the exit of the reactor, cooled, compressed and stored at high pressure and ambient temperature.

All the spent sorbent is regenerated and the CaO produced is separated from the rest by using cyclone separators, cooled and stored at ambient temperature.

When the thermal energy from the CSP is insufficient, or during evening peaks of electricity, the heat required to drive the power cycle is provided by the carbonation reactor. The CaO regenerated during the charge of the storage, and the CO<sub>2</sub> necessary for the reaction, are conveyed from their respective storage to the carbonator reactor, flowing first through a heat exchanger network that increase the inlet temperature at the reactor.

Inside the carbonator enters also recirculation CO<sub>2</sub> used to transfer the heat of exothermic reaction from the reactor to the power cycle. The modulation of the power production by the Brayton cycle can be carried out either by the auxiliary compressor and the bleed valve described above, or by controlling the mass flow rates of the reagents to be sent to the carbonation reactor. In both ways it is possible to change the turbine inlet temperature of the working fluid and therefore the generation of electricity.

The work done during the Thesis aims to analyse in detail the integration between the Calcium Looping and the Brayton cycle illustrated in Fig 5.9. In the next chapters, the same power cycle is connected with the same system of CaL performed previously but with different flow rates are modelled. The calcium looping has been designed to meet the nominal power of the power cycle 24/24 which is equivalent to the most stressful condition. The sizing of the storage is instead calculated considering that the solar thermal energy available for 8/24 hours must regenerate the calcium carbonate to produce the reagents necessary for the carbonator.

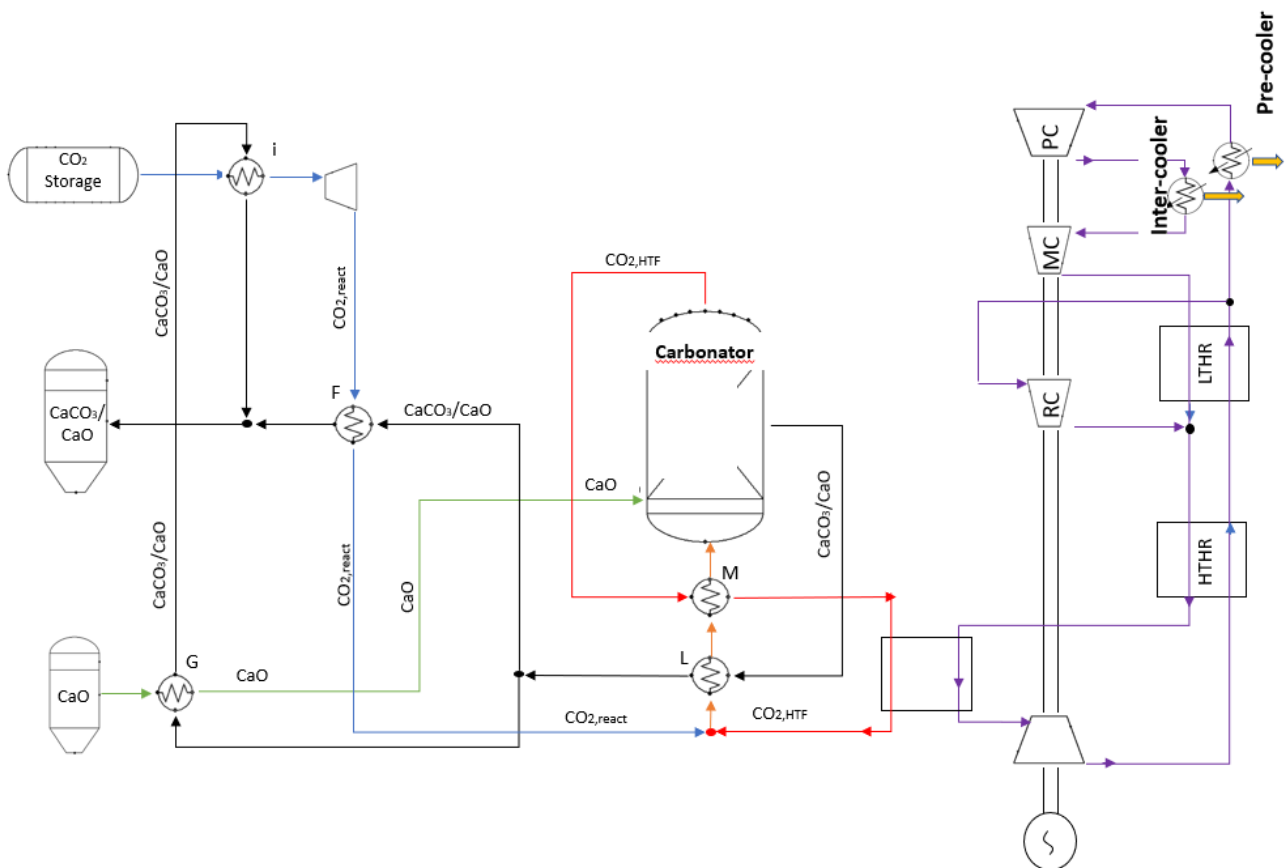


Figure 5.9: Plant configuration (carbonator-side) resulting from the previous pinch analysis integrated with s-CO<sub>2</sub> Brayton cycle

#### 5.4. Modelling

As was done in the previous chapter, the commercial software Chemcad<sup>TM</sup> was used for the modelling and simulation of the s-CO<sub>2</sub> Brayton cycle power plant integrated with calcium looping technology. Both the Brayton cycle plant and the CaL unit were simulated through several components such as reactors, flow mergers/splitter, heat exchangers turbine and compressors. The plant is equipped with a solid-solid heat exchanger, gas-solid heat exchanger and with gas-gas regenerator.

Some simplifying assumptions has made:

Other assumptions are listed below:

- Operation of all components is at steady state;
- Only thermodynamic equilibrium has been considered neglecting the kinetic of reactions;
- The ambient temperature and pressure are constant and equal to 20°C and 1 bar, respectively;
- The pressure losses were neglected;
- The heat losses in the piping and in the rest of the system were neglected with the exception of the carbonator reactor in which about 4% of heat produced is lost.
- The performance of the main reactors e.g. Carbonator and Calciner were represented using the chemical and phase equilibrium through the Gibbs free energy minimization at the operating temperature;
- A complete calcination of calcium carbonate takes place into solar calciner;
- Minimum temperature difference (pinch temperature) is 20°C for all main heat exchangers and 10°C for intercooler;

Several and others assumption are summarized in the following tables:

Table 5.7: Assumptions for the Solar Calcium Looping system

Reference case		
Solar heat provided to Calciner	2162	MWth
Termal dispersion in Carbonator	3,85%	%
Calciner Temperature	900	°C
Calciner Pressure	1	bar
Ambient Temperature	20	°C
CaO average conversion	70%	%
Carbonator Temperature	830	°C
Carbonator Pressure	2	bar
CO2 storage conditions	74	bar
Daylight hours	8	h
Pump isentropic efficiency	90%	%
Isentropic efficiencies of steam turbine and compressor	83%	%

Table 5.8: Assumption for the Brayton cycle

Assumption		
Parameters	Value	Unit
Turbine efficiency	0,93	[-]
Compressor efficiency	0,89	[-]
Min $\Delta\tau$	20	[°C]
Mass flow rate	2640	[kg/h]
Turbine Inlet temperature	650	[°C]
Compressor inlet temperature	51	[°C]
Maximum Pressure	250	[bar]
Pressure Ration	3,4	[-]
RPR	0,5	[-]

The Chemcad model analysed is shown in the following figure.

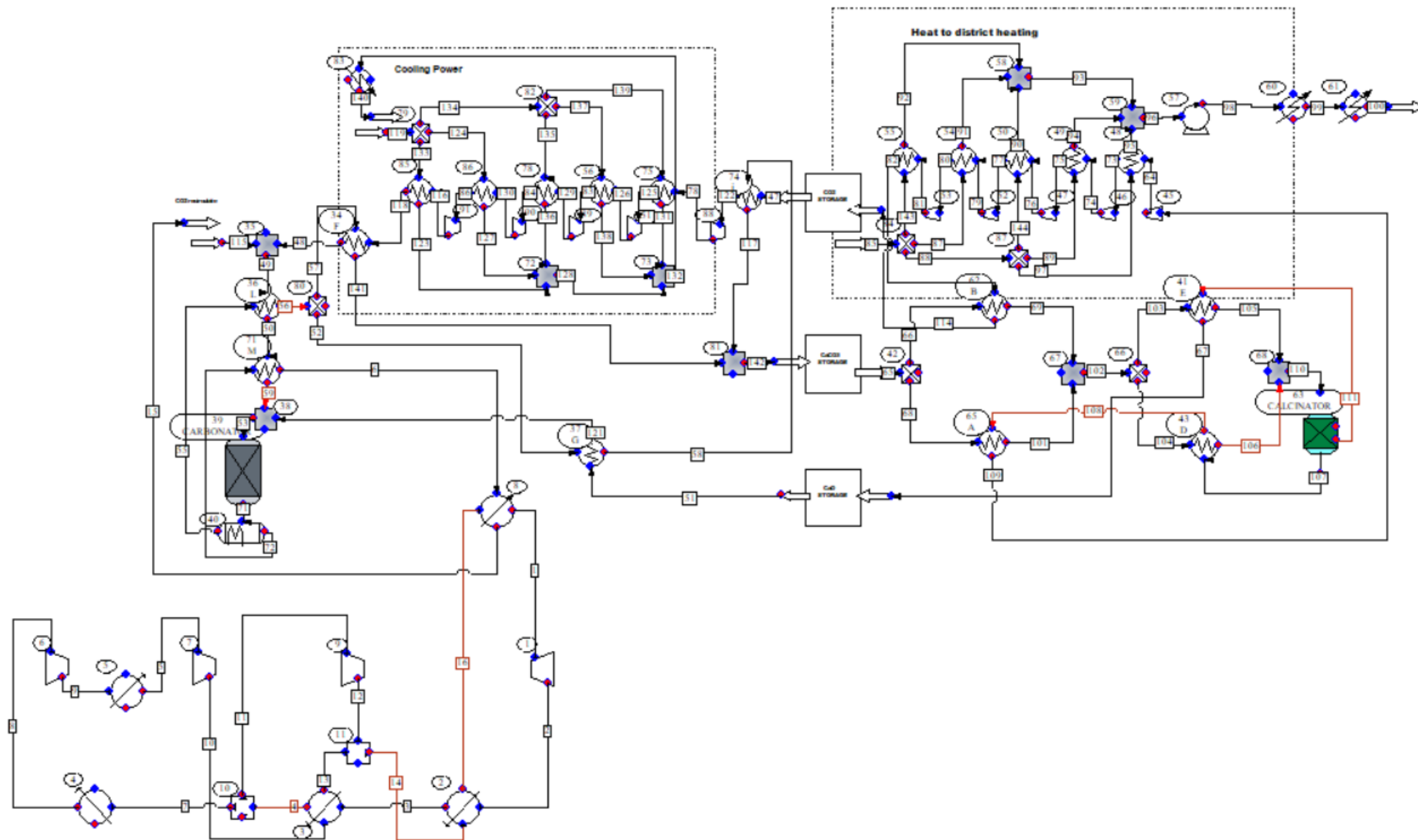


Figure 5.10: ChemCad model for Solar CaL integrated Brayton cycle power plant

The IS-CaL Brayton cycle is showed in Figure 5.10. It was assumed that the carbonation reaction occurs onto isothermal GIBBS reactor (a Chemcad™ model based on the Gibb's free energy minimization). The heat of reaction is transferred at the power cycle by means of heat transfer fluid but the 4% of the heat is lost to the environment.

The thermodynamic equilibrium is supposed to be reached in both Carbonator and Calciner reactors. In calciner reactor all  $\text{CaCO}_3$  is regenerated in Calcium oxide and  $\text{CO}_2$  while only the 70% of the CaO react with the  $\text{CO}_2$  into carbonator reactor.

In Chemcad™ the average conversion is considered by introducing an element with the same chemical property of the CaO but inert in presence of the carbon dioxide and thus does not produce calcium carbonate. It was introduced in the simulation of the plant in to properly solve the energy balance of the CaL system. It is known that the thermal energy input required by the calciner is mainly due to the decomposition of calcium carbonate. Consequently, the calciner energy consumption is estimated based on the average possible quantities of solids sent into the reactor

The CaL process requires a continuous make-up flow of fresh limestone to counteract the deactivation of lime with the number of carbonation/calcination cycles while a corresponding purge is also extracted from the calciner. The calcined purge is obviously a potential material to be fed to the cement plant and others. Due to the high resistance of the new sorbents at higher number of cycles, a continuous make-up flow is not simulated.

#### 5.4.1. Optimum configuration and parametric analysis

Once all the parameters that optimize the integration of the two systems have been found, a further analysis must be performed on the only independent key parameter: the CaO conversion. The degree of conversion is a function of the type of material used and the number of carbonation / calcination cycles performed. Whatever the thermodynamic conditions of operation, the degree of conversion will tend to decrease as the number of cycles increases.

Therefore, a parametric analysis was carried out by varying the most critical parameter (e.g. CaO conversion). This parameter has a significant influence on the storage vessels, on the solids flow rates and on the power consumption.

During parametric analysis, the power production of the s- $\text{CO}_2$  Brayton cycle is fixed. Therefore, a minimum heat power has to be released into carbonator reactor. The same amounts of reagents participate in the carbonation reaction, however, the un-reactant CaO flow rate increase. The obtained results are illustrated in the Figure below.

The Figures 4.17 and 4.18 show the effect of the CaO conversion on the thermal power in both main reactors in which the carbonation and calcination reaction occur. By fixing the quantities of the compounds that must react in the reactors, the necessary thermal powers in the calciner to regenerate the material ( $\Phi_{\text{calcination}} = 2141 \text{ MW}$ ) and the heat provided by carbonator ( $\Phi_{\text{carbonation}} = 713.85 \text{ MW}$ ) reactors remain constant. However, the sensible heat necessary to heat up the reactants to the temperature of the respective reactors, slumped significantly at high CaO conversion.

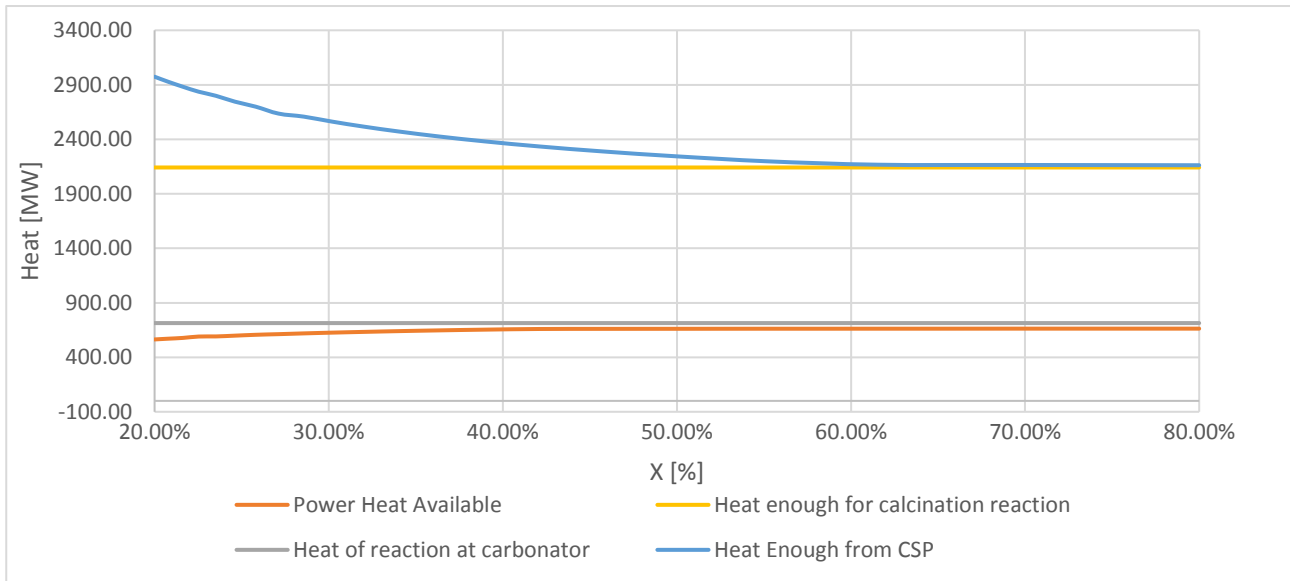


Figure 5.11: Thermal power fluxes of main reactors to vary CaO conversion

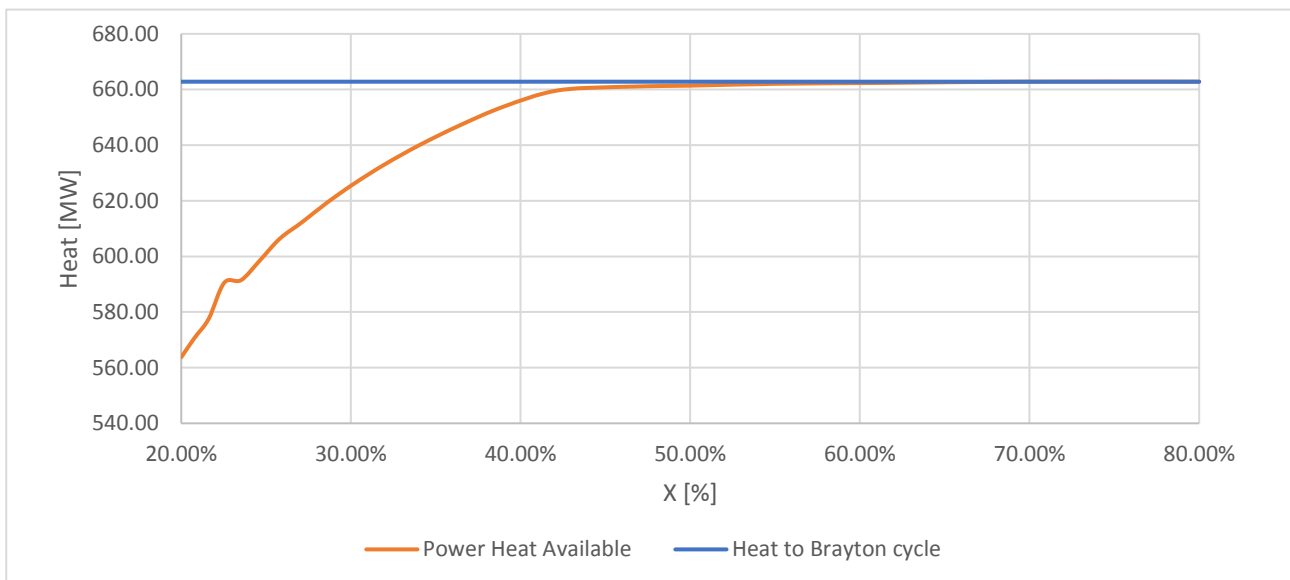


Figure 5.12: The heat enough from Brayton cycle is fixed, while change the heat provides by the storage system.

This leads to rise the heat demand necessary for total calcination, and to decline the thermal power available in the carbonation reactor. Therefore, in case of loss of performance of the sorbent, it may be necessary:

- Reduce the electric power produced, thus requiring less energy to the carbonator;
- Use an external resource that provides the missing power;
- Increase the flow rate of the reagents, making the system operate at nominal power but for less hours a day;
- If the performance has been reduced a lot (around  $X=0.35$ ), replace the solid material with a new one.

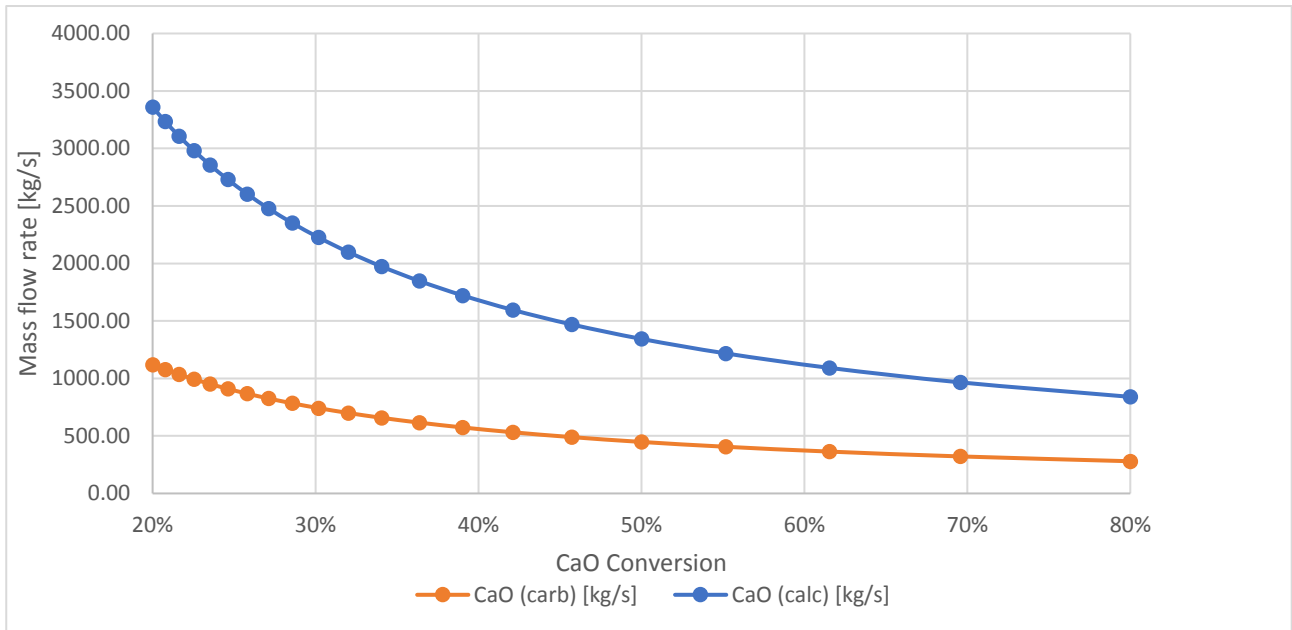


Figure 5.13: Solids mass flow rate at different CaO conversion

At fixed power heat Brayton cycle, changing CaO conversion it is possible compute the molar rate and then storage volume of each component. Remember that in this analysis the molar of the compound that participate really at the reaction are the same, as well as the CO<sub>2</sub> flowed in the carbonator side. Only the CaO unreacted increase.

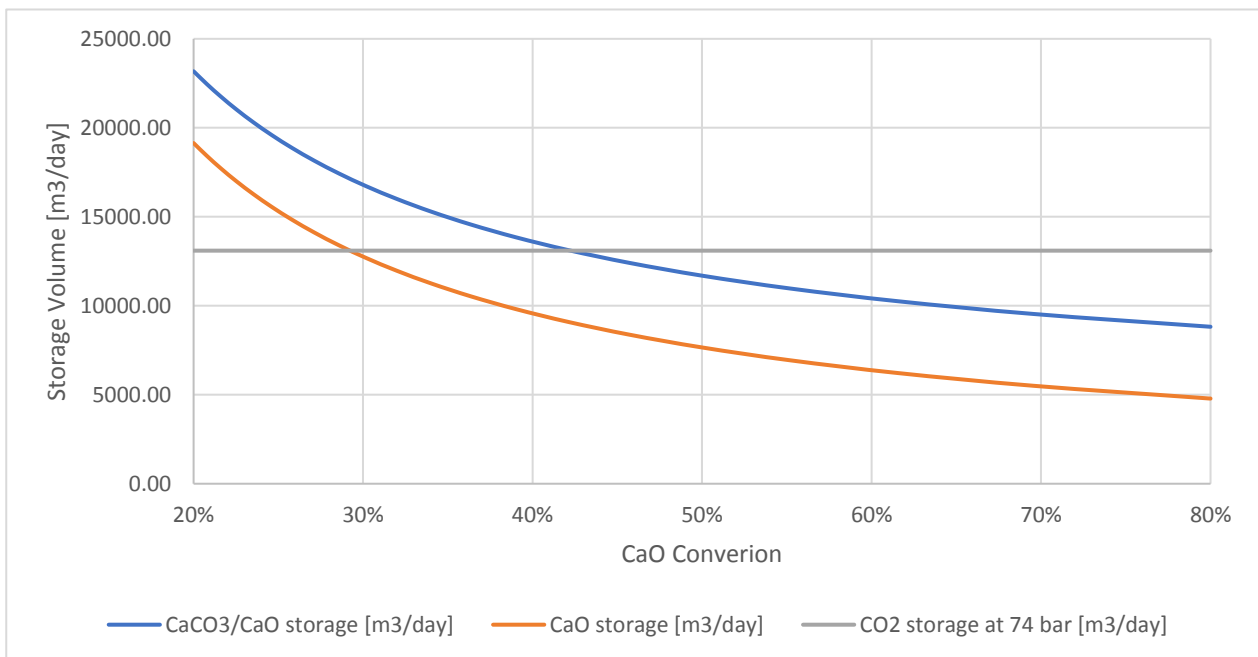


Figure 5.14: Storage volume as a function of average CaO conversion of the solids and CO<sub>2</sub> at 74 bar and 20°C

Figure 5.14 shows that increasing the CaO conversion, storage volume of the solid streams decreases while the CO<sub>2</sub> storage remain steady because of the power heat come into calciner reactor and flow out to Brayton cycle are kept constant. The CO<sub>2</sub> storage volume is not sensible to the CaO conversion, but it strongly depends (section 2.3) on the thermodynamic storage conditions.

In the following table are summarize the parameter used to compute the storage volume of components:

Table 5.9: Parameters used to compute storage volume

MM CO <sub>2</sub> [kg/kmol]	44
MM CaO [kg/kmol]	56
MM CaCO <sub>3</sub> [kg/kmol]	100
$\rho$ CO <sub>2</sub> (P=74 bar T=20°C) [kg/m <sup>3</sup> ]	773,99
$\rho$ CaO [t/m <sup>3</sup> ]	3,37
$\rho$ CaCO <sub>3</sub> [t/m <sup>3</sup> ]	2,93
Daylight hours [h]	8
hours of storage [h]	16

The mass flow rate of CaO produced in the calciner reactor is equal to the Calcium oxide consumed onto carbonator to provide the heat of reaction at Brayton power cycle as illustrated in Fig.5.15.

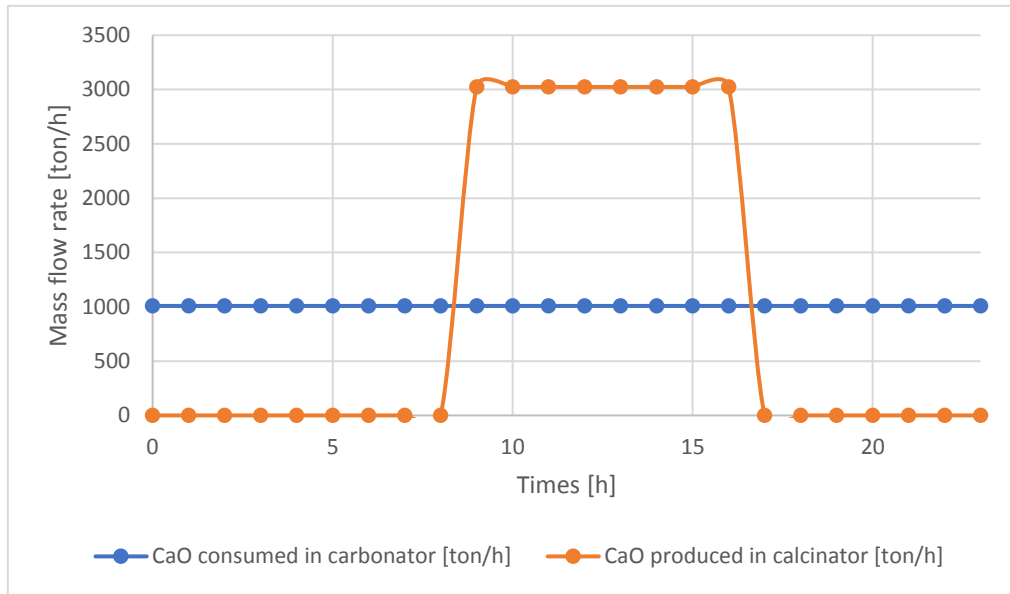


Figure 5.15: Mass flow rate of Calcium oxide consumed and produced respectively in different operational times

The efficiency of the storage system is computed as the follow:

$$\eta_{storage} = \frac{Q_{carbonator+LCO_2,expansion}}{Q_{CSP+LCO_2,compression}} \quad (5.2)$$

When CaO conversion goes down, the sensible heat necessary to heat an higher solids mass flow rate at the entrance of both reactors must be provided. Therefore, the heat provided by the CSP to regenerate the spent sorbent increase, and part of the heat of reaction into carbonator reactor is used to heat up the reactants.

When conversion degree is equal to 40% (Fig 5.16), the system loses more than 10% efficiency and maybe is better change the sorbent material.

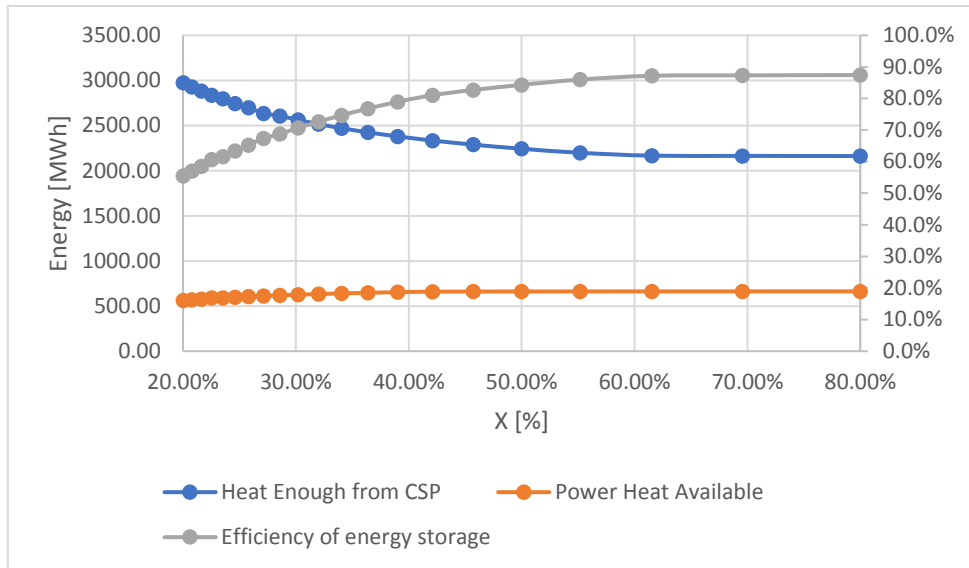


Figure 5.16: Thermal power fluxes (left axis) and energy storage efficiency (right axis) function of CaO conversion

When into the system efficiency also the heat to district heating and cooling power is consider, obviously the storage efficiency increases a lot. To consider the recovery power, the equation of the efficiency is modified in this way:

$$\frac{Q_{carbonator} + L_{CO_2 expansion} + Q_{chiller} + Q_{district heating}}{Q_{CSP} + L_{CO_2 compression} + L_{pump}} \quad (5.3)$$

Each term represents an energy and is calculated by multiplying the thermal or mechanical power by the respective operation time.

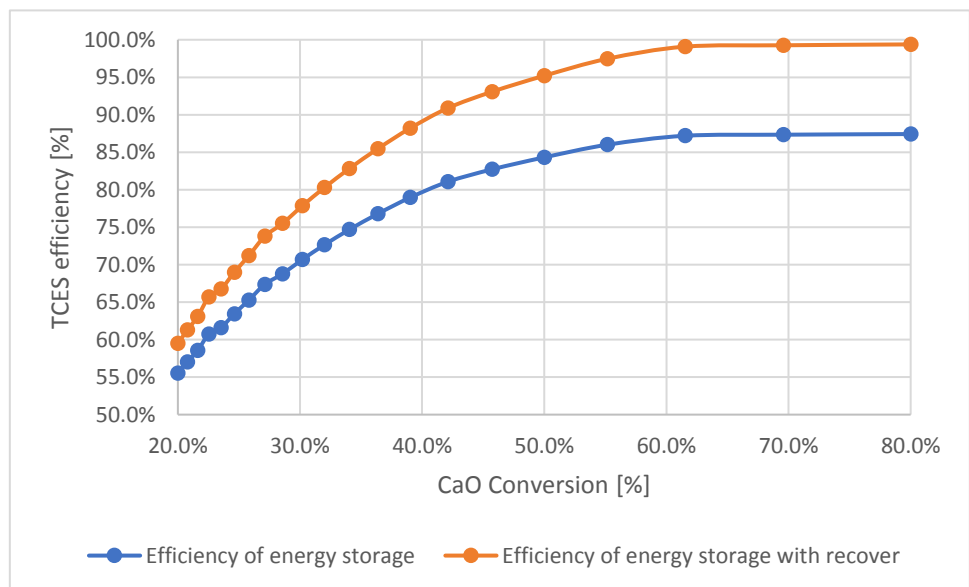


Figure 5.17: Thermodynamic efficiency energy storage with and without low thermal energy recovery in chiller and district heating

The two efficiencies went up significantly increasing CaO conversion and they reached a good peak of 87.4% and 99.4% respectively. Therefore, it is better to work with a material having excellent conversion performance and recover the various energies available at low temperature to achieve very high levels of efficiency for a storage system.

The optical and thermodynamic efficiencies of the CSP were not considered.

With the CaO conversion equal to 0.4 the efficiency with energy recovery plummet from 99.4% to 88.2%.

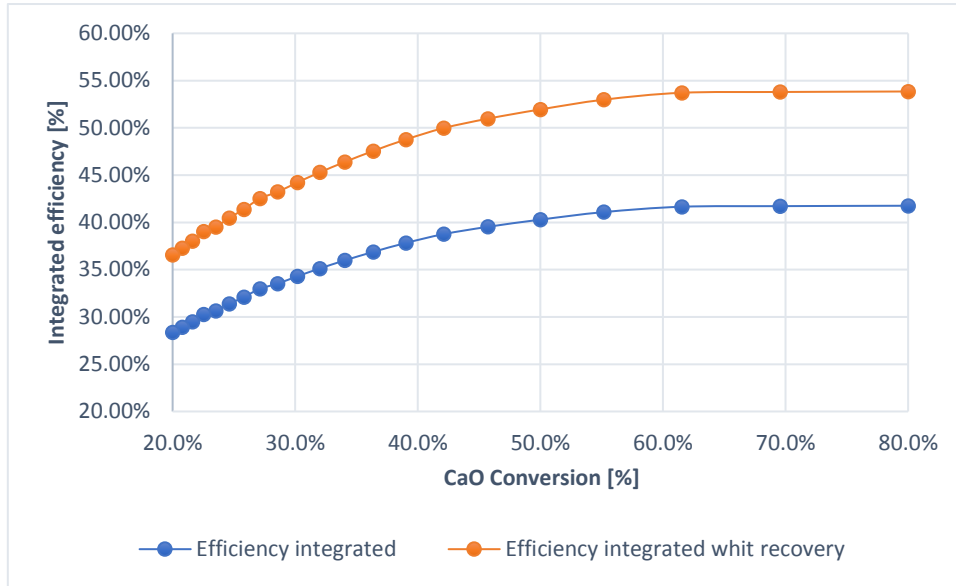


Figure 5.18: Thermodynamic integrated efficiency with and without low thermal energy recovery

It is important to remember that the efficiency of the starting s-CO<sub>2</sub> Brayton cycle is 46.1%. When the thermochemical storage system is integrated into the power cycle, the thermodynamic efficiency will certainly be lower, and it vary with the CaO conversion parameter. The Net electrical efficiency (blue line) is calculated by the following reaction:

$$\eta_{NET} = \frac{L_{turbine,Brayton} + L_{CO_2,expansion}}{Q_{CSP} + L_{CO_2,compression}} \quad (5.4)$$

While the gross efficiency is defined as:

$$\frac{L_{turbine,Bryton} + L_{CO_2expansion} + Q_{chiller} + Q_{district heating}}{Q_{CSP} + L_{CO_2compression} + L_{pump}} \quad (5.5)$$

The maximum integrated efficiency with and without recover heat from compression/expansion of CO<sub>2</sub> into CaL system reach the peak of 41.76% and 53.85%

The thermodynamic efficiency at low values of CaO conversion went down. Therefore, when the conversion degree of the sorbent decreases a lot, the material should be changed.

All the electrical and thermal powers produced and consumed by the various components, and the values of the plant efficiencies at a fixed CaO conversion value set at 0.7 are summarized in the following table.

Table 5.10: Thermal and electrical input and output for each macro-component

Calciner side	Power Heat from CSP to calciner	-2162,00	MW
	Daylights hours	8,00	h
	Energy heat from CSP	-17296,00	MWh
	Electric power to compress CO2	-185,04	MW
	Electric energy to compress CO2	-1480,32	MWh
	Power pump to water networking	-1,18	MW
	Energy to pump water networking	-9,44	MWh
	Power to district heating	206,00	MW
Carbonator side	Energy to district heating	1648,00	MWh
	Electric power from compressed CO2	21,17	MW
	Electric energy from compressed CO2	508,08	MWh
	Cool power	26,10	MW
	Cool energy	626,40	MWh
	Power to Brayton cycle	662,81	MW
Brayton Cycle	Energy to Brayton cycle	15907,44	MWh
	HP Turbine	476,87	MW
	Re-compressor	-90,63	MW
	Main compressor	-46,99	MW
	Pre compressor	-33,66	MW
	Power output from Brayton	305,59	MW
	Daily work	24,00	h
Efficiency	Energy output from Brayton	7334,23	MWh
	Efficiency of energy stored	87,3%	%
	Efficiency of energy stored with recover	99,3%	%
	Efficiency of s-CO2 Brayton	46,1%	%
	Efficiency integrated	41,7%	%
	Efficiency integrated whit recovery	53,8%	%

## References

- [1] IRENA; « Concentrating Solar Power» International Renewable Energy Agency; 2012.
- [2] Y. Ahn, et al « REVIEW OF SUPERCRITICAL CO<sub>2</sub> POWER CYCLE TECHNOLOGY AND CURRENT STATUS OF RESEARCH AND DEVELOPMENT »; ELSEVIER; 2015
- [3] M. Binotti, et al « Preliminary assessment of sCO<sub>2</sub> power cycles for application to CSP Solar Tower plants »,ELSEVIER, 2016
- [4] Z. Guo, et al;, « Optimal design of supercritical CO<sub>2</sub> power cycle for next generation nuclear power conversion systems », ELSEVIER; 2018.
- [5] K. Wang, et al « A systematic comparison of different S-CO<sub>2</sub> Brayton cycle layouts based on multi-objective optimization for applications in solar power tower plants » ELSEVIER; 2018

## 6. Conclusion

A novel solution for CO<sub>2</sub> capture and energy storage by means of a calcium-based process (Calcium Looping, CaL) and concentrated solar power (CSP) technologies is presented and thoroughly investigated.

The first part of this Thesis is focused on the energy analysis of a direct reduced iron process (Midrex) decarbonised via CaL and compared to the conventional Midrex process integrated with an electric arc furnace (EAF) producing 1 Mt/y. The new components added in the decarbonised plant are:

- the Bi-reformer of methane (BMR) used to convert methane into a mixture of CO and H<sub>2</sub> via steam methane reforming (SMR) and dry methane reforming (DMR) at 950°C;
- SE- WGS (Sorption Enhanced Water Gas Shift, SE-WGS) using the **CaL** technology to enhance the production of the hydrogen via the intensification of the water gas shift (WGS) reaction with the capture of CO<sub>2</sub> at 650°C;
- Carbonator reactor used to capture the CO<sub>2</sub> from the flue gas produced in iron making mills.

The hydrogen is used as reductant in the production of DRI (Direct Reduction Iron) into a shaft furnace in order to reduce the emission of CO<sub>2</sub>. The heat requested during the production of DRI is furnished by the combustion of conventional fuels (i.e. methane and coal). Flue gas will be decarbonised via carbonator reactor.

A reduction of 40 kg/t ls compared to the reference plant is obtained. The waste heat is recovered producing 0.19 MWe/t ls. The heat is recovered from: (i) the SE-WGS (about 33% of total energy recovery), (ii) flue gas combustion (23%), (iii) hot CaCO<sub>3</sub> produced during the capture of CO<sub>2</sub> into carbonator and SE-WGS, (iv) flue gas exist carbonator and finally (v) the EAF offgas (6%) as showed in Fig. 6.1.

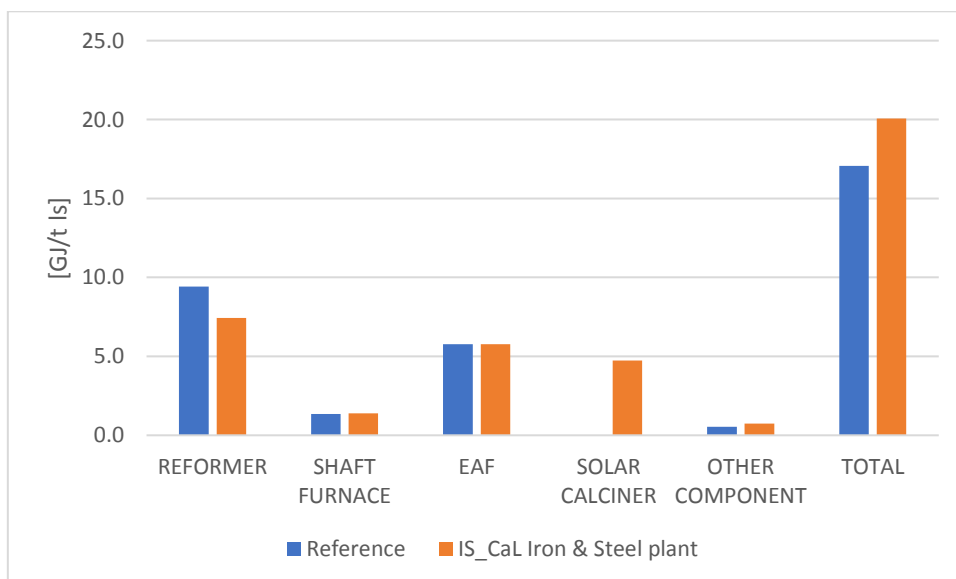


Figure 6.1: Thermal energy requirement for both plants considered

The energy consumed by the novel plant is 18.4 GJ/t ls (see Fig. 6.1) to respect the 17 GJ/t ls consumed by the Midrex plant. Conversely, the CO<sub>2</sub> emitted directly in atmosphere are reduced of 86% while the equivalent CO<sub>2</sub> emission reduction is 69% due to CO<sub>2</sub> emitted from power production. The mainly emission is due to electricity production (Fig 6.2) therefore a direct coupled with renewable power plant (e.g. ISCaL) is suggested to further reduce the CO<sub>2</sub> emission.

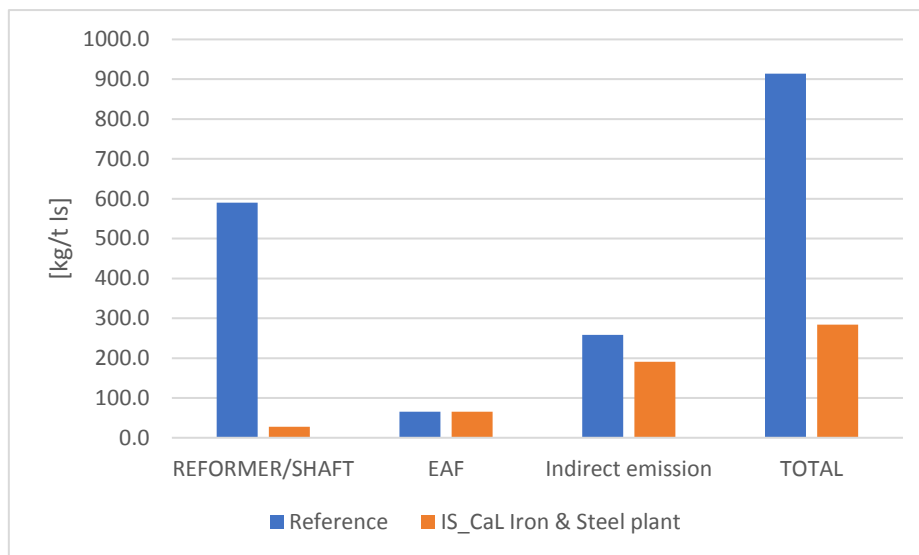


Figure 6.2: Direct and indirect CO<sub>2</sub> emission for both plants considered

The value of the SPECCA (2 GJ/ tCO<sub>2</sub>) index is comparable with other CCS systems.

The integration of the calcium looping process for thermochemical energy storage (TCES) of the solar energy excess was investigated. The solar energy is used to decompose CaCO<sub>3</sub> into CaO and CO<sub>2</sub> at high temperature and stored at ambient temperature. Solar energy is harvested into central tower receiver and transferred into calcination reactor by heat transfer fluid or, alternatively, calcination reaction can happen directly into a solar receiver. The solar energy is then stored in chemical form which can be used in a different place and in different times without heat loss overcoming the fluctuation of power generation from solar energy. During energy release, CO<sub>2</sub> is expanded into a turbine and sent into a carbonator where it reacts with CaO coming from a silos, and releasing reaction heat at high temperature, used for power production.

The second part of this work analyses two power cycle configurations with the main goal of optimizing the performance of the overall system integration. In particular, an integration with a conventional Rankine cycle produced 320 MWe and an early-stage supercritical CO<sub>2</sub> Bryton cycle of 305 MWe are proposed. A pinch analysis is performed to optimize these energy systems. A parametric analysis was carried out to evaluate the reduction of plant efficiency when the CaL process coefficients (e.g. carbonation extent, temperature and pressure of carbonation reactor) changes.

Fig. 6.3 shows the net and gross efficiencies of the two plant at different CaO conversion.

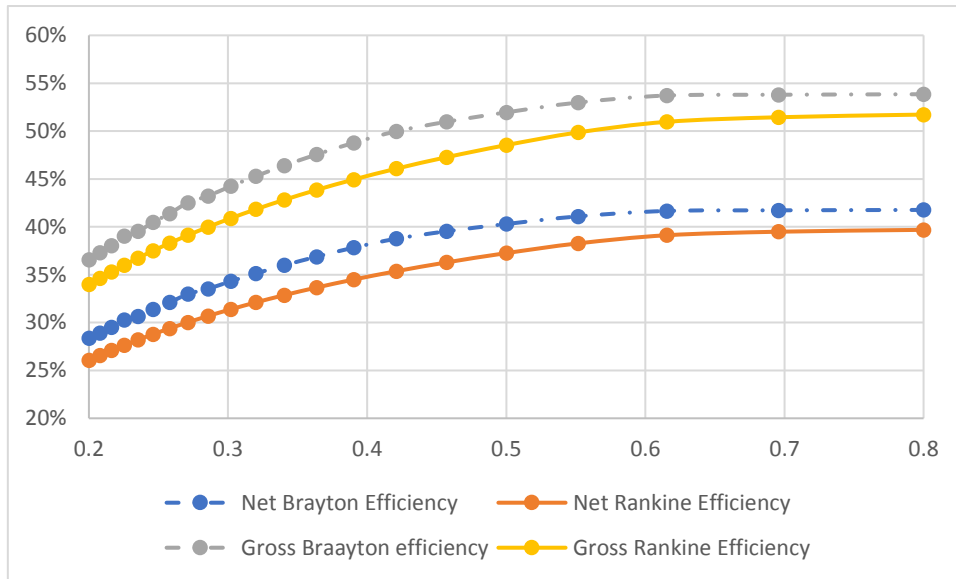


Figure 6.3: Net and Gross efficiencies of the two power plants integrated with ISCaL at different material performance

In the s-CO<sub>2</sub> Brayton cycle, the CO<sub>2</sub> has the ability to: (i) gather heat from solar field and (ii) be used as working fluid in the thermodynamics cycle. It can potentially lead to high efficiency reaching high temperature operation and a compact system layout, reducing the investment cost.

The s-CO<sub>2</sub> Brayton cycle is more efficient of the Rankine power cycle reaching respectively 54% and 42% at X=0.8 while the Rankine cycle is always less than two percentage point at different CaO conversion. However, the use of ISCaL process in conventional Rankine cycle makes this solution a good candidate for the decarbonisation of power sector compared to the low-TRL s-CO<sub>2</sub>.